

LECTURES IN THEORETICAL PHYSICS

Vol VII C -- Statistical Physics, Weak Interactions, Field Theory
University of Colorado Press, Boulder, 1965

THE NATURE OF CRITICAL POINTS*

Michael E. Fisher†
The Rockefeller Institute
New York, New York

Preface

These lecture notes present an informal review of the experimental facts and theories concerning critical points, especially in fluid and magnetic systems. The main emphasis is on the fundamental problems and recent theoretical developments. In writing the notes I have retained the informal style of the lectures and have not attempted, for example, to give a complete bibliography of the field. Relatively little background knowledge is assumed and the mathematical level is quite low. Readers familiar with the subject but interested in the newer developments might wish to skim the early chapters or start directly with, say Chapter VII.

Much of the material in these notes was first presented as a series of invited lectures at Yale University. I would like to thank Professor W. P. Wolf of Yale for the stimulus that lead to their preparation.

Contents

Chapter I

1. Introduction	7
2. Critical Point of a Fluid	9
3. Curie Point of a Ferromagnet	14
4. Binary Solutions	18
5. Antiferromagnetism	20
6. Homogeneous Binary Alloys	22

* Presented at the THEORETICAL PHYSICS INSTITUTE, University of Colorado, Summer 1964.

† On leave of absence 1963-64 from The Wheatstone Physics Laboratory, King's College, London, England.

Contents (Continued)

<u>Chapter II</u>	
7. Simple Models	24
8. Simpler Models	27
9. Basic Statistical Mechanical Formulas	28
10. Equivalence of Ising Magnet and Lattice Gas	30
<u>Chapter III</u>	
11. General Statistical Questions	35
12. The Mathematical Mechanism of Phase Transitions	39
13. Singularities in the Canonical Partition Function	42
<u>Chapter IV</u>	
14. The Mean Field and Van der Waals Equation	45
15. Classical Critical Point Predictions	49
16. Phenomenological Treatment of Critical Points	51
17. Validity of Classical Theory	52
<u>Chapter V</u>	
18. Two-dimensional Ising Models	54
19. Exact Solution of the Ising Model	57
20. Further Results	61
21. Three Dimensions and Magnetic Fields	63
<u>Chapter VI</u>	
22. Series Expansions	64
23. The Counting Problem	67
24. Lattice Constants	70
25. Correlation Functions and Susceptibility	70
<u>Chapter VII</u>	
26. The Misuse of Power Series	73
27. The Ratio Method	76
28. Extensions	82
29. Ferromagnetic Susceptibility of the Square Lattice	85
<u>Chapter VIII</u>	
30. Compressibilities and Susceptibilities	87
31. Critical Isotherms	91
32. Specific Heats	91
<u>Chapter IX</u>	
33. Low Temperature Behaviour	96
34. Padé Approximants	98
35. Analytical Character	100
36. Application to the Ising Model	103
37. Physical Conclusions	106
38. Further Applications	107

Contents (Continued)

Chapter X

39. Dependence on Dimensionality	109
40. Droplet Model of Condensation	111
41. Relation for the Critical Exponents	114
42. A Thermodynamic Inequality	115

Chapter XI

43. The Theory of Antiferromagnets	118
44. Exactly Soluble Antiferromagnetic Model	122
45. Properties of the Superexchange Model	126
46. Perpendicular Susceptibility of the Ising Model	131

Chapter XII

47. Counting Theorem for the Susceptibility	133
48. Extrapolation to the Antiferromagnetic Singularity	135
49. Comparison with Experiment	137
50. Relation to Correlation Functions	138
51. Correlation in a Simple Antiferromagnet	140
52. Energy-Susceptibility Relation	143
53. Other Properties	147

Chapter XIII

54. Critical Scattering	150
-------------------------	-----

Appendix

Existence and Properties of the Free Energy	152
---	-----

List of Figures

2.1 Typical isotherms for a simple fluid.	9
2.2 Phase diagram for a simple fluid.	10
2.3 Coexistence curve for neon, argon, krypton, etc. (from E. A. Guggenheim, J. Chem. Phys. <u>13</u> , 253(1945)).	11
2.4 Coexistence curve for xenon close to T_C (from M. A. Weinberger and W. G. Schneider, Can. J. Chem. <u>30</u> , 422(1952)).	12
2.5 Constant volume configurational specific heat for argon at critical density (from M. E. Fisher (to be published) after measurements by M. I. Bagatskii, A. V. Voronel' and B. G. Gusak, Soviet Phys. JETP <u>16</u> , 517(1963)).	14
3.1 Spontaneous magnetization and initial susceptibility of a ferromagnet near its Curie point.	15
3.2 Sketch of the specific heat of nickel in zero field.	16
3.3 Ideal magnetization curve of a ferromagnet.	17
3.4 Phase diagram for a ferromagnet.	17

List of Figures (Continued)

4.1	Coexistence curve for a binary fluid mixture.	19
4.2	Coexistence curve illustrating a lower critical point of a binary solution.	19
5.1	Sketch of the susceptibility of a typical antiferromagnet. The dashed line indicates the free spin susceptibility.	20
5.2	Specific heat of the antiferromagnet $\text{NiCl}_2 \cdot 6\text{H}_2\text{O}$ (from W. K. Robinson and S. A. Friedberg. <i>Phys. Rev.</i> <u>117</u> , 402(1960)).	21
5.3	Cube of the sublattice magnetization of MnF_2 , as measured by the NMR frequency, versus temperature (from P. Heller and G. B. Benedek, <i>Phys. Rev. Letters</i> <u>8</u> , 428(1962)).	23
5.4	Phase diagram for a typical antiferromagnet.	23
11.1	Canonical free energy and pressure versus specific volume illustrating possible (solid line) and impossible (dashed line) behaviour.	37
11.2	Grand canonical pressure and density illustrating possible behaviour.	38
12.1	Possible distribution of zeros of $\Xi(z, \Omega)$ in the complex z plane.	40
12.2	Possible limiting distribution of zeros in z plane.	41
13.1	Energy versus β showing approach to a first order phase change.	43
14.1	(a) Van der Waals isotherm below T_C showing Maxwell construction.	48
	(b) Van der Waals free energy below T_C showing "double tangent" construction.	49
18.1	Kagomé lattice: note $q = 4$.	57
19.1	Loci of zeros of the Ising partition function in the complex $v = \tanh(J/2kT)$ plane.	58
19.2	Exact specific heat of the plane square Ising lattice (solid curve), Bethe's approximation (dotted curve) and the Kramers-Wannier and Kikuchi approximation (dashed curve). (From C. Domb <i>Adv. in Phys.</i> <u>9</u> , Nos. 34, 35 (1960).)	60
22.1	An allowed configuration of bonds on the plane square lattice.	66
26.1	Successive approximations based on truncating the series for $\chi_O(T)$ compared with the expected behaviour.	74
26.2	Successive approximations based on truncating the series for $1/\chi_O(T)$ compared with the expected behaviour.	75

List of Figures (Continued)

- 27.1 Ratios of coefficients of the susceptibility series of the triangular ($q=6$) and f.c.c. ($q=12$) lattices (from C. Domb and M. F. Sykes, J. Math. Phys. 2, 63 (1961)). 78
- 27.2 Ratios c_n/c_{n-1} for walks on the square lattice (a) with only reversals and squares disallowed, (b) with no self-intersections, (c) with no self-intersections or nearest neighbour contacts (from M. E. Fisher and B. J. Hiley, J. Chem. Phys. 34, 1253(1961)). 80
- 28.1 Plot of the refined critical point estimates $\beta_n = \mu_n^*/q$ for (A) the square lattice, (B) the simple cubic lattice and (C) the body-centered cubic lattice (from Domb and Sykes, loc. cit.). 83
- 28.2 Reciprocal susceptibilities of two- and three-dimensional Ising models compared with the Weiss mean field prediction (from C. Domb and M. F. Sykes, Proc. Roy. Soc. A240, 214(1957)). 85
- 30.1 Reciprocal compressibility of xenon above T_C from M. E. Fisher, J. Math. Phys. 5, 944 (1964) . 88
- 30.2 Plot of the effective exponent $\gamma^*(T)$ for nickel (from J. S. Kouvel and M. E. Fisher, Phys. Rev. 736, A1626 (1964)). 90
- 31.1 Critical isotherm for nickel (from J. S. Kouvel and M. E. Fisher, loc. cit.). 92
- 32.1 Specific heat of the f.c.c. Ising lattice from series estimates (solid curve), from the Kikuchi (dashed curve) and Bethe (dotted curve) approximations. (From C. Domb, Adv. in Phys. 9, Nos. 34, 35(1960).) 94
- 32.2 Logarithmic plot of the reduced configurational specific heat of argon (circles and line a) compared with Ising model predictions (curves b, c, d and e). (From M. E. Fisher, Phys. Rev. 136, A1599 (1964)). 95
- 33.1 Complex u plane illustrating the physical region on the real positive axis, and interfering singularities which limit the radius of convergence. 97
- 35.1 Illustrating the distribution of zeros and poles of the Padé approximants to the functions of Equations (35.2) and (35.3). 101
- 37.1 Spontaneous magnetization of two- and three-dimensional Ising lattices (from D. M. Burley, Phil. Mag. 5, 909(1960)) . 107
- 43.1 Temperature variation of the susceptibilities of a typical antiferromagnetic material. 119

List of Figures (Continued)

- 43.2 Behaviour of the specific heat and susceptibilities of an antiferromagnet according to the mean field and related approximations. Note that the peaks in $C(T)$ and in $\chi(T)$ occur at the same temperature. 120
- 44.1 Bond transformation. 122
- 44.2 Decorated square lattice. 125
- 45.1 Sketch of the transition curve for the plane superexchange model. 127
- 45.2 Constant temperature magnetization curves for the superexchange model. Note $\mathcal{Q} = 2M/M_{\max}$ and $\alpha = H/H_C$. (From M. E. Fisher, Proc. Roy. Soc. A254, 66(1960).) 128
- 45.3 Parallel susceptibility of the superexchange model versus temperature in zero field (solid line) and in a field $H = \frac{1}{4}H_C$ (dashed curve). (From M. E. Fisher, Proc. Roy. Soc. A254, 66(1960).) 129
- 45.4 Comparison of the reduced susceptibility $\xi(T) = kTX/m^2$ and the function $1 - [U(T)/U(0)]$. Note that the scale of ordinates has been doubled and that K^{-1} is proportional to T . (From M. E. Fisher, Proc. Roy. Soc. A254, 66(1960).) 131
- 46.1 Perpendicular susceptibility of (a) the plane square Ising lattice, (b) the square superexchange lattice compared with (c) the parallel susceptibility of the superexchange model. From M. E. Fisher, J. Math. Phys. 4, 124(1963). 132
- 49.1 Parallel susceptibilities of (a) the body centred cubic ($q=8$) and (b) the simple cubic ($q=6$) Ising lattices near the antiferromagnetic critical point which is marked by a circle. (From M. F. Sykes and M. E. Fisher, Physica 28, 930(1962).) 137
- 51.1 Qualitative behaviour of the correlation functions of a simple antiferromagnet. 142
- 52.1 Comparison of the magnetic specific heats (upper pair of curves and right hand scale) with the susceptibility gradients (lower pair of curves and left hand scale) versus $\theta = T/T_C$ for MnF_2 (solid curves) and MnO (broken curves). Note the different zero levels of the two vertical scales. (From M. E. Fisher, Phil. Mag. 7, 1731(1962).) 146
- 52.2 Comparison between the magnetic energy and the susceptibility for dysprosium aluminum garnet. The

List of Figures (Continued)

	critical point is at 2.49°K. (From W. P. Wolf and A. F. G. Wyatt, Phys. Rev. Letters <u>13</u> , 368 (1964).)	148
52.3	Comparison of the specific heat of DAG with the gradient $\partial(TX)/\partial T$ normalized by a factor corresponding to $F(T) = 1$ in Equation (52.4). (From W. P. Wolf and A. F. G. Wyatt, Phys. Rev. Letters <u>13</u> , 368 (1964).)	149

List of Figures—Appendix

A.1	A domain Ω containing two separated subdomains.	155
A.2	Illustrating the convexity of the free energy density $g(\rho)$.	158

 Chapter I
1. Introduction

The study of phase transitions and critical points cuts across the familiar divisions of the sciences. Much of the original thinking about the states of matter and their interrelations was done by engineers who wanted to design efficient heat engines, turbines, and other devices. In present times it overlaps the domains of low-temperature physics, solid-state physics, physical chemistry, chemical engineering, and metallurgy. At further remove some of the ideas developed in the study of phase transitions have been applied in biochemistry and biophysics to the study of macromolecules, and in nuclear physics in the understanding of nuclear structure and spectra.

Needless to say I will not, in these lectures, attempt to cover the whole field! My approach to the subject will be mainly that of a theorist aiming at a general understanding of the phenomena rather than a detailed description of the peculiarities of specific physical and chemical systems. My philosophy at this stage has been well expressed by Frenkel (in a review article devoted to the theory of metals, quoted by Tamm in his obituary of Frenkel).

Frenkel states his views on the task of a theoretical physicist as follows:

The more complicated the system considered, the more simplified must its theoretical description be. One cannot demand that a theoretical description of a complicated atom, and all the more of a molecule or a crystal, have the same degree

of accuracy as of the theory of the simplest hydrogen atom. Incidentally, such a requirement is not only impossible to fulfill but also essentially useless. . . . An exact calculation of the constants characterizing the simplest physical system has essential significance as a test on the correctness of the basic principles of the theory. However, once it passes this test brilliantly there is no sense in subjecting it to further tests as applied to more complicated systems. The most ideal theory cannot pass such tests, owing to the practically unsurmountable mathematical difficulties unavoidably encountered in applications to complicated systems. In this case all that is demanded of the theory is a correct interpretation of the general character of the quantities and laws pertaining to such a system. The theoretical physicist is in this respect like a cartoonist, who must depict the original, not in all details like a photographic camera, but simplify and schematize it in a way as to disclose and emphasize the most characteristic features. Photographic accuracy can and should be required only of the description of the simplest system. A good theory of complicated systems should represent only a good "caricature" of these systems, exaggerating the properties that are most difficult, and purposely ignoring all the remaining inessential properties.

It is fair to add, however, that it is not always easy to see beforehand just what are the essential properties of a system in relation to the particular phenomena studied. Indeed in our discussion of critical points there will appear some surprises in this direction! Of course it is one of the jobs of theory to decide just what properties of the system, or more formally of its Hamiltonian, are responsible for the observed behaviour at a critical point.

In the spirit of Frenkel's remarks I will consider mainly the simplest examples of the various types of physical systems displaying critical phenomena—especially monoatomic fluids, simple ferromagnets and anti-ferromagnets and binary alloys. I will not discuss superconductivity or superfluidity which at the present time seem to stand apart, owing to their essentially quantum mechanical origin; although one may hope that eventually a theory will be developed which will also encompass them naturally.

Nor will I consider ferroelectricity in which the long-range nature of the Coulomb forces appears to play a dominant role.

In the next few sections the salient features of the systems of interest will be reviewed briefly and I will point out some striking experimental results that challenge our theoretical imagination!

2. Critical Point of a Fluid

If a gas is compressed at a temperature below its critical temperature T_C it reaches a certain density ρ_G and then condenses at constant pressure to a liquid of greater density ρ_L . As T is increased towards T_C the discontinuity ($\rho_L - \rho_G$) becomes smaller and disappears altogether at the critical point where $T = T_C$, $\rho_L = \rho_G = \rho_C$ and $p = p_C$. These familiar facts are illustrated in the typical (p, v) isotherms ($v = 1/\rho$) sketched in Figure 2.1.

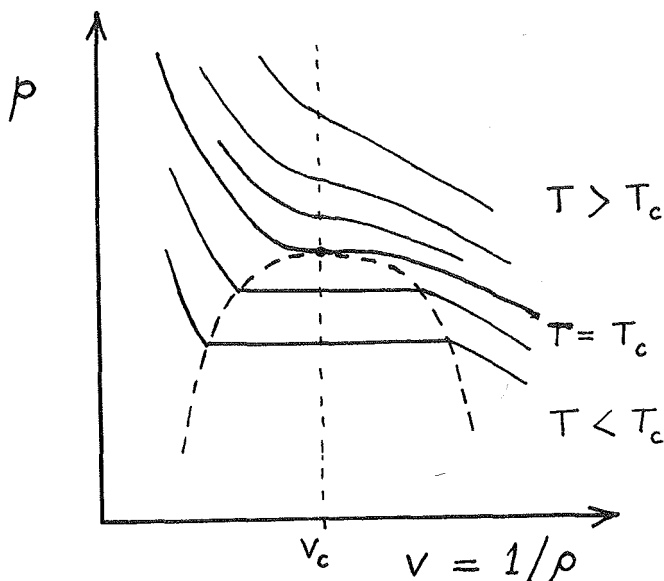


Figure 2.1. Typical isotherms for a simple fluid.

By compressing a gas at a temperature above T_C , one can, experimentally, pass from the gaseous to the liquid state without any discontinuity and, as far as can be told, without an "anomaly" in any of the derivatives of the free energy. This topological fact is illustrated in Figure 2.2 which shows the phase diagram for a simple system with one solid phase. The critical point is, of course, located at the end of the vapour pressure curve. Whether, despite the experimental results, there is some subtle kind of higher order singularity which persists above the critical point on a continuation of the vapour pressure curve, is a difficult theoretical question. The answer is generally believed to be "No" and we shall accept this in these lectures. Recently, however, I have constructed some soluble (although necessarily somewhat artificial) models for which such a

distinction between liquid and gas does remain above the critical point!

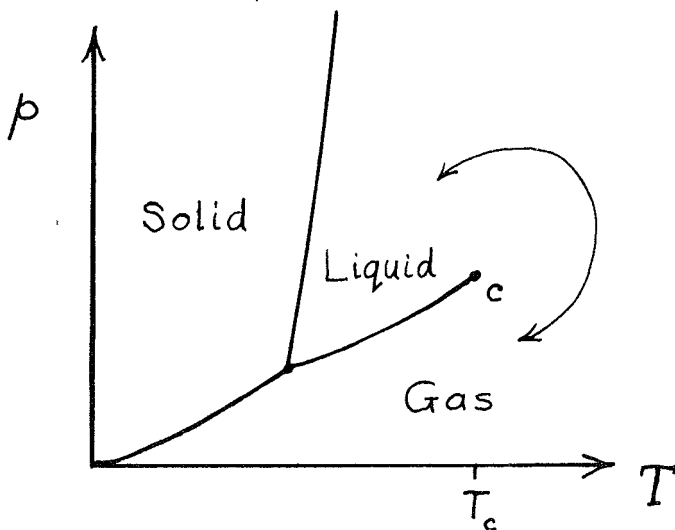


Figure 2.2. Phase diagram for a simple fluid.

Be that as it may, one does, in passing over the critical point, observe a well defined maximum in the isothermal compressibility.

$$K_T = -\frac{1}{V} \left(\frac{\partial V}{\partial p} \right)_T = \frac{1}{\rho} \left(\frac{\partial \rho}{\partial p} \right)_T, \quad (2.1)$$

which occurs close to the critical density ρ_c . If we lower the temperature at constant density $\rho = \rho_c$ the compressibility increases rapidly (corresponding to the flattening of the isotherms in Figure 2.1) and the critical point may be characterized by

$$K_T(\rho = \rho_c, T) \rightarrow \infty, \quad (T \rightarrow T_c +). \quad (2.2)$$

This fact, and other properties of K_T , make it a quantity of central theoretical interest.

As observed, we may also characterize the critical point by the "closure" of the coexistence curve, i.e., by

$$(\rho_L - \rho_G) \rightarrow 0 \quad (T \rightarrow T_c -). \quad (2.3)$$

Figure 2.3 (taken from a paper of Guggenheim in 1945) shows experimental data on the coexistence curve for the simple gases Ne, Ar, Kr, Xe, N₂, etc. (These are ideal "physicists' gases"!) We observe

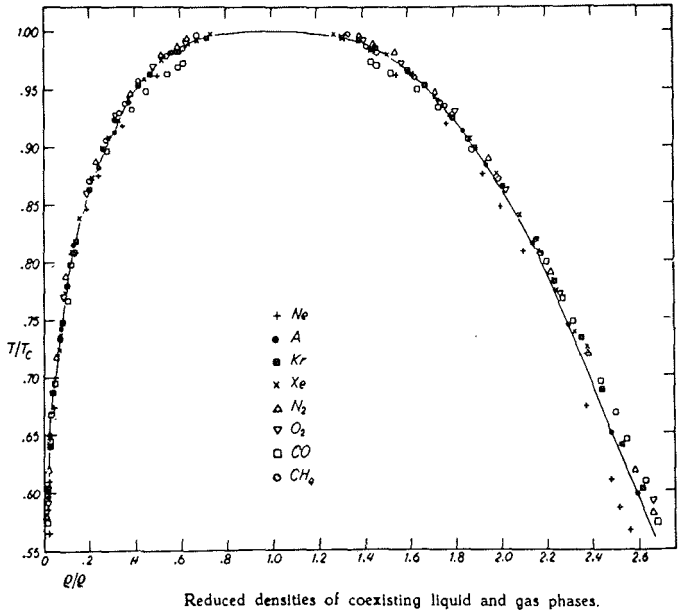


Figure 2.3. Coexistence curve for neon, argon, krypton, etc. [from E. A. Guggenheim, *J. Chem. Phys.* 13, 253(1945)].

first that they follow, to a good approximation, a law of corresponding states which means essentially that there is a unique behaviour for the theorist to calculate. Of more crucial interest to us, however, is the shape of the solid curve drawn through the data which gives a very good fit near T_C (to within ± 0.5 per cent in $\Delta\rho/\rho_C$ and $\Delta T/T_C$ from $T/T_C \cong 0.6$ to within $\frac{1}{2}$ per cent of T_C). Guggenheim looked for a simple power law and discovered

$$(\rho_L - \rho_G) \cong A(T_C - T)^{\frac{1}{3}}, \quad (2.4)$$

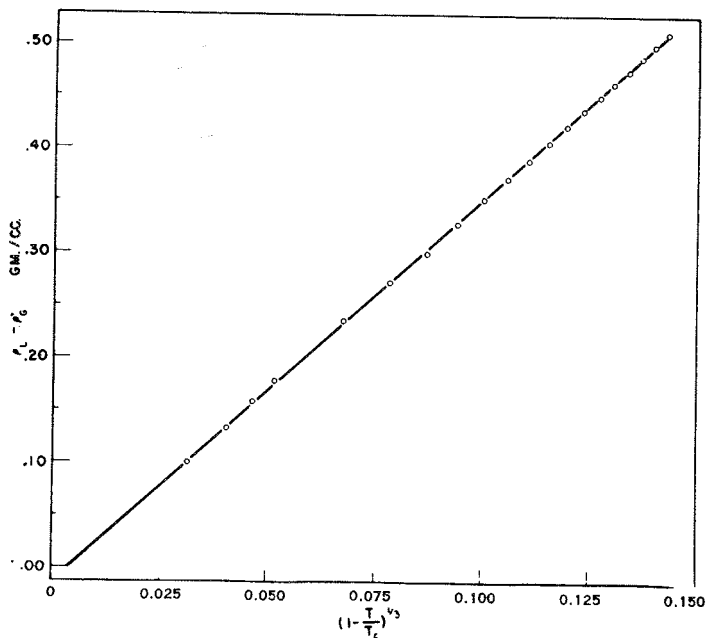
i. e., a one-third power law! (One should also note the law of

rectilinear diameter which is quite well obeyed by most gases, namely,

$$\frac{1}{2}(\rho_L + \rho_G) = \rho_C[1 + a(T_C - T)/T_C] \quad (2.5)$$

where a usually has a value close to 2.5.)

Actually Michels, Blaisse and Michels in 1937 had noted that for CO_2 the index $\beta=0.357$ in (2.4) gave a very good fit to their data. A more recent and very careful test of the one third law (by Weinberger and Schneider) is illustrated in Figure 2.4. The density discontinuity ($\rho_L - \rho_G$) for xenon is plotted versus $[1 - (T/T_C)]^{1/3}$ and a very good straight line is observed. It should be noted that the data go up to temperatures differing from T_C by only one part in 30,000, the temperature being controlled to within $\pm 0.001^\circ\text{C}$!



Plot of $\rho_L - \rho_G$ vs. $(1 - T/T_C)^{1/3}$.

Figure 2.4. Coexistence curve for xenon close to T_C [from M. A. Weinberger and W. G. Schneider, *Can. J. Chem.* 30, 422(1952)].

A small peculiarity in Figure 2.4 is that the straight line, through the data points, does not intercept the origin ($\rho_L = \rho_G = \rho_C$ when $T = T_C$) as it should.* This may be understood by postulating, more generally,

$$(\rho_L - \rho_G) = A(T_C - T)^\beta \quad (T \rightarrow T_C -) \quad (2.6)$$

and asking the data what value of the exponent β they prefer—rather than forcing $\beta = \frac{1}{3}$ on them! One discovers that

$$\beta = 0.345 \pm 0.015 \quad (2.7)$$

best expresses the experimental measurements. This value is a little larger, but is not inconsistent with $\frac{1}{3}$.

Finally we must note that the critical point is associated with a striking thermal anomaly. It has been known for some time that the specific heat C_V exhibits a maximum above T_C near $\rho = \rho_C$ and that this maximum increases as the critical point is approached. It has only been revealed recently, however, by Russian measurements on argon (and on oxygen) how sharp the peak really is—see Figure 2.5 where the configurational specific heat at constant critical volume is plotted versus T from the triple point to above the critical point. Experimentally we may conclude

$$C_V(T) \rightarrow \infty \quad (T \rightarrow T_C \pm, \rho = \rho_C) \quad (2.8)$$

where the "infinity" seems to be limited by the considerable difficulties of measurement but in any case exceeds the usual kinetic specific heat $(3/2)k$, by a factor of eleven or twelve.

Of course, the way in which $C_V(T)$ and $K_T(T)$ diverge to infinity will be of prime interest to us but we will review the experimental data on these points when we have discussed some of the theories.

*We might remark, parenthetically, that some ten to fifteen years ago the question was raised, notably by O. K. Rice (see, for example, J. Phys. (Colloid) Chem. 54, 1293(1950)), as to whether the coexistence curve might have a "flat top." Although this has not been ruled out theoretically, more recent and accurate experiments establish that the coexistence curves for simple systems do not have a significant flat top.

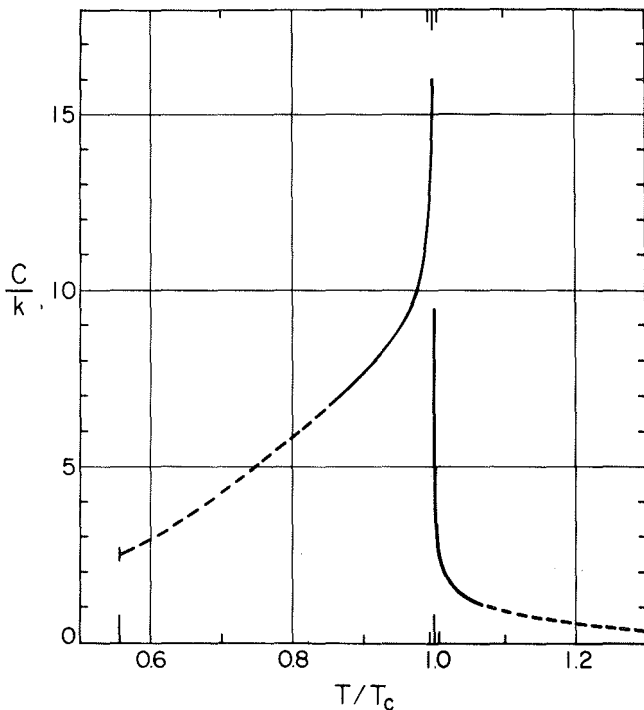


Figure 2.5. Constant volume configurational specific heat for argon at critical density [from M. E. Fisher (to be published) after measurements by M. I. Bagatskii, A. V. Voronel' and B. G. Gusak, Soviet Phys. JETP 16, 517(1963)].

3. Curie Point of a Ferromagnet

A ferromagnet is characterized by a spontaneous or residual magnetization which remains even when a magnetizing field H is reduced to zero. Physically, of course, the phenomenon arises because the forces between the electronic spins are such as favour parallel alignment. Formally we may define the spontaneous magnetization as

$$M_0(T) = \lim_{H \rightarrow 0^+} M(T, H) \quad (3.1)$$

where $M(T, H)$ is the equilibrium magnetization in a field H . *

*We must remember that the magnetization process in real magnets is rather complicated and hysteresis and other nonequilibrium phenomena may be difficult to avoid experimentally, especially at

As the temperature is increased, the spontaneous magnetization decreases and finally vanishes sharply at the Curie point T_C (see Figure 3.1), i.e.,

$$M_0(T) \rightarrow 0 \quad (T \rightarrow T_C^-). \quad (3.2)$$

Above T_C the magnetization in zero field is identically zero. However, the initial susceptibility

$$\chi_0(T) = \left(\frac{\partial M}{\partial H} \right)_{T, H=0} \quad (3.3)$$

is positive and as $T \rightarrow T_C$, $\chi_0(T)$ diverges to infinity, signalling, as it were, the onset of spontaneous magnetization (see Figure 3.1).

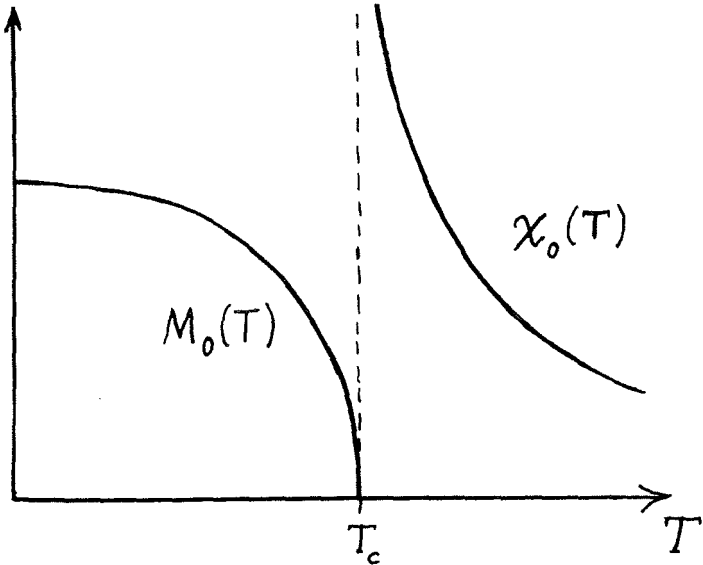


Figure 3.1. Spontaneous magnetization and initial susceptibility of a ferromagnet near its Curie point.

low-temperatures. The problem may be reduced by working with single-crystal single-domain specimens. A further point concerns the magnetic field H : we will always mean the "true" or "internal field" but owing to the demagnetizing effects, which find their origin in the long-range dipolar nature of magnetic forces, this will differ from the "external field" observed by the experimentalist. Corrections, dependent on the shape of the specimen, must be made to obtain H and this becomes especially significant for ferromagnets with low Curie temperatures.

If the specific heat in zero field is measured, an anomaly is observed at T_C , although in the case of iron and nickel—the classical ferromagnets—this is superimposed on a relatively large lattice specific heat of Debye type (see Figure 3.2). However, the more

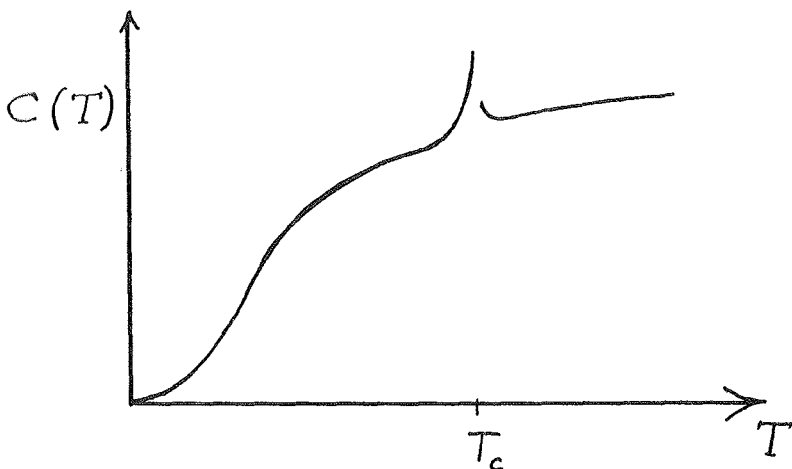


Figure 3.2. Sketch of the specific heat of nickel in zero field.

recently discovered ferromagnets Gd, EuO, EuS, etc. have critical points in the low-temperature region and the magnetic specific heats may be studied without interference from lattice contributions. Such experiments are in progress.

If we change the sign of the field H in (3.1) the sign of $M_0(T)$ changes. Consequently the (ideal) magnetization curve below T_C has a discontinuity $2M_0$ as a function of field (see Figure 3.3). If we make a correspondence between changes in magnetization and changes in density of a fluid and similarly between the magnetic field and the pressure, we see that there is an analogy between a magnetic isotherm below T_C and a p, ρ isotherm of a fluid below its critical point: rotate Figure 3.3 anticlockwise through a right angle and compare with Figure 2.1. Similarly if we complete the spontaneous magnetization curve by reflecting it in the $M=0$ axis in Figure 3.1 and rotate the resulting figure anticlockwise through a right angle, we see a close analogy with gas-liquid coexistence curve, Figure 2.3!

It is evident that the magnetic susceptibility $\chi(T)$ will similarly be analogous to the fluid compressibility K_T . In particular, both diverge as $T \rightarrow T_C$.

The analogy continues if we look at the phase diagram or (H, T) plane of a ferromagnet (see Figure 3.4). The Curie point, like

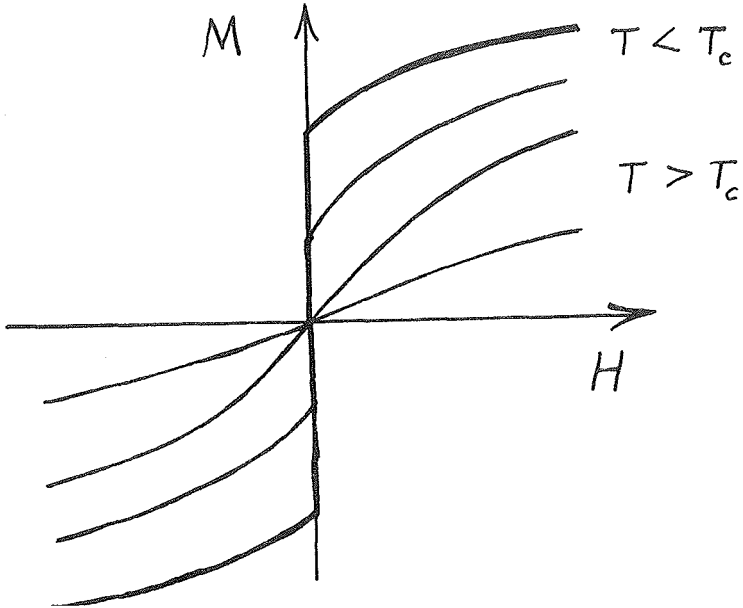


Figure 3.3. Ideal magnetization curve of a ferromagnet.

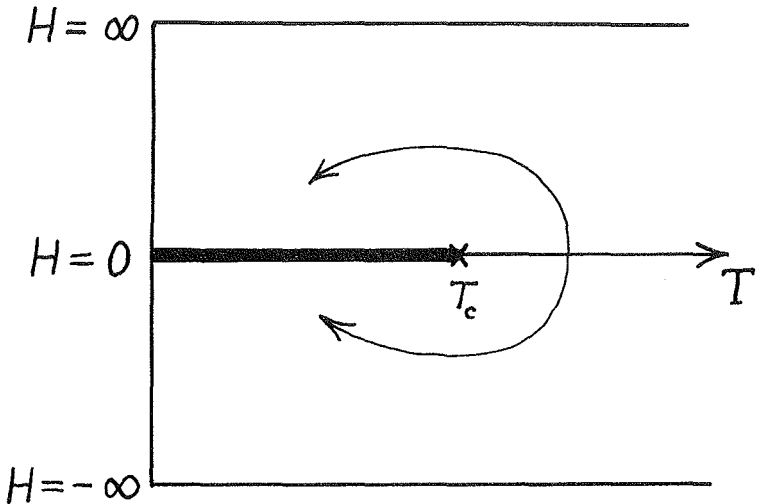


Figure 3.4. Phase diagram for a ferromagnet.

the critical point, appears at the end of a line of discontinuity. (There is no phase transition in a nonzero field.) By passing around the Curie point (or critical point as we shall usually call it) we see that the two opposite magnetic "phases" can be transformed continuously into one another as can liquid and gas.

We will show theoretically that this analogy, between what are at first sight very different physical systems, is not merely superficial, but can be made quite precise. A strong hint of its significance is given by the way in which $M_0(T)$ vanishes as $T \rightarrow T_C$. Magnetic resonance experiments by Heller and Benedek (as yet unpublished*); but see also Section 5) on the insulating ferromagnet EuS indicate that

$$M_0(T) = A(T_C - T)^\beta, \quad (T \rightarrow T_C^-) \quad (3.4)$$

where the index $\beta = 0.33 \pm 0.01$! In other words a one third law seems also to apply to ferromagnets!

4. Binary Solutions

If in a binary fluid mixture of two components A and B, the A molecules preferentially attract A molecules while the B molecules preferentially attract B molecules, the system may undergo phase separation into an A-rich phase and a B-rich phase. At constant overall pressure the conditions of equilibrium depend on the temperature and the solution composition as expressed in terms of the mole fractions x_A and x_B ($x_A + x_B = 1$). Coexistence curves of the usual appearance for gases are observed (see Figure 4.1) with a critical temperature above which only one homogeneous phase occurs.

A typical system studied is perfluoromethylcyclohexane in carbon tetrachloride (such systems have convenient critical temperatures and compositions). This has been the subject of very accurate experiments by O. K. Rice and coworkers whose most recent results confirm that the coexistence curve obeys the law

$$[x_1 - x_2] \cong A|T_C - T|^\beta, \quad (T \rightarrow T_C) \quad (4.1)$$

with β close to 0.33! Indeed this one third power law is known to hold to good approximation for many different binary solutions. (See the book by J. S. Rowlinson, "Liquids and Liquid Mixtures," Butterworths, London, 1959.)

The analogy with the single component fluid is clear: we merely forget about one of the components, say B, and regard the

*The experimental results have now been published in Phys. Rev. Letters 14, 71 (1965).

space it occupies as "vacuum." Then x_A corresponds to ρ and the partial pressure to p .

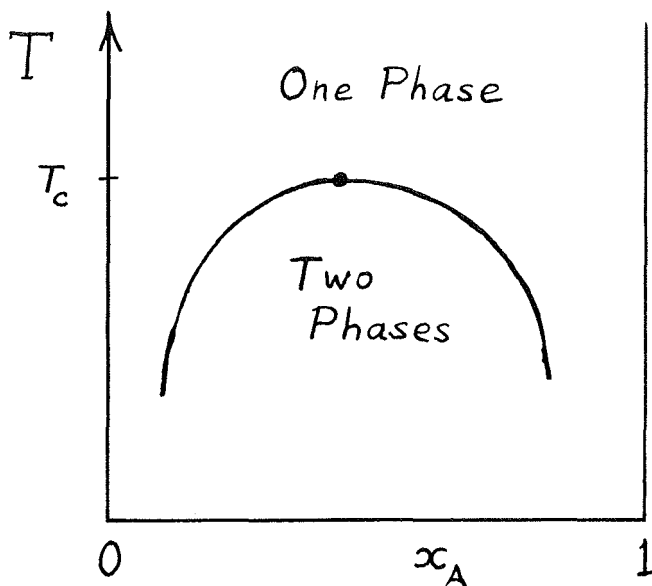


Figure 4.1. Coexistence curve for a binary fluid mixture.

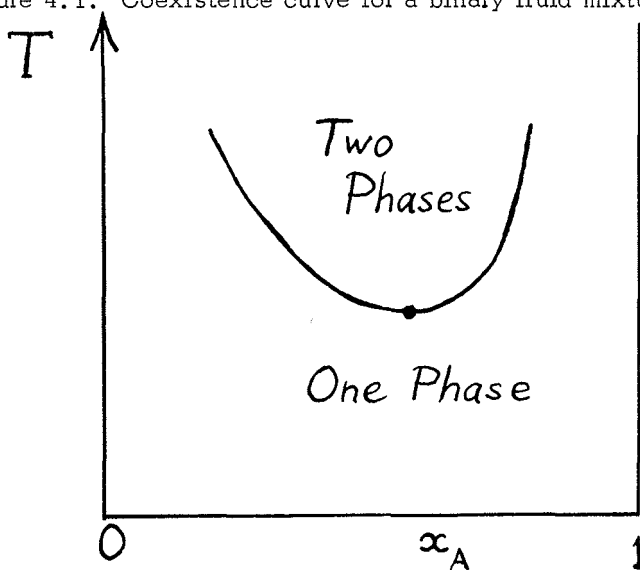


Figure 4.2. Coexistence curve illustrating a lower critical point in a binary solution.

It is interesting to note that certain binary mixtures exhibit a lower critical point below which the system remains in one phase and above which phase separation occurs (see Figure 4.2 on preceding page). Experiment shows that even in the vicinity of these lower critical points the one third law (4.3) is followed quite closely!

5. Antiferromagnetism

The physical systems discussed above might be characterized as "like-attracts-like": molecules of type A attract molecules of type A rather than of type B in binary solutions; "up" spins attract "up" spins and repel "down" spins in ferromagnets; molecules of a fluid attract one another and coalesce in condensation. Other systems might be characterized as "like-repels-like" or "unlikes attract." The most prominent examples of this are antiferromagnets in which neighboring spins tend to align antiparallel, and homogeneous binary alloys which tend to crystallize with a regular alternation of A and B ions.

Historically, antiferromagnets were detected by a susceptibility versus temperature curve falling below the free, uncoupled, curve and exhibiting a more-or-less sharp maximum (see Figure 5.1). At a temperature near this susceptibility maximum a sharp anomaly in the specific heat is observed. Friedberg's measurements on $\text{NiCl}_2 \cdot 6\text{H}_2\text{O}$

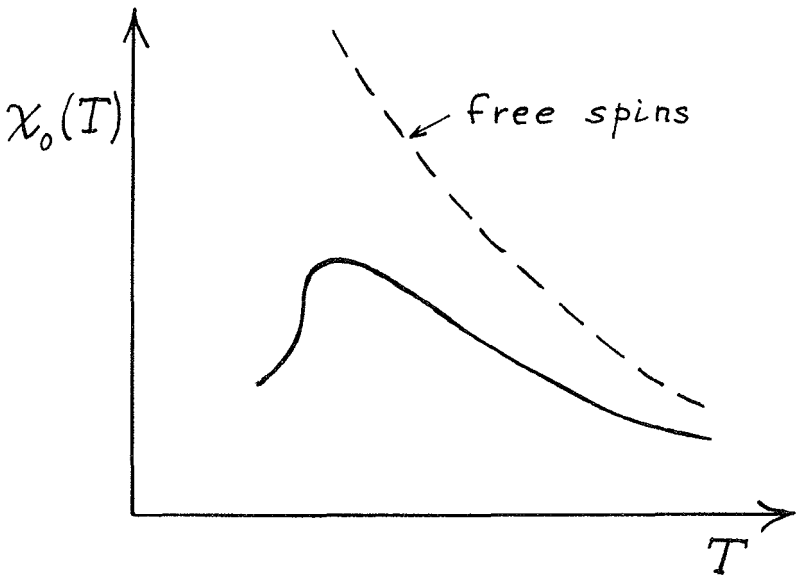


Figure 5.1. Sketch of the susceptibility of a typical antiferromagnet. The dashed line indicates the free spin susceptibility.

shown in Figure 5.2 illustrate the typical lambda shape of the magnetic specific heat (superimposed here on a relatively small lattice contribution). The occurrence of a sharp specific heat peak at a temperature T_C (often called the Neél temperature) suggests that some sort of ordering process sets in below that point. This is confirmed very directly by neutron scattering experiments which show that above T_C the spin directions are disordered (becoming completely random as $T \rightarrow \infty$ although exhibiting some short-range order near T_C), while below T_C a long-range alternating order occurs. Thus, the antiferromagnet MnF_2 has a body centered cubic lattice (of magnetic ions) and below T_C spins on alternate lattice sites point "up" and "down" (with respect to the "easy axis").

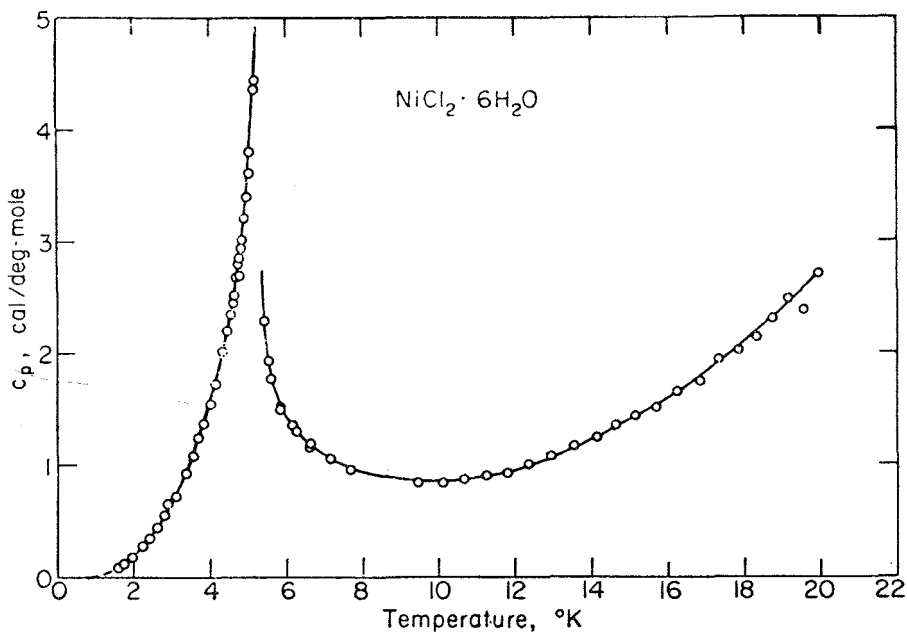


Figure 5.2. Specific heat of the antiferromagnet $\text{NiCl}_2 \cdot 6\text{H}_2\text{O}$ [from W. K. Robinson and S. A. Friedberg, *Phys. Rev.* **117**, 402(1960)].

The long-range order may be measured by the intensity of the "super-lattice" line in the neutron scattering which appears below T_C . Its position corresponds to a periodicity appropriate to the larger magnetic unit cell implied by the alternating order. The square root of this intensity is proportional to what is usually termed the

"sublattice magnetization," $M_0'(T)$. This is rather analogous to the spontaneous magnetization of a ferromagnet, except in that it cannot be observed magnetically, since it is always cancelled by an equal but opposite "magnetization" on the second sublattice. As the temperature rises towards the critical point, $M_0'(T)$ falls sharply and vanishes at T_C .

The most accurate measurements of the sublattice magnetization have been performed by Heller and Benedek who observed the nuclear magnetic resonance of the fluorine nuclei in MnF_2 . The average field at a fluorine nucleus is proportional to the sublattice magnetization of one set of manganese ions, consequently M_0' is in turn proportional to the measured resonance frequency (in zero external field). Heller and Benedek found that

$$M_0'(T) = A(T_C - T)^\beta \quad (T \rightarrow T_C^-) \quad (5.1)$$

with

$$\beta = 0.335 \pm 0.005. \quad (5.2)$$

This "one third law" held with remarkable accuracy up to within millidegrees of the critical point ($\Delta T/T_C = 0.007\%$) as can be seen from Figure 5.3 where the cube of the resonance frequency ($\sim M_0'^3$) is plotted versus T . The result of Equation (5.2) really does suggest that β is exactly one third!

The analogy between an antiferromagnet and a ferromagnet in zero field (which corresponds essentially to calling "up spins" "down spins" on alternate lattice sites) no longer holds in a magnetic field. Antiferromagnetic ordering is not destroyed by a field although the critical temperature drops as H increases. This topological distinction can be seen from a typical antiferromagnetic phase diagram shown in Figure 5.4. It is not possible to pass from the ordered to the disordered region without undergoing some detectable phase changes (notably a specific heat anomaly). We will not, however, discuss the additional phase that appears at lower temperatures in some antiferromagnets nor the many interesting but complicated spiral and layer spin orderings that have been discovered in ferrimagnets, metamagnets and related magnetic systems.

6. Homogeneous Binary Alloys

Many binary alloys undergo an order-disorder phase change associated with a thermal anomaly. The most famous and historically

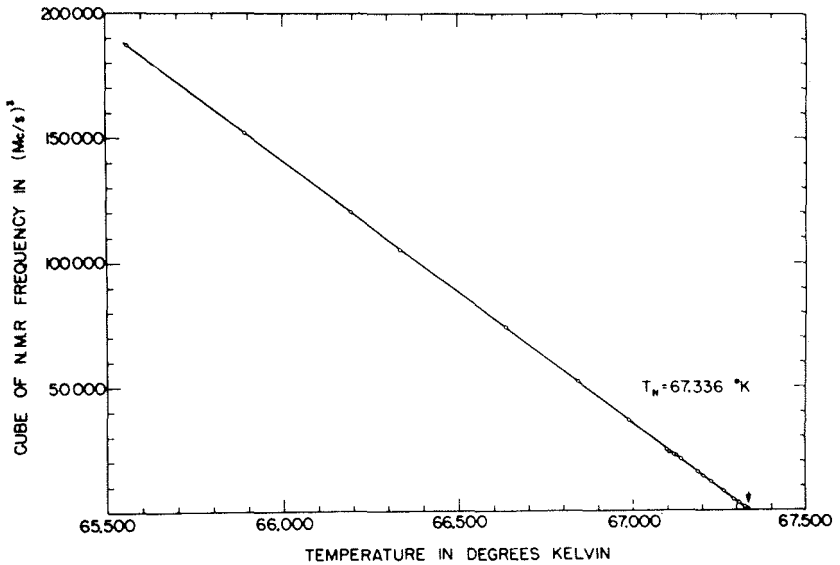


Figure 5.3. Cube of the sublattice magnetization of MnF_2 , as measured by the NMR frequency, versus temperature [from P. Heller and G. B. Benedek, *Phys. Rev. Letters* 8, 428 (1962)].

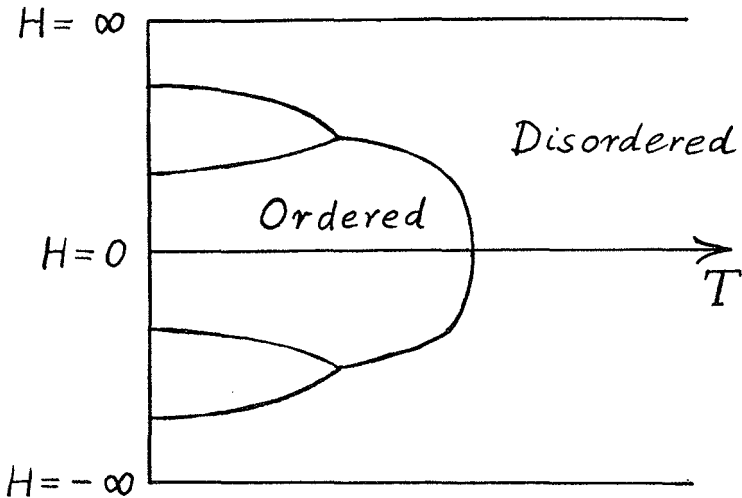


Figure 5.4. Phase diagram for a typical antiferromagnet.

important example is β -brass, which is approximately 50 per cent CuZn. The specific heat displays a large and sharp lambda anomaly, the peak of which locates the ordering temperature T_C . Other examples are FeCo, FeNi, Cu₃Au, and Ni₃Mn. X-ray and neutron scattering experiments verify the appearance of superlattice reflections below T_C indicating the presence of long range alternating order with A ions preferentially on one sublattice and B ions preferentially on the other sublattice. The intensity of the superlattice line (or its square root $R(T)$) again measures the degree of long range order. As $T \rightarrow T_C$ - the order $R(T)$ drops and vanishes at T_C . To my knowledge, however, there are at present no experiments accurate enough to decide if a $(T_C - T)^{\frac{2}{3}}$ law is followed here also.

One does not have, in this case, a direct analogue of the susceptibility of a ferro- or antiferromagnet. However, the diffuse low angle scattering above T_C corresponds essentially to a wavelength dependent (ferromagnetic) susceptibility and becomes large as T_C is approached from above.

The topology of the phase diagram is similar to that of an antiferromagnet in that the ordered phase cannot be reached from the disordered phase without crossing a line of phase change.

Chapter II

After our healthy dose of experimental results, let us turn to theory! The first task, recalling Frenkel's advice, is to construct some simple physical models on which to base our theoretical calculations.

7. Simple Models

Our first model is so familiar that the theorist is apt to forget that it is only a model of real physical systems. This is:

A. The Classical Continuum Gas which normally embodies three assumptions:

- (i) the use of classical mechanics,
- (ii) pairwise forces,
- (iii) central forces.

Actually, the use of classical mechanics seems quite justifiable for most gases near their critical temperatures. Only in the case of hydrogen, helium, and perhaps neon should one have serious reservations.

Quantum mechanical calculations of many-body forces between atoms and molecules show that assumption (ii) is not entirely correct. However, except at high densities the three-body and higher order forces are numerically small and it seems safe to neglect them

near critical densities (ρ_C is usually about a third of ρ_{\max}) in a first discussion.

The assumption (iii) of central forces with a potential $\varphi(r)$ should be a good one for the monotonic gases. Presumably it is less accurate for diatomic and other nonsymmetric molecules but the law of corresponding states evidence indicates that this should not be crucial for critical phenomena.

One knows, of course, that the correct pair potential, $\varphi(r)$, should have a strongly repulsive core followed by a relatively weak attractive well and an attractive tail decaying as $1/r^6$. For theoretical purposes it is often useful, however, to consider a potential of strictly finite range b [$\varphi(r) \equiv 0$ for $r > b$]: one feels that this should not matter too seriously.

By considering $\varphi(r)$ as an "effective potential" between molecules of one species and neglecting the second species, we can also use the model to discuss binary solutions.

B. Heisenberg Model for Magnetism.

This model is based on the principle assumption of

(i) Well-localized spins.

One supposes the spins can be localized to a good approximation on the lattice of magnetic ions so that a spin variable \vec{S}_j may be associated with the j th lattice site. This should be justifiable for insulating crystals but is certainly open to question for good conductors such as iron and nickel. Indeed in the latter case the zero temperature saturation moment indicates that only 0.6 of the usual electronic magnetic moment is available per ion.

Accepting (i) we may write the general Heisenberg Hamiltonian for N ions

$$\mathcal{H} = - \sum_{i=1}^N \sum_{j=1}^N J_{ij} \vec{S}_i \cdot \vec{S}_j - g\beta_B \sum_{i=1}^N \vec{S}_i \cdot \vec{H} \quad (7.1)$$

where \vec{H} is the magnetic field $g\beta_B$ is essentially the magnetic moment per spin, and

$$J_{ij} = J(\vec{r}_{ij}) \quad (7.2)$$

is the "exchange energy" between spins i and j . (Note that J is positive for ferromagnetic coupling and negative for antiferromagnetic coupling.)

The Hamiltonian (7.2) embodies the further assumptions of

(ii) Pairwise interactions, which again seems reasonable in a first approach.

(iii) Complete isotropy; that is, \mathcal{H} is invariant under rotation

of the total spin. All real magnetic materials show some anisotropy. Although this is frequently quite small numerically it can play an important role, especially in antiferromagnets, by "stabilizing" the direction of magnetization. It may be taken into account by adding to \mathcal{H} terms of the form $\sum_i (S_i^z)^2$, for example, by modifying

$$J_{ij} \vec{S}_i \cdot \vec{S}_j \quad \text{to} \quad \sum_{\alpha, \beta} J_{ij}^{\alpha\beta} S_i^\alpha S_j^\beta$$

where $\alpha, \beta = x, y, z$, or by adding dipolar forces of the form

$$\left[\vec{S}_i \cdot \vec{S}_j - 3(\vec{S}_i \cdot \vec{r}_{ij})(\vec{S}_j \cdot \vec{r}_{ij}) \right] / r_{ij}^3.$$

However, in many cases we may hope to avoid these refinements and indeed simplify (7.1) still further by restricting the interactions to nearest neighbour pairs described by a single exchange constant J . Although there is ample evidence to show that second and further neighbour interactions are not in general negligible they should not matter crucially if they do not oppose the ordering tendencies of the dominant first neighbour interactions. Conversely, when this is not true one sees the more complicated magnetic behaviour which we have elected not to discuss.

Our last "fairly realistic" simple model is for:

C. Binary Alloys.

One assumes:

- (i) A fixed lattice, each site of which is occupied by an A or a B atom.
- (ii) That only fixed nearest neighbour interaction energies ϵ_{AA} , $\epsilon_{AB} = \epsilon_{BA}$ and ϵ_{BB} enter (although one may consider more distant interactions).

Assumptions (i) and (ii) imply the neglect of any interactions with the lattice vibrations. This cannot be very accurate since if the masses m_A and m_B are distinct even the zero point lattice energy will depend on the degree of order. However, if the ϵ do not vary too rapidly with lattice spacing and the masses are not too different, lattice vibrations probably lead only to a "renormalization" of the interaction energies (and presumably to an increase in the range of the effective direct interactions). The assumptions also neglect effects due to different atomic sizes of A and B ions which might well be important if these differ appreciably. Nevertheless, one feels that the model ought to yield a fairly reliable description of the ordering phenomenon.

B. Simpler Models

Of the three models discussed, the classical continuum gas model is probably the most realistic. Unfortunately, however, it is so difficult to discuss mathematically except at low densities that essentially no progress has been possible in calculating critical behaviour reliably. Accordingly, we will simplify and schematize still further by introducing the:

A'. Lattice Gas.

In the most general form of the model one introduces a regular space lattice of spacing δ and requires that the molecules be restricted to the lattice site and that no site be occupied by more than one molecule. Essentially, this merely replaces the configurational integrals in the partition function by approximating Riemann sums. Consequently, if the lattice spacing δ is small compared with the distances over which the pair potential varies appreciably, any errors should be negligible except perhaps at densities near close-packing. Indeed, one can verify by explicit calculation for various one-dimensional systems that in the limit $\delta \rightarrow 0$ (holding $\varphi(r)$ constant) the lattice gas results agree exactly with the continuum model results for $\rho > \rho_{\max}$.

Unfortunately in practice if δ is small, the mathematical difficulties are still severe. One is thus forced, at least in the first instance, * to consider the extreme case where the hard core of the potential is represented merely by the restriction forbidding double occupancy of lattice sites while the attractive part is represented by a nearest neighbour energy, i. e. ,

$$\begin{aligned}\varphi(\vec{0}) &= \infty \\ \varphi(\vec{\delta}) &= -|\varphi_0| \\ \varphi(\vec{r}) &= 0, \quad |\vec{r}| > \delta.\end{aligned}\tag{8.1}$$

Some artificial features of such a model can easily be seen. The high density behavior cannot be correct and one should clearly not expect close numerical agreement in comparison with real gases.

However, the model, which as we will indicate is now mathematically equivalent to the binary alloy model C (except for the sign of $\varphi(\vec{\delta})$) still contains the "seeds of reality" and it transpires that it yields a surprisingly accurate account of the critical point phenomena.

Finally, let us simplify the Heisenberg model. Although in many ways this is not as intractable as the continuum gas model (thus

*Recently some progress has been made for hard cores extending to first neighbour sites.

the low temperature properties may be described accurately, even though only asymptotically, in terms of spin waves and progress can also be made at high temperatures), the noncommutation of the operators makes extensive calculation difficult. Accordingly, let us introduce the

B'. Ising Model of Magnetism—by replacing the isotropic Heisenberg coupling $\vec{S}_i \cdot \vec{S}_j$ by the anisotropic Ising coupling $S_i^z \cdot S_j^z$.

If the field \vec{H} is parallel to the z-axis, the Ising Hamiltonian may be diagonalized trivially and the operators S_i^z may be replaced by "semiclassical" variables taking the $2S+1$ values

$$S, S-1, \dots, -(S-1), -S.$$

In the simplest and most commonly considered case, $S = \frac{1}{2}$ and $S_i^z = \pm \frac{1}{2}$ corresponding just to "up" and "down" spins. In practice we will usually also suppose that the interactions are restricted to nearest neighbours. However, one should remember that longer range interactions can be discussed (and some progress has been made). Furthermore, if the field is not parallel to the z-axis the noncommutative properties of the S_i^α will come into play. Indeed, it has proved possible to calculate the perpendicular susceptibility of the Ising model exactly in two dimensions!

One of the most artificial aspects of the Ising interaction is its extreme anisotropy which results, in particular, in an essentially complete absence of spin wave behaviour at low temperatures. However, our interests will be at higher temperatures close to the critical point where this deficiency can be expected to be less significant (and where the concept of a spin wave loses its validity). On the other hand, some extremely anisotropic magnetic crystals have been discovered (notably the antiferromagnet dysprosium aluminium garnet*), and these should be well approximated by Ising models even at lower temperatures!

9. Basic Statistical Mechanical Formulas

Having accepted a model of a physical system we must calculate its thermodynamic properties with the aid of statistical mechanics. To establish our notation let us put down the basic formulas with which we will work.

For a classical system of N identical particles of mass m with coordinates $\vec{r}_1 \dots \vec{r}_N$ confined in some domain Ω of volume

*Studied by W. P. Wolf and coworkers: M. Ball, M. J. M. Leask, W. P. Wolf and A. F. G. Wyatt, *J. Appl. Phys.*, **34**, 1104(1963); M. Ball, M. T. Hutchings, M. J. M. Leask and W. P. Wolf, *Proc. 8th Int. Congr. on Low Temperature Physics* (in press).

$V = V(\Omega)$ the canonical configurational partition function is

$$Q(N, \Omega) = \frac{1}{N!} \int_{\Omega} d\vec{r}_1 \dots \int d\vec{r}_N \exp(-\beta U_N) \quad (9.1)$$

where $\beta = 1/kT$ and $U_N = U_N(\vec{r}_1 \dots \vec{r}_N)$ is the total potential energy of interaction. The factor $1/N!$ is present since we must only count distinct configurations of the particles. The connection with thermodynamics is provided by

$$-\frac{F}{kT} = \frac{-F_N}{NkT} = \frac{1}{N} \ln Q(N, \Omega) - 3 \ln \Lambda \quad (9.2)$$

where the Helmholtz free energy per particle F , is regarded as a function of T (or β) and the specific volume,

$$v = 1/\rho = V/N \quad (9.3)$$

and where

$$\Lambda^2 = h^2/2\pi mkT \quad (9.4)$$

h being Planck's constant. The equation of state is given by

$$p = -\left(\frac{\partial F_N}{\partial V}\right)_T = -\left(\frac{\partial F}{\partial v}\right)_\beta = p(\beta, v). \quad (9.5)$$

In practice it is often more convenient to work with the grand canonical partition function

$$\Xi(z, \Omega) = \sum_{N=0}^{\infty} z^N Q(N, \Omega) \quad (9.6)$$

where the activity z is related to the chemical potential μ (or Gibbs free energy per particle) by

$$z = e^{\beta\mu}/\Lambda^3. \quad (9.7)$$

The corresponding grand canonical pressure and density follow from

$$\frac{p}{kT} = \pi(\beta, z) = [1/V(\Omega)] \ln \Xi(z, \Omega) \quad (9.8)$$

$$\rho = z \left(\frac{\partial \pi}{\partial z}\right)_\beta = \left(\frac{\partial p}{\partial \mu}\right)_\beta. \quad (9.9)$$

For a quantum mechanical system, such as a ferromagnet, one must define the partition function by

$$Z(\Omega) = \text{Tr}_{\Omega} \{ \exp(-\beta \mathcal{H}_{\Omega}) \} \quad (9.10)$$

where \mathcal{H}_{Ω} is the Hamiltonian for the domain Ω , and the trace is taken with a set of orthogonal normalized states complete in Ω and of appropriate symmetry. The free energy density $f(\beta)$ is then given by

$$-\frac{f}{kT} = -\frac{F_{\Omega}}{kTV(\Omega)} = [1/V(\Omega)] \ln Z(\Omega). \quad (9.11)$$

For a magnet, f will normally be expressed as a free energy per spin (but it should be noted that this is still a free energy density while F defined in (9.2) is not a density). The magnetization density is obtained from

$$M = -\left(\frac{\partial f}{\partial H}\right)_{\beta}. \quad (9.12)$$

10. Equivalence of Ising Magnet and Lattice Gas

We may now formulate explicitly the partition function for the Ising model. For the present we will consider only the case $S = \frac{1}{2}$ with the field H parallel to the z -axis. On diagonalizing the Hamiltonian in a basis of up and down spins at each site, the trace operation becomes simply a sum over $S_i^z = \pm \frac{1}{2}$ for all $i = 1, 2, \dots, \mathfrak{n}$. (We use a script symbol \mathfrak{n} here for the number of spins, or lattice sites, so as to avoid confusion with N , the number of atoms in a lattice gas. In later sections, when there is no risk of confusion, we will use the more conventional N for the number of spins and lattice sites.) It is convenient to introduce the scalar variables

$$s_i = 2S_i^z = \pm 1, \quad (10.3)$$

which in the literature have been variously denoted σ_i^z , σ_i , or μ_i . If we write for the magnetic moment per spin

$$m = \frac{1}{2} g \beta_B \quad (10.4)$$

the Hamiltonian becomes

$$\mathcal{H} = - \sum_{(ij)} \left(\frac{1}{2} J_{ij}\right) s_i s_j - mH \sum_{i=1}^{\mathfrak{n}} s_i \quad (10.5)$$

where the first summation is over all pairs (i, j) of distinct spins.

One should be warned that in the literature on the Ising model an alternative convention is common in which the symbol J_{ij} replaces $\frac{1}{2}J_{ij}$ as we have defined it here and in (7.1). Introducing the temperature and field variables

$$K_{ij} = J_{ij}/2kT, \quad L = mH/kT, \quad (10.6)$$

the partition function is

$$Z(T, H, N) = \sum_{s_i = \pm 1} \exp \left[\sum_{(ij)} K_{ij} s_i s_j + L \sum_{i=1}^N s_i \right]. \quad (10.7)$$

It is useful to notice that when the interactions are restricted to the q nearest neighbour spins of a given spin (so that one has only the single exchange parameter $J_{ij} = J$) the partition function is merely a polynomial in the temperature and field variables

$$x = e^{-2K}, \quad \text{and} \quad y = e^{-2L}, \quad (10.8)$$

except for a leading factor

$$\exp [N(\frac{1}{2}qK + L)] \quad (10.9)$$

corresponding to the configuration with all spins up. (Notice that if q is the coordination number of the lattice, the number of bonds is $\frac{1}{2}qN$, ignoring boundary corrections.)

To formulate the lattice gas model we suppose the lattice has N sites ("cells") and that a lattice cell has volume v_0 . Since each site is either occupied by one atom or is vacant we may introduce the occupation variables

$$\begin{aligned} t_i &= 1 && \text{if the } i\text{th site is occupied} \\ &= 0 && \text{if the } i\text{th site is vacant.} \end{aligned} \quad (10.10)$$

Evidently the total number of atoms in a given configuration specified by a set $\{t_i\}$ is

$$N = \sum_{i=1}^N t_i. \quad (10.11)$$

The grand partition function may thus be written

$$\Xi(\beta, z, n, v_0) = \sum_{N=0}^{\infty} z^N \sum_{N\{t_i\}} \exp \left[-\beta \sum_{(ij)} \varphi(\vec{r}_{ij}) t_i t_j \right] \quad (10.12)$$

where \vec{r}_{ij} is the distance vector for the i th and j th sites and the symbol $N\{t_i\}$ on the second sum denotes that we sum over values of $t_i = 0$ or 1 subject to the condition (10.11), i.e., over all distinct configurations of N atoms. However, if we substitute for N in (10.12) with (10.11), we may replace the two summations by a single unrestricted summation over all $t_i = 0$ or 1 , so that

$$\Xi = \sum_{t_i=0,1} \exp \left[\ln z \sum_{i=1}^n t_i - \sum_{(ij)} \beta \varphi(\vec{r}_{ij}) t_i t_j \right]. \quad (10.13)$$

To see that the calculation of Ξ for the lattice gas is mathematically equivalent to the calculation of Z for the magnet consider the identity

$$t_i = \frac{1}{2}(1 - s_i) \quad (10.14)$$

which associates (by common convention) an "up" spin on the i th site of the magnet with the absence of an atom in the gas and a "down" or "overtuned" spin with the presence of an atom. Evidently

$$t_i t_j = \frac{1}{4} - \frac{1}{4} s_i - \frac{1}{4} s_j + \frac{1}{4} s_i s_j \quad (10.15)$$

so that the quadratic in t_i in (10.13) can be reduced to a quadratic in the s_i . Comparison with (10.7) then leads directly to the identifications

$$\varphi(\vec{r}_{ij}) = -2J_{ij} \quad (10.16)$$

and

$$\ln z = -2L - 2\beta E_0 \quad (10.17)$$

or

$$\mu = -2mH - 2E_0 + 3kT \ln \Lambda \quad (10.18)$$

where the essentially uninteresting constant is

$$E_0 = -\frac{1}{4} \sum_{j \neq 0} \varphi(\vec{r}_{0j}) = \frac{1}{2} \sum_{j \neq 0} J_{0j}. \quad (10.20)$$

When each site has just q nearest neighbours interactions,

$$E_0 = \frac{1}{2} qJ, \quad (10.21)$$

and for the activity one gets simply

$$z = yx^q. \quad (10.22)$$

Thus we conclude that the grand canonical partition function of the lattice gas corresponds to the canonical partition function for the Ising ferromagnet and that changes in chemical potential (or activity) correspond to changes in magnetic field. From the standard formulas of the last section we find that the lattice gas pressure is given by

$$pv_0 = -f - mH - \frac{1}{2} E_0 \quad (10.23)$$

while density depends on the magnetization:

$$\rho = \frac{1}{2v_0} \left[1 - \frac{M}{m} \right]. \quad (10.24)$$

Notice that zero density corresponds to positive saturation magnetization while $\rho = \rho_{\max} = 1/v_0$ (close packing) corresponds to negative saturation.

This formula might have been anticipated directly from the definition (10.14) since it is equivalent to

$$\rho = \langle t_1 \rangle = \frac{1}{2} (1 - \langle s_1 \rangle) = \frac{1}{2} (1 - M) \quad (10.25)$$

where the angular brackets denote the thermodynamic average and where for simplicity we have now chosen units in which $m=1$ and $v_0=1$.

In the same units we find for the compressibility

$$4\rho^2 K_T = \chi(T) \quad (10.26)$$

and for the specific heats

$$\rho C_V(T) = C_M(T). \quad (10.27)$$

(In zero field we may identify C_M with C_H .)

The expressions (10.16) to (10.27) spell out formally the analogy between a ferromagnet and a gas which we noticed in studying

the experimental data.* Of course, these relations are only exact for an Ising ferromagnet and a lattice gas. However, in as far as we believe that these models are at all "realistic," we may now draw the theoretical conclusion that we should expect the critical behaviour for gases and ferromagnets to be very similar! In particular, in addition to the correspondence between the spontaneous magnetization and coexistence curves, the divergence of the susceptibility and compressibility, and the specific heat anomalies should match.

In discussing the Ising model theoretically, it is often easier to think in terms of the magnetic analogy because the symmetries of the model are then apparent. We will, however, freely use either interpretation and leave the reader to supply the complementary one.

Finally, let us note that a grand canonical formulation of the binary alloy model C can be obtained by introducing, in addition to the occupancy variables t_i for the A species (say), complementary variables

$$\bar{t}_i = 1 - t_i \quad (10.28)$$

which will take the values 1 or 0 according as a B ion occupies the i th site or not. The total energy of a configuration may now be written

$$E\{t_i\} = \sum_{(ij)} \left[\epsilon_{AA}(\vec{r}_{ij}) t_i t_j + \epsilon_{AB}(\vec{r}_{ij}) (t_i \bar{t}_j + \bar{t}_i t_j) + \epsilon_{BB}(\vec{r}_{ij}) \bar{t}_i \bar{t}_j \right]. \quad (10.29)$$

Clearly this can also be reduced to the Ising model form and one finds the relation

$$J_{ij} = \epsilon_{AB}(\vec{r}_{ij}) - \frac{1}{2} \left[\epsilon_{AA}(\vec{r}_{ij}) + \epsilon_{BB}(\vec{r}_{ij}) \right]. \quad (10.30)$$

If only nearest neighbour interactions enter, the relevant energy parameter is

*One should perhaps draw attention to one detail in which the analogy is a little more complicated than anticipated. Equation (10.18) shows that the magnetic field is to be identified (up to a constant) with the chemical potential whereas we had previously identified changes in field with changes in pressure. The correct formula for the pressure, (10.23), involves the free energy as well as the field. In general, however, the changes in f will be of higher order than the changes in H so then there is no serious loss of accuracy in making the identifications $\Delta H \sim \Delta\mu \sim \Delta p$.

$$\epsilon = \epsilon_{AB} - \frac{1}{2}(\epsilon_{AA} + \epsilon_{BB}).$$

A binary alloy with the same numerical concentration for each species will, by symmetry, correspond to the Ising model in zero field (and hence zero mean magnetization). More generally, the concentration difference corresponds to the magnetization and the field H must be chosen accordingly (at each temperature).

Chapter III

11. General Statistical Questions

Before going ahead in an attempt to calculate explicitly the partition functions for our chosen models, we will pause to consider a few fundamental questions that might be asked when one uses statistical mechanics to discuss phase transitions. Two natural questions are:

- (a) Is statistical mechanics applicable to phase transitions?
- (b) Is there a unique statistical mechanical answer? In particular do the canonical and grand canonical ensembles agree?—even at a critical point?

Historically the affirmative answer to (a) was strongly doubted. People wondered how atoms separated by macroscopic distances could "know" when they should condense. It was suggested that extra conditions might be needed to tell the system which phase to go into. It was thought that one ought to calculate the (Gibbs) free energy separately for each phase and decide where a phase change took place by equating the two free energies. The phase with the lower free energy would be realized (while the higher one could correspond to a "metastable phase").

Today, however, with the striking example of Onsager's solution of the plane Ising model before us, the answer to (a) should be "Yes." Onsager's work (which we will describe) showed unequivocally how a phase change could and should come out of a rigorous statistical calculation without the need for any additional constraints or supplementary conditions. One proviso to our "Yes" is, however, needed: true equilibrium must have been established in the experimental situations we wish to describe. This requirement is not always so easy to fulfill in the laboratory since "settling times" often become very long near critical points, and irreversible and metastable tendencies often plague systems which are close to first order phase changes. We will, however, always assume that equilibrium is attained.

Despite our affirmative answer to (a) which, to my knowledge, is no longer questioned, there are people who still seem to think and talk as if they accepted the historical doubts! (Of course, it should

be said that as a matter of the practical computation of a numerical answer, it may well be a good tactic to calculate approximately and separately for each phase. However, the question of principle is what matters here.)

The uniqueness question (b) must be answered negatively if we have in mind finite physical systems. Thus the canonical free energy per particle, even of a large system, does depend to some extent on the size and shape of the system, and it also differs from the corresponding grand canonical free energy. However, we know that to obtain true thermodynamic behaviour we must consider the limit of a very large system in which the intensive parameters, temperature, density, chemical potential, etc., are held fixed. Formally we can define the thermodynamic limit for the canonical ensemble by choosing a sequence of domains Ω_k ($k=1, 2, 3, \dots$) whose volumes $V=V(\Omega_k)$ approach infinity. (It is not enough just to specify the volume and forget about the shape!) The correct limiting free energy per particle is then given by

$$-\frac{F}{kT} = \lim_{k \rightarrow \infty} (1/N) \ln Q(N, \Omega_k) - 3 \ln \Lambda \quad (11.1)$$

where the limit is taken at fixed density

$$\rho = N/V(\Omega_k). \quad (11.2)$$

Of course, the existence and uniqueness of this limit can be expected only for "reasonable" shapes of domain and for systems with "reasonable" forces. Completely rigorous existence proofs have been given only recently.* For our present purposes the following set of sufficient conditions is useful to know:

(A) On the pair potentials:

$$(i) \quad |\varphi(r)| \leq C/r^{3+\epsilon} \quad \text{as } r \rightarrow \infty \quad (11.3)$$

$$(ii) \quad \varphi(r) \geq C'/r^{3+\epsilon'} \quad \text{as } r \rightarrow 0 \quad (11.4)$$

where C , C' and ϵ , ϵ' are positive constants.

The first condition says the potential must decay reasonably rapidly at infinity (and rules out dipolar and unshielded Coulomb forces) while the second condition ensures that the potential has a sufficiently strong repulsive core to prevent the system "collapsing."

(B) On the domains:

The sequence Ω_k may be constructed from any finite set

*See D. Ruelle, *Helv. Phys. Acta.* 36, 183, 789 (1963); M. E. Fisher, *Arch. Ratl. Mech. Anal.* 17, 377 (1964).

of bounded domains by an arbitrary sequence of isotropic expansions such that $V(\Omega_k) \rightarrow \infty$ as $k \rightarrow \infty$.

A necessary condition on the domains is that the volume $V_\sigma(h, \Omega)$ within a distance h of the boundary should satisfy

$$\lim_{h \rightarrow 0} V_\sigma(h, \Omega_k) / V(\Omega_k) = 0. \quad (11.3)$$

Under conditions (A) and (B) one can prove that $F(\beta, v)$ is a well-defined continuous function of β and v . Furthermore F is a monotonic decreasing function of v differentiable almost everywhere. This means (compare with Equation (9.5)) that the pressure is well defined everywhere except for possible step discontinuities (which have not been ruled out in general—see Figure 11.1).

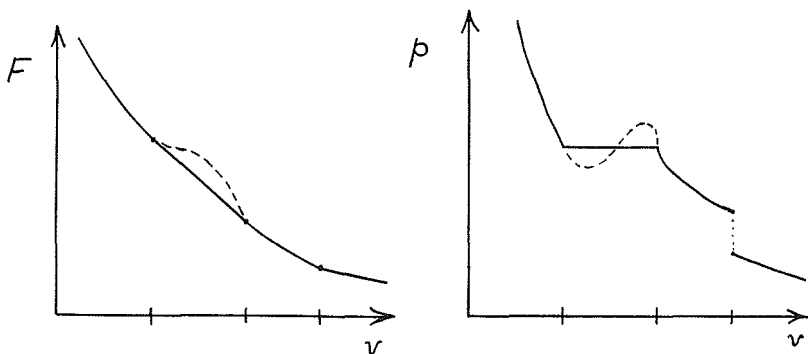


Figure 11.1. Canonical free energy and pressure versus specific volume illustrating possible (solid line) and impossible (dashed line) behaviour.

An important theorem that follows (a proof of these results for a sequence of doubling cubes under slightly more restrictive conditions on the potentials is given in Appendix A) is:

Theorem: The canonical pressure $p(v)$ is a monotonic non-increasing function of the specific volume v .

Thus the pressure falls as v increases or, as in condensation, remains constant (nonincreasing) over some interval (see Figure 11.1). However, we see that "Van der Waals" or "metastable loops," such as illustrated by the dashed lines in Figure 11.1, can never arise in a correct canonical calculation. If we calculate a canonical pressure and find such a loop, we have made a mistake!

The magnetic analogue of our theorem is that H is a monotonic nondecreasing function of M (and vice versa). Thus equally in the magnetic case a rigorous calculation based on the partition function cannot yield a hysteresis loop.

The thermodynamic limit for the grand canonical ensemble is defined in the analogous manner once a sequence of domains Ω_k is given. As before, one can prove that the grand canonical pressure $\bar{p}(z)$ is a unique, continuous, differentiable (almost everywhere) function of the activity z . Furthermore, if the grand canonical density $\bar{\rho}(z)$ is computed by Equation (9.9), the function $\bar{p}(\bar{\rho})$ agrees exactly with the canonical pressure function $p(\rho)$ even at critical and condensation points. The same holds for all other thermodynamic quantities computed in the two ensembles. Indeed, it has recently been shown that this result is true for the correlation functions also. One must, of course, remember that the grand canonical ensemble does not explicitly describe the two-phase region in a condensation process since $\bar{\rho}(z)$ changes discontinuously at a condensation point (see Figure 11.2).*

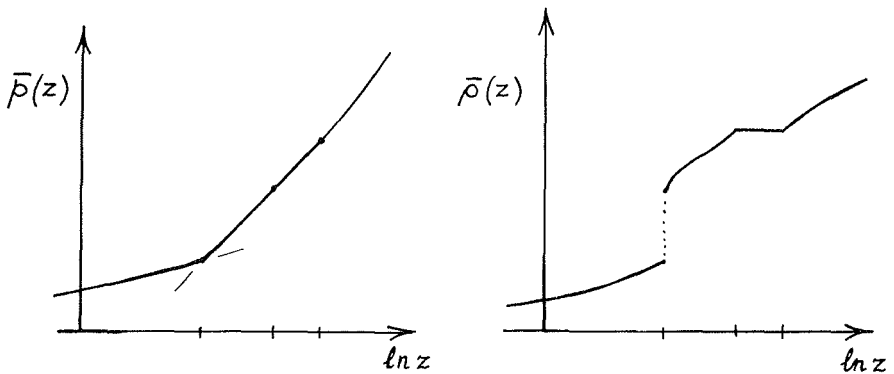


Figure 11.2. Grand canonical pressure and density illustrating possible behaviour.

To summarize, we see that if we want well-defined thermodynamically correct answers we must always compute the thermodynamic limit. If we do this we may use whichever ensemble is the most convenient in the knowledge that the answers will be unchanged. In the discussions that follow we will always assume that the thermodynamic limit is taken unless we expressly mention otherwise.

*Conversely, the canonical ensemble would not describe the intermediate points of a discontinuity in $p(v)$ (if such a phenomena were observed) whereas the grand canonical ensemble would do so. The pressure must increase linearly with $\ln z$ through the jump (see Figure 11.2).

12. The Mathematical Mechanism of Phase Transitions

Our examination of phase transitions and critical points has shown that they correspond to mathematical singularities in the free energy $F(\beta, \nu)$ or in the grand potential $\pi(\beta, z)$ and their derivatives; thus the compressibility becomes infinite at the critical point, the spontaneous magnetization vanishes identically, and $\rho(z)$ is discontinuous at a condensation point. For theoretical purposes we will consider any nonanalytic point* of $F(\beta, \nu)$ or $\pi(\beta, z)$ occurring for real positive β, ν or z as a phase transition point.

However, when we look at the partition functions that we have written down we observe that they are completely smooth analytic functions for real β and z . Indeed they are usually entire analytic functions over the whole complex β and z planes. (Recall that the Ising partition function was merely a polynomial in x and y). Of course, this result is only true for finite systems; but it does establish that a finite system cannot display a true phase transition. Evidently, only the limiting free energy per particle (and limiting grand potential) could have mathematical singularities of the type we seek. This shows again the importance of taking the thermodynamic limit in the study of phase transitions.

It might be objected, however, that all real systems studied in the laboratory are actually finite! The answer to this objection is, of course, that the number of particles in a typical macroscopic system is of order

$$N \cong 10^{22} \text{ to } 10^{24}$$

so that we might expect departures from the ideal limiting behaviour only of order 1 in 10^{22} ; but such accuracy is way beyond the possibilities of most experiments. However, we know from fluctuation theory that this is an oversimplification; we should expect relative fluctuations, e.g., $\Delta T/T_C$, $\Delta p/p_C$ to be of order $1/\sqrt{N} \cong 10^{-11}$. Fortunately, this is also safely beyond normal experimental accuracy. Nevertheless we should be on our guard, especially near a critical point. For example, it is plausible that the maximum of a specific heat peak of a finite system grows only as

$$\ln N \cong 50$$

so that really accurate experiments at critical points might reveal a

*Nonanalytic means that the function cannot be expressed by a Taylor series expansion about the point in question which converges in every neighbourhood of the point. It is not necessary that any particular derivative of $F(\beta, \nu)$ or $\pi(\beta, \nu)$ display a discontinuity or become infinite.

finite size dependence. At present, however, even the most accurate experiments on carefully purified, homogeneous systems do not seem to reach these limits.

Since a phase transition only appears in the thermodynamic limit it is natural to ask, "How can a phase transition grow?" An illuminating answer to this question for the grand canonical ensemble was first given by Yang and Lee (Phys. Rev. 87, 404(1952)) and is now quite well known.

If, as in the lattice gas model, the particles have an infinite "hard core," $\Xi(z, \Omega)$ is just a polynomial in z of degree R , equal to the maximum number of particles that can be packed in Ω . Now a polynomial is completely characterized by its zeros. (Indeed, the zeros are the only analytic feature a polynomial has!) We may thus write*

$$\Xi(z, \Omega) = \prod_{r=1}^R \left[1 - \frac{z}{z_r} \right] \quad (12.1)$$

where the zeros $z_r = z_r(\beta)$ will lie in the complex z -plane off the real axis (for real β) as indicated in Figure 12.1. For the grand potential

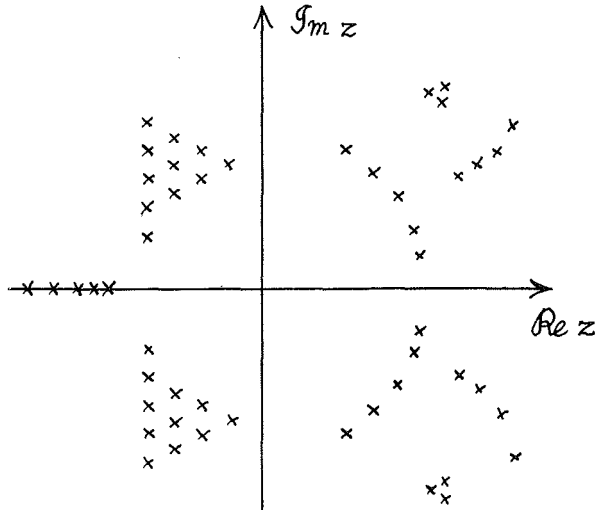


Figure 12.1. Possible distribution of zeros of $\Xi(z, \Omega)$ in the complex z plane.

*More generally if there is no hard core but the potentials satisfy (11.4), say, $\Xi(z)$ will be an entire function with an infinite number of zeros. The factorization formula (12.1) will still be valid, however, if $R = \infty$.

of the finite system we have

$$\pi(z, \Omega) = \sum_{r=1}^R V_{\Omega}^{-1} \log \left(1 - \frac{z}{z_r} \right) \quad (12.2)$$

which expresses π as the total (two-dimensional) electrostatic potential due to R positive point charges of strength $1/V(\Omega)$ at the positions z_r . As we take the thermodynamic limit, $R \rightarrow \infty$ and the zeros may close up to form lines of charge density as illustrated in Figure 12.2. For a

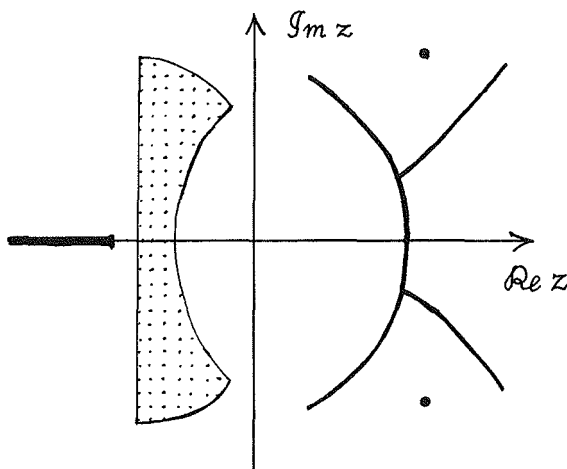


Figure 12.2. Possible limiting distribution of zeros in z plane.

finite system, the zeros cannot touch the real axis but in the limit a line of charge might cut the axis. If this happens at $z = z_t$ we know from elementary electrostatics that the potential (i.e., the pressure) will be continuous at z_t but its derivative the field (which corresponds to the density) will be discontinuous.* Such a point will thus represent a first order transition.

In general we must also expect that some of the charge may coalesce to form macroscopic point charges in the limit (see dots in Figure 12.2). Furthermore, one cannot rule out the possibility that the charge might spread out over some finite area of the z -plane as suggested by the dots in Figure 12.2. If this happened in the neighborhood of the positive real axis, it would correspond again to some sort of phase transition. It is generally believed, however, that "lines of charge" are more "natural" than areas. One heuristic

*Assuming the charge density on the real axis is not zero.

argument in favour of this is Lee and Yang's strong result for the Ising model with totally attractive potentials ($J_{ij} \geq 0$). They proved that all zeros lie on the circle

$$|z| = z_t = x^q, \quad (12.3)$$

i. e., $y_t = 1$ which corresponds to zero magnetic field (see Equations (10.22) and (10.8)). Unfortunately, they were not able to calculate the density of charge on this circle for the two-dimensional model (although in one dimension it is not difficult to find). The theorem fails if antiferromagnetic interactions are allowed.

13. Singularities in the Canonical Partition Function

It is not always realized that the Yang-Lee analysis in terms of the zeros of $Z(z, \Omega)$ has a direct analogue for the canonical partition functions $Q(\beta, N, \Omega)$ and $Z(\beta, N, \Omega)$ at fixed density $N/V(\Omega)$. Since these partition functions are essentially sums of terms of the form $e^{-\beta E}$ they are entire functions of β . Consequently, subject to a few conditions, we may express the free energy per particle for the finite system in terms of the complex zeros $\beta_r = \beta_r(v)$ of $Z(\beta, \Omega)$. In general these will be infinite in number so that

$$\begin{aligned} -\frac{F}{kT} &= N^{-1} \ln Z(\beta, N, \Omega) \\ &= \sum_{r=1}^{\infty} N^{-1} \ln [1 - (\beta/\beta_r)] + \text{const.} \end{aligned} \quad (13.1)$$

(For the Ising model, however, we may use the temperature variable x rather than β , and there will then be only a finite number of zeros.)

As in the grand canonical case, the zeros will lie off the real positive temperature axis (β axis) for a finite system but may close up on the axis in the thermodynamic limit. The point β_c where a limiting line of zeros cuts the axis will locate a critical temperature. In the limit $N \rightarrow \infty$ we expect the summation in (13.1) to go over into an integration.

We will show explicitly (in Section 19) that this sort of behaviour is just what happens for the two-dimensional Ising model in zero field. It may nevertheless be useful to examine in a little detail a simpler example based on the "mock partition function."

$$Z(\beta, N) = 2 e^{NK(\beta)} \cosh \frac{1}{2} N\epsilon (\beta - \beta^*) \quad (13.2)$$

where we suppose $K(\beta)$ is an entire function of β and that ϵ and β^*

are fixed. This $Z(\beta)$ is, of course, just the sum of two exponentials and is clearly an entire function. Notice that the zeros

$$\beta_r = \beta^* \pm (2r + 1) \pi i / N\epsilon \quad (r = 0, 1, 2, 3, \dots) \quad (13.3)$$

are spaced at constant intervals $|\Delta\beta| = 2\pi/N\epsilon$ along a line parallel to the $\text{Im}\{\beta\}$ axis but cutting the $\text{Re}\{\beta\}$ axis at β^* . As $N \rightarrow \infty$ the zeros close up to yield a uniform line density. Now

$$N^{-1} \ln Z(\beta, N) = K(\beta) + N^{-1} \ln \cosh \left[\frac{1}{2} N\epsilon(\beta - \beta^*) \right] + (\ell n 2)/N, \quad (13.4)$$

and so the energy per particle is

$$\begin{aligned} U(\beta) &= -\frac{\partial}{\partial \beta} N^{-1} \ln Z(\beta, N) \\ &= -K'(\beta) - \frac{1}{2} \epsilon \tanh \left[\frac{1}{2} N\epsilon(\beta - \beta^*) \right]. \end{aligned} \quad (13.5)$$

This is a perfectly smooth analytic function of β (see solid line in Figure 13.1). However, as we let N increase, the variation of $U(\beta)$ becomes very rapid near $\beta = \beta^*$ and in the limit $N \rightarrow \infty$ we find

$$\begin{aligned} U(\beta) &= -K'(\beta) - \frac{1}{2} \epsilon, & (\beta > \beta^*) \\ &= -K'(\beta) + \frac{1}{2} \epsilon, & (\beta < \beta^*). \end{aligned} \quad (13.6)$$

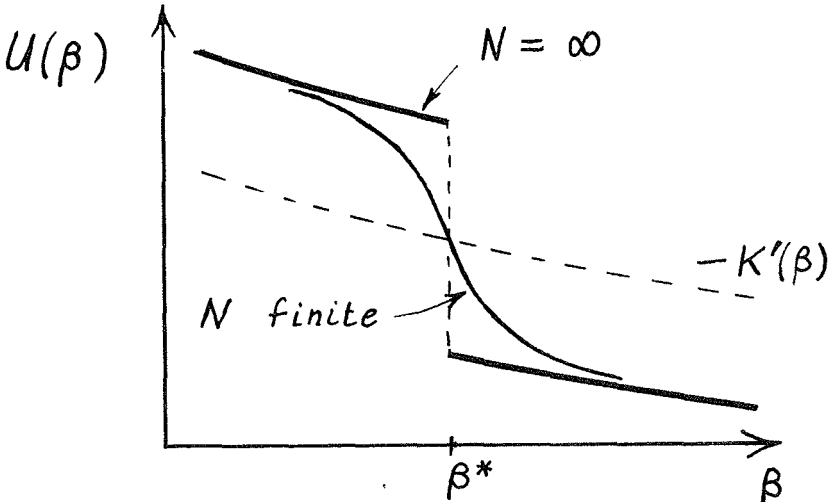


Figure 13.1. Energy versus β showing approach to a first order phase change.

Thus the limiting energy function is nonanalytic at $\beta = \beta^*$ which we identify as a first order transition point with energy discontinuity

$$\Delta U = \epsilon, \quad (\beta = \beta_0). \quad (13.7)$$

On the other hand, in terms of the zeros (13.3), we have[†]

$$N^{-1} \ell_n Z(\beta, N) = K(\beta) + N^{-1} \sum_{r=-\infty}^{+\infty} \ell_n [\epsilon\beta - \epsilon\beta^* - (2r+1)\pi i/N] + \text{constants}. \quad (13.8)$$

Now put

$$\theta = -(2r+1)\pi/N, \quad d\theta = -2\pi/N, \quad (13.9)$$

so that

$$N^{-1} \sum_r$$

becomes

$$(2\pi)^{-1} \int d\theta \quad \text{as } N \rightarrow \infty$$

and the limiting free energy per particle is

$$-F/kT = K(\beta) + (1/2\pi) \int_{-\infty}^{\infty} g(\theta) \log [\epsilon(\beta - \beta^*) + i\theta] d\theta. \quad (13.10)$$

For generality we have introduced the line density $g(\theta)$ which is simply unity in this case. Differentiating under the integral sign we get

$$U(\beta) = -K'(\beta) + \frac{1}{2\pi i} \int_{-\infty}^{\infty} \frac{\epsilon g(\theta) d\theta}{\theta - i\epsilon(\beta - \beta^*)} \quad (13.11)$$

where the contour runs along the real θ axis. The integrand has a simple pole at $\theta_0 = i\epsilon(\beta - \beta^*)$. As β varies, this pole crosses the axis when $\beta = \beta^*$ and its contribution to the integral then changes by $2\pi i \epsilon g(0)$. Of course, this just corresponds to the energy discontinuity found previously.

In the present case $g(\theta)$ is constant but the above argument would go through in general provided $g(\theta)$ can be extended into a function of θ analytic in the complex θ plane at $\theta=0$. (For real θ

[†]Using the factorization of $\cos \alpha = \cosh i\alpha$.

we must have $g(\theta)$ real, positive with $g(-\theta) = g(\theta)$.) It is by no means clear that we should always expect such analyticity. On the contrary, the subtlety of the thermodynamic behaviour at a transition point is probably reflected in the nature of the nonanalyticity of $g(\theta)$ at $\theta = 0$ (accepting for the moment that a line of charge will be what occurs).

To see this more clearly suppose that $g(\theta)$ varies as $a|\theta|$ as $\theta \rightarrow 0$. I will leave it as an exercise to show that this implies a "continuous" or "second order" transition at $\beta = \beta^*$ where the energy varies as

$$U(\beta) = U(\beta^*) + A(\beta - \beta^*) \log |\beta - \beta^*| + \dots \quad (13.12)$$

Differentiation yields a symmetric logarithmically diverging specific heat! Conversely, such a specific heat singularity implies a non-analyticity of $g(\theta)$.

Chapter IV

Let us now leave aside general considerations and discuss the explicit calculation of the critical behaviour of our chosen models. I will start by reviewing briefly the well established approximate theories which, for want of a better name, I will term the "classical theories" of the critical point. †

14. The Mean Field and Van der Waals Equation

A fundamental idea in the standard treatments of many-body systems and phase transitions is the "mean field" or "internal field" whose genesis goes back to Pierre Weiss (1907) if not farther. One attempts to replace the complicated pairwise interactions between particles (or between spins) by a uniform internal field with which each particle interacts directly. Of course this field must be chosen in a self-consistent manner so that, say, the average interaction of each particle with its neighbours is correctly preserved.

In the case of a magnet the mean field is taken proportional to the total magnetization and each spin is considered to move freely in a sum of the internal and external (i.e., true) magnetic fields. The details of the theory are rather well known ‡ and will not be reproduced here. Rather I will follow Uhlenbeck and sketch Ornstein's

†Of course, "classical" is used here with its dictionary meaning: "often referred to, standard," rather than as a synonym for "nonquantum-mechanical."

‡See, for example, Kittel, "Solid State Physics," John Wiley & Sons, New York (1956), p. 402.

(1908) derivation of the Van der Waals equation which employs the same basic idea. Let us recall, however, that for a Heisenberg ferromagnet of spin S , with a lattice of coordination number q and nearest neighbour interactions of strength J , a critical point is predicted by the mean field theory at

$$kT_c = \frac{1}{3} S(S+1)q(2J). \quad (14.1)$$

To obtain an approximate equation of state for a classical fluid with pairwise forces let us suppose that the potential $\varphi(r)$ is characterized (i) by a small hard core of radius \underline{a} and (ii) by a weak attractive tail $\varphi_0(\vec{r})$ of relatively long-range \underline{b} . The idea is to evaluate the configurational integral

$$Q_N = \frac{1}{N!} \int \cdots \int e^{-\beta U_N} d\vec{r}_1 \cdots d\vec{r}_N \quad (14.2)$$

by treating the two parts of the potential separately.

For most allowable configurations, the mean potential energy of one molecule will be approximately

$$\int \varphi_0(\vec{r}) \rho d\vec{r} = (-\omega\bar{\varphi})\rho \quad (14.3)$$

where $\rho = N/V$ is the mean density, $\omega \cong (4/3)\pi b^3$ is the volume of the effective sphere of interaction, and $-\bar{\varphi}$ is the corresponding mean strength of the potential. For the total potential (excluding, of course, the hard core contribution) we have

$$- \langle U_N \rangle \cong \frac{1}{2} N\rho\omega\bar{\varphi} \quad (14.4)$$

where the factor $\frac{1}{2}$ must be included to avoid the double counting of each pair interaction. Replacing U_N in (14.2) by its mean value (14.4) yields

$$Q_N \cong (1/N!) e^{\frac{1}{2}N\rho\omega\bar{\varphi}} \int \cdots \int d\vec{r}_1 \cdots d\vec{r}_N \prod_{(ij)} \theta_a(r_{ij}) \quad (14.5)$$

where we have taken account of the hard cores by introducing the theta functions defined by

$$\begin{aligned} \theta_a(r) &= 0 & \text{if } r \leq a \\ &= 1 & \text{otherwise.} \end{aligned} \quad (14.6)$$

Now the integral remaining in (14.5) is just that needed for the partition function of a gas of nonattracting hard spheres of radius \underline{a} . As such, its computation is a difficult and essentially unsolved problem. For a one-dimensional gas, however, the exact value is $(V - Nv_0)^N$ where V is the total (one-dimensional) volume and v_0 is the (one-dimensional) volume of each particle. For the present purposes this should be sufficiently exact in three dimensions also, if we set $v_0 \cong (4/3)\pi a^3$. (Notice that for a lattice gas with a single site hard core the exact result for a lattice of n sites in all dimensions is just $n!/(n-N)!$.) Accepting this result and using Stirling's formula yields, in the limit $N \rightarrow \infty$, the free energy

$$-F/kT = \frac{1}{2} \beta \rho \omega \bar{\varphi} + \ell n (v - v_0) + 1. \quad (14.7)$$

Consequently the equation of state is

$$\frac{p}{kT} = \frac{\rho}{1 - \rho v_0} - \frac{1}{2} \left(\frac{\omega \bar{\varphi}}{kT} \right) \rho^2. \quad (14.8)$$

This is, of course, identical with the more familiar Van der Waals form

$$\left(p + \frac{A}{v^2} \right) (v - B) = RT, \quad (14.9)$$

but has the merit that the two terms on the right hand side explicitly represent the separate contributions of the hard core repulsions and the weak long-range attractions. (For a lattice gas the first term on the right of (14.8) would be $(1/v_0) \ell n (1 - \rho v_0)$.)

A plot of the isotherms (14.8) shows that at high temperatures p increases monotonically with ρ . However, at a density

$$\rho_C = \frac{1}{3}(1/v_0) = \frac{1}{3} \rho_{\max} \quad (14.10)$$

and a temperature

$$kT_C = \frac{4}{27} \left(\frac{\omega}{v_0} \right) \bar{\varphi} \quad (14.11)$$

the isotherm flattens out and the compressibility K_T becomes infinite for the first time. We naturally identify this point as the critical point. It is interesting to notice the similarity of (14.11) with the mean field prediction (14.1); consider the identifications: $\frac{1}{3} S(S+1) \equiv 4/27$, $q \equiv (\omega/v_0) =$ (attractive volume/repulsive volume of potential), and $2J \equiv \bar{\varphi}$. (Note, incidentally, that for a lattice Van der Waals gas $\rho_C = \frac{1}{2}(1/v_0) = \frac{1}{2} \rho_{\max}$.)

At temperatures below T_C , as given by (14.11), all the isotherms display the famous Van der Waals loops, the pressure being no longer monotonic in the specific volume (see Figure 14.1a). Now our rigorous theorems tell us that this cannot be correct! Consequently, we must agree that our approximations are no longer valid in this region and we should not expect to draw reliable conclusions from them either below T_C or at the critical point, where, after all, the "disease" is just setting in. Although I maintain that this is the correct interpretation which we must place on the theory (and on similar theories elsewhere), this viewpoint was not accepted historically.

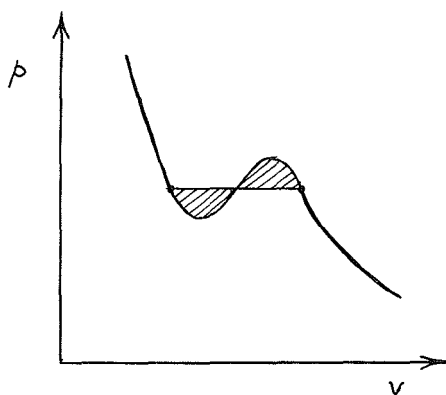


Figure 14.1a. Van der Waals isotherm below T_C showing Maxwell construction.

Maxwell proposed that the disease be cured by a supplementary appeal to thermodynamics (recall the discussion of Section 11). On this basis he proposed an "equal area" construction which gave a prescription for cutting off the loops by a horizontal line corresponding, presumably, to the coexistence of phases. This construction is particularly unsatisfactory in that it entails giving meaning to the thermodynamically unstable parts of the isotherm where the compressibility is negative! More convincing is the "double tangent" construction illustrated in Figure 14.1b which does not require the complete isotherm. This construction is equivalent to equating the Gibbs free energy, as a function of pressure, for the two branches of the isotherm. It must be recognized, however, that all these devices are in the nature of repairs to what is really a faulty, albeit very suggestive, theory.* (Nevertheless, we will see that the

*It is interesting to note that if a grand canonical formalism is used, the Maxwell or Gibbs constructions come rather naturally and it is

Van der Waals theory does have a theoretical validity in a certain limiting sense (see Section 17).

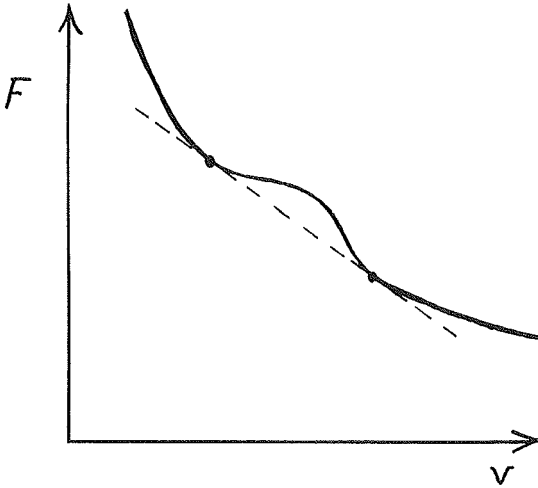


Figure 14.1b. Van der Waals free energy below T_C showing "double tangent" construction.

15. Classical Critical Point Predictions

Now what predictions do the Van der Waals and mean field theories make about the critical behaviour? We may summarize as follows:

(a) Compressibility and Susceptibility

$$K_T = \frac{B^\pm}{|T - T_C|} = \chi_0(T), \quad (T \rightarrow T_C^\pm). \quad (15.1)$$

where above the critical point K_T is taken at $\rho = \rho_0$, while below T_C it represents the compressibility at condensation. The amplitude B^- is appreciably smaller than B^+ . The simple hyperbolic divergence of $\chi_0(T)$ above T_C is the famous Curie-Weiss law.

(b) Coexistence Curve and Spontaneous Magnetization

$$(\rho_L - \rho_G) = A(T_C - T)^{\frac{1}{2}} = M_0(T), \quad (T \rightarrow T_C^-). \quad (15.2)$$

i. e., a square root law or, in our previous notation, $\beta = \frac{1}{2}$.

(c) Specific Heats ($\rho = \rho_C$; $H = 0$)

easier to feel that "nothing has been done"!

$$C_V(T) = C_C^\pm - D_C^\pm |T - T_C| = C_M(T)$$

with

$$\Delta C = C^- - C^+ > 0, \quad (15.3)$$

so that $C(T)$ drops discontinuously as T increases through T_C but varies smoothly on either side of T_C .

(d) Critical Isotherm ($T = T_C$)

$$p - p_C = a(\rho - \rho_C)^3 \quad (p \rightarrow p_C) \quad (15.4a)$$

$$H = aM^3, \quad (H \rightarrow 0). \quad (15.4b)$$

i. e. , a cubic law.

Now it turns out that these predictions show a surprising degree of invariance under improvements of the theory! To be more explicit, if we use a better approximation like Bethe's, which takes some account of the short-range order, we still obtain the formulas (15.1) to (15.4) near T_C . The amplitudes A, B, C, D , etc., alter somewhat, and the expression for the critical point in terms of molecular parameters changes by some 5 to 20 per cent (in typical cases) but the predicted analytic behaviour is unchanged. The same is true of various higher order cluster treatments such as Kikuchi's method and its generalizations developed by De Boer and collaborators, of the constant coupling method and of the truncated Green's function approach, etc. Many of these approximations give more accurate accounts of the properties of the model away from the critical region, e. g. , at high temperatures or low temperatures or high fields, and they often yield more accurate estimates of T_C but (except for a few very misleading approximations) the predictions (15.1) to (15.4) are common to all!

The same invariance holds in the theory of gases. Thus Dieterici's equation, the superposition approximation, the ring approximation, the hypernetted integral equation, etc., all yield essentially similar critical behavior.

Unfortunately, this invariance does not mean the classical results are correct! Certainly the square root coexistence and magnetization laws do not match up with the experimentally observed one third law. At one time people were inclined to blame the admittedly over simplified aspects of the models used for such disagreements, but we will show that this was unjustified. Let us ask, however, "Why do all the theories make the same predictions?"

16. Phenomenological Treatment of Critical Points

In answer to the question just raised we will describe a phenomenological treatment of a system near a critical point which has been developed particularly by Landau and the Russian school. It is based on the natural, and apparently harmless, assumption that the free energy may be expanded as a Taylor series in convenient variables at the critical point. This assumption looks quite general and nonspecific but we will show that, when supplemented by a thermodynamic argument, it necessarily leads to the classical critical point predictions. At the same time one can see that it is explicit or implicit in all the approximate theories cited.

We will give the argument for a ferromagnet since we considered a gas previously. As independent variables, let us choose the temperature and the magnetization.* The appropriate free energy is then the magnetic Gibbs free energy per spin, namely,

$$g = g(T, M) = f + HM, \quad (16.1)$$

in terms of which the field and the entropy are

$$H = \left(\frac{\partial g}{\partial M} \right)_T \quad \text{and} \quad S = - \left(\frac{\partial g}{\partial T} \right)_M. \quad (16.2)$$

Now expand g in powers of M . By symmetry only even powers can occur, so that,

$$g = a(T) + c(T)M^2 + e(T)M^4 + \dots \quad (16.3)$$

By Equation (16.2)

$$H = 2c(T)M + 4e(T)M^3 + \dots \quad (16.4)$$

and so the inverse susceptibility is

$$\frac{1}{\chi} = \left(\frac{\partial H}{\partial M} \right)_T = 2c(T) + 12e(T)M^2 + \dots \quad (16.5)$$

But by our assumption we may expand the coefficients in terms of $\Delta T = T - T_C$, so that,

$$c(T) = c_1 \Delta T + c_2 \Delta T^2 + \dots$$

*The magnetization is chosen rather than the field H , since we know that the free energy varies abruptly with H .

$$e(T) = e_0 + e_1 \Delta T + \dots \quad (16.6)$$

where we have set $c_0 \equiv 0$ since we know that $1/\chi \rightarrow 0$ as $T \rightarrow T_C$ when $M = 0$. Substituting in (16.5) yields

$$\chi(T) \cong \frac{(1/2c_1)}{(T - T_C) + 6(e_0/c_1)M^2} \quad (16.7)$$

In zero field above T_C we have from (16.4) that $M = 0$ and (16.7) reduces to the Curie-Weiss law (15.1)!

Below T_C in zero field the relation (16.4) gives three solutions, namely, $M = 0$ and

$$M_0^2 \cong \left(\frac{c_1}{2e_0} \right) (T_C - T) \quad (16.8)$$

It is easy to see from (16.3) that the solution $M=0$ corresponds to a maximum of the free energy $g(T, M)$ and so is thermodynamically "unstable." The two solutions (16.8), on the other hand, are both "stable." We recognize (16.8) as nothing but the square root Law (15.2) for the spontaneous magnetization! Substituting (16.8) in (16.7) shows that the initial susceptibility also obeys a Curie-Weiss law below T_C but with amplitude $(1/4c_1)$ so that $B^- = \frac{1}{2}B^+$ in (15.1).

Since $c(T_C) \equiv 0$, Equation (16.4) yields the cubic critical isotherm (15.4). Finally from the entropy we can derive the specific heat. In zero field above T_C

$$C_H = -T \left(\frac{\partial^2 a}{\partial T^2} \right) = C^+ - D^+ \Delta T + \dots \quad (16.9)$$

expanding $a(T)$. Below T_C in zero field we must substitute (16.8) into (16.3) before differentiation. This yields an additional term,

$$C_{H=0} = C^+ + \left(\frac{c_1^2 T_C}{2e_0} \right) + D^- \Delta T + \dots \quad (16.10)$$

so that there is a specific heat discontinuity of magnitude $(c_1^2 T_C / 2e_0)$.

17. Validity of Classical Theory

Despite the naturalness and seeming generality of the phenomenological arguments, we know experimentally that they cannot be valid. The accurate measurements cited in earlier sections definitely rule out a square root law for the coexistence or spontaneous magnetization curves. Similarly accurate experimental specific heat curves are not satisfactorily described as simple discontinuities.

We will show, when we examine experimental data again in later sections, that the Curie-Weiss and cubic critical isotherm laws are also not realized in real systems. Consequently on experimental grounds we cannot accept the Taylor series assumption.

Theoretically, the rigorous calculations on the Ising model which we describe next lead to the same conclusion. Certainly for the two-dimensional Ising model with nearest neighbour forces, an expansion of F in powers of $(T - T_C)$ cannot be made. Good evidence indicates that the same is true in higher dimensions if the forces are of "short range."

Recently, however, theoretical calculations by various authors have shown that for "infinitely long ranged" and "infinitely weak" attractive forces the classical predictions should become correct. To be more explicit, Kac, Uhlenbeck and Hemmer (J. Math. Phys. 4, 216(1963)) have considered a one-dimensional gas with the pair potential

$$\begin{aligned}\varphi(r) &= \infty, & (r < a) \\ &= -\kappa e^{-\kappa r}, & (r > a).\end{aligned}\tag{17.1}$$

(Note that $\int_a^\infty \varphi(r) dr$ is independent of κ .) For $\kappa > 0$ this potential satisfies the conditions of Section 11 so the limiting free energy and pressure exist and are monotonic in v . An exact calculation verifies this and shows that no phase transition occurs. However Kac, Uhlenbeck and Hemmer now consider the limit $\kappa \rightarrow 0$ in which the potential becomes infinitely weak but of infinite range (and, of course, cannot really be considered a proper potential any longer). In this limit they show rigorously that the equation of state becomes precisely the Van der Waals equation except that the flat portions of the isotherms no longer have to be grafted on by supplementary thermodynamic arguments but come properly out of the mathematics!

This result, which might have been guessed on the basis of Ornstein's derivation of the Van der Waals equation, and which is also suggested by work of Brout, has been extended to two- and three-dimensional Ising models by Baker, Siegert and Kac and Helfand. If one has a short-range attractive potential of fixed form, one may always introduce a scaling factor κ so that as $\kappa \rightarrow 0$ the range of the potential becomes infinite but $\int \varphi_\kappa(\vec{r}) d\vec{r}$ remains constant. Then, at least above T_C , if the limit $\kappa \rightarrow 0$ is taken after the thermodynamic limit, one always gets a Van der Waals or mean field type of equation of state for which the classical critical point predictions are valid.

It is clear that this "Van der Waals limit" is rather pathological and hence detailed results that follow from it are quite probably somewhat misleading. Nevertheless the results suggest strongly that

for physical systems with weak, very long-range attractive forces the equation of state should be rather Van der Waals-like except, perhaps, in the immediate critical region. Brout's arguments, and some others we will mention later, indicate that for forces of fixed short-range the behaviour should also become more Van der Waals-like as the dimensionality d of the system is increased! The limit $d \rightarrow \infty$, in fact, seems to yield essentially the same results as the $\kappa \rightarrow 0$ limit. But, from a practical viewpoint, one must remember that Nature provides us with a space of fixed low dimension and that the physical systems we are interested in are characterized, in the main, by short-range forces which we cannot alter.

Chapter V

18. Two-Dimensional Ising Models

We will now review the exact results that have been obtained in the study of plane Ising models. This will give us insight into the deficiencies of classical theory and will thereby serve as a foundation for a discussion of the three-dimensional models. We will mainly use the language appropriate to a ferromagnet.

The Ising model was introduced in a paper by E. Ising in 1925 (Z. Phys. 31, 253) and solved by him for a one-dimensional chain with nearest neighbour interactions for all fields and temperatures. As is well known, the solution is obtained readily by a matrix method*. One considers the partial partition functions $Z_N(\uparrow)$ and $Z_N(\downarrow)$ for a chain of N spins with the last spin fixed up or down respectively. If $\vec{\zeta}_N$ denotes the column vector

$$\vec{\zeta}_N = \begin{bmatrix} Z_N(\uparrow) \\ Z_N(\downarrow) \end{bmatrix}, \quad (18.1)$$

we find easily that the addition of a further spin to the chain leads to the recurrence

$$\vec{\zeta}_{N+1} = \underline{\underline{M}} \vec{\zeta}_N$$

where the elements of the 2×2 transition matrix

*A useful introductory review of the theory of the Ising model is G. F. Newell and E. W. Montroll, Rev. Mod. Phys. 25, 352 (1953). A more recent and comprehensive review is C. Domb, Adv. in Phys. 9, Nos. 34, 35 (1960).

$$\underline{M} = \begin{bmatrix} M(\uparrow\uparrow) & M(\uparrow\downarrow) \\ M(\downarrow\downarrow) & M(\downarrow\uparrow) \end{bmatrix} = \begin{bmatrix} x^{-\frac{1}{2}}y^{-\frac{1}{2}} & x^{\frac{1}{2}}y^{-\frac{1}{2}} \\ x^{\frac{1}{2}}y^{\frac{1}{2}} & x^{-\frac{1}{2}}y^{\frac{1}{2}} \end{bmatrix} \quad (18.2)$$

correspond to the extra Boltzmann factors introduced by the new spin (see Eq. (10.8)). The total partition function

$$Z_N = Z_N(\uparrow) + Z_N(\downarrow) \quad (18.3)$$

can now be expressed exactly in terms of the eigenvectors and eigenvalues of \underline{M} . For the calculation of the thermodynamic limit only, the largest eigenvalue $\lambda_0 = \lambda_0(K,L)$ is required and the free energy per spin is

$$-\frac{f}{kT} = \lim_{N \rightarrow \infty} N^{-1} \ln Z_N = \ln \lambda_0(K,L). \quad (18.4)$$

It is found that the linear chain has no phase transition; the specific heat in zero field $C(T)$ rises smoothly from zero to a rounded maximum and decays as $1/T^2$ as $T \rightarrow \infty$. Of course the mean field approximation would predict a transition! However, the Bethe approximation which treats the interaction of one spin with its immediate neighbours exactly and only uses the mean field for the shell of neighbouring spins turns out to be exact in this case.

Historically the next really significant step was taken by Kramers and Wannier in 1941 (Phys. Rev. 60, 252, 263) who developed the matrix method for the nearest neighbour plane square lattice. One must consider a lattice of m layers and specify the configuration of the m spins in the last or n th column ($N=mn$). There are in all 2^m configurations so that the transition matrix \underline{M} is now of order $2^m \times 2^m$. The largest eigenvalue $\lambda_0(m)$ yields the partition function per column of an infinitely long lattice of width m but a further limit is required to calculate the free energy per spin of the infinite plane lattice, namely,

$$-\frac{f}{kT} = \lim_{m \rightarrow \infty} \left(\frac{1}{m}\right) \ln \lambda_0(m;K,L). \quad (18.5)$$

For zero field Kramers and Wannier discovered a symmetry property of the transition matrix which implied that the partition function transformed into itself (up to a harmless multiplicative factor) under the transformation

$$x^* \longleftrightarrow \frac{1-x}{1+x} \quad (18.6)$$

which takes high temperatures into low temperatures. Thus

$$Z(\text{high } T) \leftrightarrow Z(\text{low } T), \quad (H = 0). \quad (18.7)$$

The transformation (18.6) has a unique fixed point (for real positive T) given by $x^* = x$ and it is natural to identify this with the critical temperature. In this way Kramers and Wannier located the exact critical point of the square lattice at

$$\begin{aligned} v_C &= \tanh K_C = \tanh (J/2kT_C) \\ &= \sqrt{2} - 1 = 1/(1 + \sqrt{2}), \end{aligned} \quad (18.8)$$

where we have introduced the variable

$$v = \tanh K = \frac{1 - x}{1 + x} \quad (18.9)$$

which proves very convenient in later theoretical developments. (Of course v should not be confused with the specific volume of the lattice gas).

Shortly afterwards Onsager showed that (18.6) was a special case of a duality transformation which carried the Ising problem on a planar lattice[†] into the Ising problem on the dual lattice. The transformation (18.7) was seen to be a consequence of the self-duality of the infinite square lattice. For the triangular and honeycomb lattices which are a dual pair of coordination numbers $q=6$ and $q=3$, respectively, Onsager introduced an additional star-triangle transformation. In combination with the duality transformation, this located the critical points of the triangular and honeycomb lattices at

$$1/v_C = 2 + \sqrt{3}, \quad (\Delta) \quad (18.10)$$

and

$$= \sqrt{3} \quad (\circ) \quad (18.11)$$

respectively.

The results (18.8), (18.10) and (18.11) can be written as a single formula with parameter q . However, the conjecture that the critical point depends only on q for all plane lattices is disproved by the kagomé lattice (derived from Japanese woven bamboo patterns!). This lattice has a fourfold coordination like the square lattice (see Figure 18.1), but

[†] A planar lattice may be drawn in the plane with no crossing bonds.

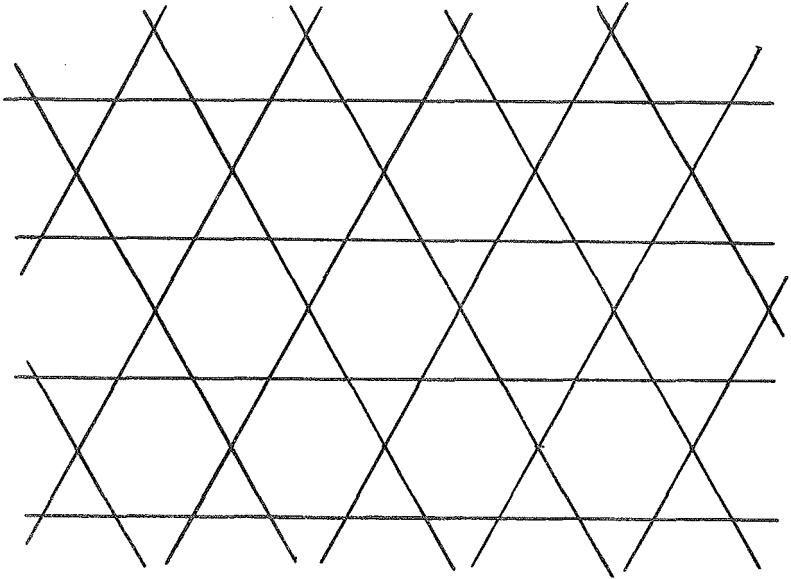


Figure 18.1. Kagomé lattice: note $q=4$.

$$v_c(\text{kagomé})/v_c(\text{square}) = 1.0512 \dots \quad (18.12)$$

Onsager went on from the topological considerations to provide in a famous, but not always fully appreciated, paper (Phys. Rev. 65, 117 (1944)) a complete rigorous solution for the square net Ising model in zero field.

19. Exact Solution of the Plane Ising Model

Onsager based his calculations on the matrix method. With no added difficulty he obtained the solution for the asymmetric square lattice with interaction energies J and J' in the horizontal and vertical directions. His result for the limiting free energy per spin is

$$-\frac{f}{kT} = \frac{1}{2} \int_{-\pi}^{\pi} \frac{d\varphi_1}{2\pi} \int_{-\pi}^{\pi} \frac{d\varphi_2}{2\pi} \ln [\text{ch } 2K \text{ch } 2K' - \text{sh } 2K \cos \varphi_1 - \text{sh } 2K' \cos \varphi_2] \quad (19.1)$$

(where we have used the useful abbreviations $\text{ch} \equiv \cosh$ and $\text{sh} \equiv \sinh$).

Notice first the occurrence of the two cosines; these are a direct reflection of the twofold translational invariance of the square net. Of course, this invariance is common to all the regular two-dimensional lattices and, indeed, the known answers for other lattices

all have a similar form but with different coefficients.

Notice secondly that, since $K, K' \sim \beta = 1/kT$, the formula (19.1) has the form

$$-\frac{f}{kT} = \sum_r \ln[1 - (\beta/\beta_r)] , \quad (19.2)$$

that is a summation over zeros in the complex β plane, as was anticipated in Section 13. This result is more obvious from Kaufman's (Phys. Rev. 76, 1232(1949)) exact expression for the partition function of a finite lattice which is expressed in terms of the product*

$$Z_N^{(1)} = \prod_{r=1}^m \prod_{s=1}^n \left\{ \frac{1+v^2}{1-v^2} \frac{1+v'^2}{1-v'^2} - \frac{2v}{1-v^2} \cos \frac{2\pi r}{m} - \frac{2v'}{1-v'^2} \cos \frac{2\pi s}{n} \right\} \quad (19.3)$$

using the variable $v = \tanh K$. For the symmetric case $K=K'$, $v=v'$, it is not difficult to calculate the zeros of $Z_N^{(1)}$. Of course, these will be indexed by the pair of integers (r, s) but one finds, nonetheless, that they lie on two circles in the complex v plane given by (see Figure 19.1)

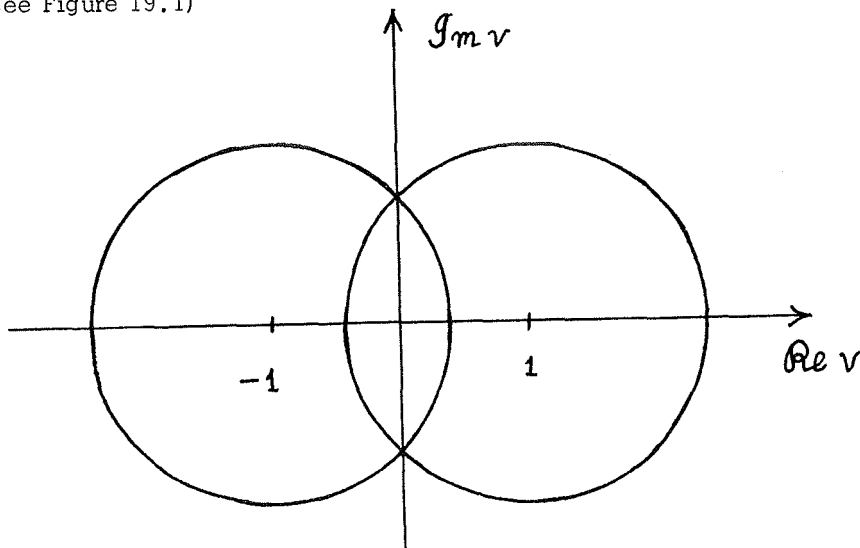


Figure 19.1. Loci of zeros of the Ising partition function in the complex $v = \tanh(J/2kT)$ plane.

*Actually, to get the particular periodic or toroidal boundary conditions used, the sum of four similar products is required, with r and s replaced by $r - \frac{1}{2}$ and $s - \frac{1}{2}$ respectively, but this will not make a significant difference.

$$v_{\theta} = \pm 1 + \sqrt{2} e^{i\theta}, \quad (0 \leq \theta \leq 2\pi). \quad (19.4)$$

The situation is just the same in the complex plane of $x=e^{-2K}$ since the bilinear transformation $x = (1 - v)/(1 + v)$ carries circles into circles. The loci of zeros cut the real v axis at the points $v = \pm(1+\sqrt{2})$ and $v = \pm(\sqrt{2} - 1)$. The former correspond to nonphysical (complex) temperatures but the latter locate the ferromagnetic and antiferromagnetic transition points in agreement with (18.8). (Note that the sign of v changes with the sign of J and that in zero field the square net is symmetric in $\pm J$). The density of zeros is found to be

$$g(\theta) = |\sin \theta| F(\theta) \quad (19.5)$$

where $F(\theta)$ is analytic and periodic in θ . Consequently, near the real v axis, $g(\theta) \sim |\theta|$.

As we mentioned in Section 13 this form for $g(\theta)$ already implies Onsager's most famous result, namely, a symmetric logarithmically infinite specific heat singularity,

$$C(T) = D \ln \left| 1 - \frac{T}{T_C} \right|, \quad (T \rightarrow T_C \pm). \quad (19.6)$$

Alternatively we may perform one integration in (19.1) to obtain (in the symmetric case)

$$-\frac{f}{kT} = \ln \operatorname{ch} 2K + \frac{1}{2\pi} \int_0^{\pi} \ln \left[\frac{1}{2} (1 + \sqrt{1 - k_1^2 \sin^2 \psi}) \right] d\psi \quad (19.7)$$

where the modulus k_1 is given by

$$k_1^2 = \frac{2 \operatorname{sh} 2K}{\operatorname{ch}^2 2K} \quad (19.8)$$

and attains the value unity only at $T = T_C$. This integral cannot be performed explicitly but by differentiating under the integral sign the energy per spin may be expressed in terms of the complete elliptic integral $K(k_1)$,

$$-\frac{U}{J} = \frac{1}{2} \coth 2K \left[1 + k_1'' \frac{2}{\pi} K(k_1) \right], \quad (19.9)$$

where

$$k_1'' = 2 \tanh^2 2K - 1 = \pm(1 - k_1^2)^{\frac{1}{2}}. \quad (19.10)$$

From this it follows that

$$U(T) = U_C + A(T - T_C)^{\ln} |T - T_C| + \dots \quad (19.11)$$

close to T_C , so that the energy is continuous at the critical point but has an infinite slope there corresponding to the logarithmic divergence of the specific heat.

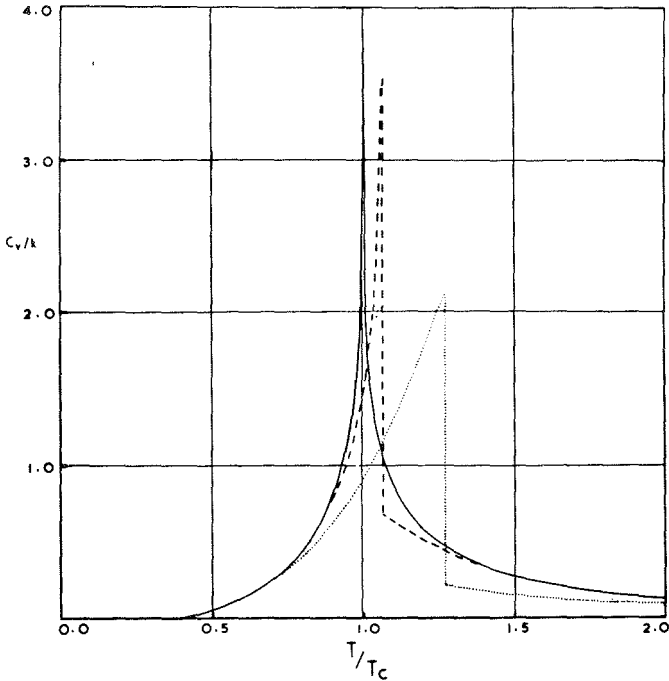


Figure 19.2. Exact specific heat of the plane square Ising lattice (solid curve), Bethe's approximation (dotted curve) and the Kramers-Wannier and Kikuchi approximation (dashed curve). (From C. Domb, *Adv. in Phys.* 9, Nos. 34, 35 (1960).)

The specific heat is plotted in Figure 19.2 (solid curve). Notice the symmetry of the singularity above and below T_C which is quite different from the characteristic asymmetry of the experimental results (see Figures 2.5 and 5.2). The dotted line in Figure 19.2 represents the results of Bethe's approximation while the dashed line

comes from the Kramers-Wannier and Kikuchi approximation. This latter approximation evidently gives the critical point more accurately but still yields a simple discontinuity. (Thus the accuracy of T_C is not a sure guide to the accuracy of qualitative behaviour.) Ironically enough, the asymmetric approximate curves compare more closely with experiment than does the exact result!

The specific heat curves for the nonsymmetric ($J \neq J'$) model still display a symmetric logarithmic singularity, but its amplitude is smaller and the critical point is lower. (A plot for the case $J' = (J/100)$ is given in Onsager's paper.)

By integrating $U(T)$ we see that the free energy varies at the critical point as

$$F(T) = F_C + a(T - T_C) + b(T - T_C)^2 \ln |T - T_C| + \dots \quad (19.12)$$

From this it is clear why the phenomenological treatment failed. The function $\ln x$ cannot be expanded as a Taylor series in x and so $F(T)$ cannot be expanded in powers of $(T - T_C)$! There is no escape from this conclusion, and it would surely be over-optimistic to expect something simpler to happen for the three-dimensional Ising model or for more realistic models.

20. Further Results

In 1948, at Cornell University, Onsager announced a formula for the spontaneous magnetization of the square lattice. He has not, as yet, published his derivation but in 1952 one was presented by Yang (Phys. Rev. 85, 808). Yang's paper is a mathematical tour-de-force and abounds in complicated elliptic integrals. The final answer, however, is surprisingly simple, namely,

$$M_0(T) = [1 - (\text{sh } 2K \text{ sh } 2K')^{-2}]^{1/8} \quad (20.1)$$

from which follows

$$M_0(T) = A(T_C - T)^{1/8}, \quad (T \rightarrow T_C^-). \quad (20.2)$$

This $\beta = 1/8$ law differs vastly from the classical prediction $\beta = \frac{1}{2}$. It also bears little resemblance to the experimental one third law, since it implies an exceedingly sharp drop of $M_0(T)$ at T_C and a very broad flat top on the coexistence curve.

In principle the result $\beta = 1/8$ could be tested on real "two-dimensional" systems, notably adsorbed monolayers. Thus for potassium on sodium bromide and n-heptane on ferric oxide, for example, experiments reveal the existence of first order phase transitions with critical points. However, an accurate check on the validity of (20.2)

seems not to have been made.

In 1949 Kaufman and Onsager (Phys. Rev. 76, 1244) went on to calculate the spin-spin correlation functions $\langle s_i s_j \rangle$. The nearest neighbour pair correlation function is clearly proportional to the energy and thus has the same $(T - T_C) \ln |T - T_C|$ singularity at the critical point. It turns out that the further correlation functions are rather similar in their variation with T and, in particular, they all have the same type of singularity at T_C . (We will need to discuss the properties of the pair correlation functions in more detail in later sections.)

Onsager's original derivation of the free energy (19.1) is anything but easy. It depends on the generation of a Lie algebra associated with the spin operators entering the transition matrix, and the subsequent reduction of this algebra. Kaufman (Phys. Rev. 76, 1232(1949)) gave a shorter derivation using theorems in abstract spinor analysis, which is simpler than Onsager's proof if one is familiar with the relevant spinor analysis! Later Kac and Ward (Phys. Rev. 88, 1332(1952)) gave a rather direct combinatorial derivation based on the construction of a determinant which counted an appropriate set of lattice configurations (see below). However, a rigorous proof that the determinant counts no more and no less than it should turns out to be rather difficult and has only recently been given by Sherman (J. Math. Phys. 1, 202(1960)) who used some ideas of Feynman. Potts and Ward used the combinatorial approach to rederive the correlation functions.

Hurst and Green (J. Chem. Phys. 33, 1059(1960)) reexpressed the configurational problem in terms of fermion operators and thereby reduced the partition function to a Pfaffian (which is a classical algebraic form equal to the square root of an antisymmetric determinant). Their analysis was later simplified and made fully rigorous by Kasteleyn (J. Math. Phys. 4, 287(1963)) who reduced the evaluation of the partition function to a dimer problem.* (See also A. M. Dykhne and Yu. B. Rumer, Soviet Phys. Uspekhi 4, 698(1962).) Montroll, Potts and Ward (J. Math. Phys. 4, 308(1963)) have used this method to rederive the correlation functions and thence the long-range order $\langle s_0 s_\infty \rangle$ which is equal to $[M_0(T)]^2$.

More recently Lieb, Schultz and Mattis (Rev. Mod. Phys., 1964) have given a further rederivation of Onsager's results based on

*A dimer is a rigid "molecule" which occupies two sites of a lattice to the exclusion of other molecules. Partition functions for planar lattices full of dimers have been recently calculated in terms of Pfaffians by P. W. Kasteleyn, loc. cit. and Physica 27, 1209(1961); H. N. V. Temperley and M. E. Fisher, Phil. Mag. 6, 1061(1961); M. E. Fisher, Phys. Rev. 124, 1664(1961).

a direct reduction of the spin operators to fermion operators. They can then use techniques developed in superconductivity theory.

Although personally I find the dimer approach the easiest and most direct, none of the methods is entirely trivial! The choice of the "simplest" really remains a matter of taste and one's particular mathematical background. What matters for our present purposes is that exact solutions can be found for a wide variety of planar lattices (although, for reasons that are not really understood in a fundamental way, plane lattices with crossing bonds have proved insoluble).

All the exact solutions* are characterized by a symmetric logarithmic specific heat singularity and in every case the free energy thus has the nonanalytic behaviour shown in Equation (19.12). Furthermore, evaluation of the spontaneous magnetization for other lattices always yields $\beta = 1/8$ (and the correlations for other lattices are also similar). These results allow us to draw the important conclusion that the analytic behaviour at the critical point of two-dimensional lattices is independent of the detailed lattice structure. (There is evidence that the inclusion of next nearest neighbour interactions makes no difference to this conclusion but presumably very long-range interactions could change the behaviour.)

21. Three Dimensions and Magnetic Fields

What rigorous results have been obtained for the Ising models (a) in three dimensions? (b) in a non-zero magnetic field?

The answer to (a) is that essentially nothing is known! But it should be mentioned that, using some old arguments due to Peierls and to Van der Waerden, one can give a rigorous proof that some sort of phase transition does take place. (The rigour has recently been supplied by R. B. Griffiths.)

The situation with respect to (b) is just a little better in two dimensions (although not, of course, in three). Thus in Section 44 we will describe a rather special (decorated) antiferromagnetic Ising lattice that can be solved completely in an arbitrary magnetic field. As mentioned before, one can also calculate the initial perpendicular susceptibilities of the usual lattices.

The parallel ferromagnetic and antiferromagnetic initial susceptibilities have never been calculated in closed form but it proves possible, as we shall explain, to say something analytically about the behaviour near T_C , at least in the case of the square lattice. One might also mention that if $\chi_0(T)$ were known exactly for the honeycomb

*After Onsager's paper the results for the triangular honeycomb, kagomé and more general checkerboard lattices were found by Wannier, Temperley, Houtappel, Syozi, Naya, Utiyama and others in the period 1950-55.

lattice, it could be found for the triangular and kagomé lattices!

The paucity of exact information, especially for the three-dimensional models which are of prime physical interest, forces us to look for other (necessarily less rigorous) approaches.

Chapter VI

22. Series Expansions

If the Hamiltonian \mathcal{H} is a bounded operator (as it is for spin systems), we may always expand the partition function as a "high-temperature series" in powers of $\beta = 1/kT$. Thus

$$\begin{aligned} Z(\beta) &= \text{Tr} \{ e^{-\beta \mathcal{H}} \} \\ &= \text{Tr} \{ 1 \} + \frac{1}{1!} \text{Tr} \{ \mathcal{H} \} \beta + \frac{1}{2!} \text{Tr} \{ \mathcal{H}^2 \} \beta^2 + \dots \end{aligned} \quad (22.1)$$

If \mathcal{H} is a sum of pair interactions invariant under translations, the successive traces in (22.1) reduce to traces over a relatively few operators and each term can be associated with a "diagram" or "graph" made up of bonds connected together in various ways. Where there is an underlying lattice the graphs can be considered drawn on this lattice. In general, such an expansion rapidly becomes very complicated. Diagrams with all combinations of multiple (or repeated) bonds must be included, the correct combinatorial factors must be found and the "weight" of each graph must be computed by taking the trace of the product in all possible orders of the operators associated with the graph.

For the Heisenberg model Rushbrooke and Wood (Proc. Phys. Soc. (London) A68, 1161(1955); Molec. Phys. 1, 257(1958)) have pushed the calculations through for general spin to obtain the partition function and initial susceptibility to terms of order β^7 . More recently, using a new approach, Domb and Wood (Phys. Letters 8, 20(1964)) have obtained two further terms for the case $S = \frac{1}{2}$ on a general lattice. (It might be practicable to obtain a further one as two terms but the labour goes up exponentially, or faster, with the number of terms computed!)

For the Ising model the commutation of the operators allows us to simplify the calculations appreciably and at the same time to obtain some insight into the underlying configurational and combinatorial problems that ultimately determine the critical behaviour. If we introduce a normalizing factor, the partition function of an Ising lattice of N spins in zero field may be written

$$\begin{aligned}
 Z(K, N) &= 2^{-N} \text{Tr} \left\{ e^{K \sum s_i s_j} \right\} \\
 &= \text{tr} \left\{ \prod_{(ij)} e^{K s_i s_j} \right\}
 \end{aligned} \tag{22.2}$$

where tr denotes $2^{-N} \sum_{(s_i = \pm 1)}$. Now the bond factor can take only the two values

$$\begin{aligned}
 f_{ij} &= e^{K s_i s_j} = e^K && \text{if } s_i s_j = 1 \\
 &= e^{-K} && \text{if } s_i s_j = -1.
 \end{aligned} \tag{22.3}$$

Hence we can write quite generally,

$$f_{ij} \equiv a + b s_i s_j. \tag{22.4}$$

The coefficients in this "linearization" can be determined by imposing the identity (22.3) for the two cases. This yields

$$a + b = e^K, \quad a - b = e^{-K}, \tag{22.5}$$

so that

$$a = \text{ch } K, \quad b = \text{sh } K, \tag{22.6}$$

and thus

$$f_{ij} = (\text{ch } K)(1 + v s_i s_j) \tag{22.7}$$

where $v = \tanh K$ is the variable introduced previously. (Note $v \rightarrow 0$ as $T \rightarrow \infty$.)

We have given this simple argument in detail since it is the prototype of a large number of useful transformations of the Ising model.* Quite generally any function $\psi(s_1, \dots, s_\ell)$ of the ℓ spin variables $s_1 \dots s_\ell$ can be expressed as a linear combination of the 2^ℓ distinct products of none, one, two, three ... spin variables. If $\psi(s_i)$ is even, that is, invariant under $s_i \rightarrow -s_i$ (all i), we only need the $2^{\ell-1}$ products of an even number of factors. An example of this technique is the solution in a magnetic field of the special antiferromagnetic model discussed in Section 44.

Now substitute (22.7) into (22.2), which yields

* See M. E. Fisher, Phys. Rev. 113, 969(1959).

$$Z(K, N) = (\text{ch } K)^{N^*} \text{tr} \left\{ \prod_{\langle ij \rangle} (1 + v s_i s_j) \right\} \quad (22.8)$$

where N^* is the number of bonds ($= \frac{1}{2} qN$ on a lattice of constant coordination number q). Consider the expansion of the product; the coefficient of v^n consists of all possible products of n "bond-pairs" $s_i s_j$. For example, in fourth order the terms $(s_1 s_2)(s_1 s_3)(s_2 s_4)(s_5 s_6)$ and $(s_1 s_2)(s_2 s_3)(s_3 s_4)(s_4 s_1)$ will appear. But notice that

$$\text{tr} \{s_i\} = 0, \quad \text{tr} \{s_i^2\} = \text{tr} \{1\} = 1, \quad (22.9)$$

from which it follows that any product which contains some particular spin variable an odd number of times (such as the first example above) will vanish on taking the trace while any even product (like the second example) has a trace of unity. Consequently, we have proved the basic graphical expansion

$$Z(K, N) = (\text{ch } K)^{N^*} \left\{ 1 + \sum_n P_n(N) v^n \right\} \quad (22.10)$$

where $P_n(N)$ is the total number of graphs of n lines (or bonds) which can be drawn on the lattice of N sites subject to the following rules: (a) each bond of the lattice may be used only once; (b) at each site of the lattice an even number of bonds must meet. An allowable configuration of bonds on the square net is shown in Figure 22.1. It will be seen that any configuration can be decomposed into

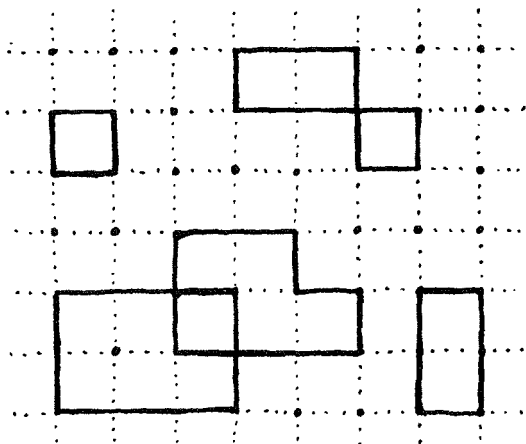


Figure 22.1. An allowed configuration of bonds on the plane square lattice.

a set of noncrossing polygons. (In three dimensions the polygons can intertwine and be knotted.)

The configurational expansion thus reduces the calculation of the partition function to the combinatorial problem of counting the allowed number of ways of placing polygons on the lattice. The expansion provides the starting point for the Kac-Ward and dimer treatments of the square net.

23. The Counting Problem

To understand the character of the expansion (22.10) and to show what is entailed in using it to obtain a high temperature expansion for the limiting free energy of an infinite lattice, let us derive the expansion for the square lattice. For simplicity we always suppose the lattice is wrapped on a large torus (that is, we impose periodic boundary conditions). All sites are then equivalent and we avoid "edge effects."

For the square net it is clear that

$$P_1(N) = P_2(N) = P_3(N) \equiv 0 \quad (23.1)$$

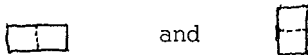
since the first closed configuration consists of a square of four bonds which may be anywhere on the lattice. If we label one corner of the square and place this corner on each of the N lattice sites, in turn we see that the total number of distinct configurations is

$$P_4(N) = N. \quad (23.2)$$

For brevity we thus say there is "one square per site" and write

$$p_4 = (\square) = 1. \quad (23.3)$$

At the next stage we see $P_5(N) = 0$ and, of course, on "loose packed" lattices such as the square, honeycomb, simple cubic and body centered cubic lattices all the odd coefficients will vanish. With six bonds we can form a hexagon which, on the square lattice, appears in the two orientations



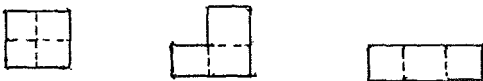
so that

$$P_6(N) = 2N. \quad (23.4)$$

We say there are two hexagons per site, and write

$$p_6 = \left(\begin{array}{c} \diagup \\ \square \\ \diagdown \end{array} \right) = 2. \quad (23.5)$$

With eight bonds we can form either an octagon or two separated squares. The octagons may be classified into the different "space types":



which can be placed in N , $4N$ and $2N$ ways respectively. In total, therefore, on the square lattice there are seven octagons per site,

$$p_8 = 7. \quad (23.6)$$

The reader is urged to try this method for the simple cubic lattice! It turns out that there are eleven space types with a total weight of $207N$ so that $p_8 = 207$ in this case. Clearly, this method rapidly becomes cumbersome as n increases and, more importantly, is very subject to error! Thus there are 73 space types of decagon and 756 types of dodecagon on the simple cubic lattice, and $p_{10} = 2412$, $p_{12} = 31754$. To calculate these numbers reliably, more sophisticated techniques have to be developed.

Returning to the eighth order term on the square lattice, we may compute the number of configurations of two separated squares by placing the first square in N ways. The second square must not have a bond in common with the first square so that it may then be placed in only $N-5$ ways. Finally, since the two squares are identical, we have a contribution $\frac{1}{2}N(N-5)$. In total, therefore,

$$\begin{aligned} P_8(N) &= 7N + \frac{1}{2}N(N-5) \\ &= \frac{1}{2}N^2 + 4\frac{1}{2}N. \end{aligned} \quad (23.7)$$

Let us now formally take the logarithm of the partition function in Equation (22.10),

$$\begin{aligned} \ln Z(K, N) - N^* \ln \chi K &= \ln \left\{ 1 + P_4(N)v^4 + P_6(N)v^6 + \dots \right\} \\ &= Nv^4 + 2Nv^6 + \left(\frac{1}{2}N^2 + 4\frac{1}{2}N\right)v^8 + \dots \\ &\quad - \frac{1}{2}(Nv^4)^2 - \dots \\ &= N \left[v^4 + 2v^6 + 4\frac{1}{2}v^8 + \dots \right]. \end{aligned} \quad (23.8)$$

We notice that the coefficient of N^2 has cancelled identically so that the answer is exactly proportional to N . We may thus divide by N and formally proceed to the limit which yields

$$-\frac{f}{kT} - \frac{1}{2} q \ell_n \text{ch } K = v^4 + 2v^6 + 4\frac{1}{2}v^8 + \dots \quad (23.9)$$

For the square net $q = 4$, and we may verify from Onsager's solution that this is the correct high-temperature expansion which converges up to the critical point. The energy and specific heat expansions may be found by term-by-term differentiation.

We see more generally that if n is less than the "circumference" of the torus (i.e., $n < N^{1/d}$ in d dimensions), $P_n(N)$ is just a polynomial in N of degree $m \leq n/4$ (or $\leq n/3$ if triangles can occur). Thus

$$P_n(N) = NP_n^{(1)} + N^2P_n^{(2)} + \dots + N^mP_n^{(m)} \quad (23.10)$$

On taking the logarithm of Z formally, the coefficients of N^2, N^3, N^4, \dots etc. vanish as above (this corresponds to the extensive property of the free energy) and one finds that

$$\begin{aligned} -\frac{f}{kT} &= \lim_{N \rightarrow \infty} N^{-1} \ell_n Z(K, N) \\ &= \frac{1}{2} \bar{q} \ell_n \text{ch } K + \sum_n P_n^{(1)} v^n \end{aligned} \quad (23.11)$$

where, in general, the mean coordination number is $\bar{q} = 2 \lim(N^*/N)$ ($N \rightarrow \infty$). Thus only the coefficient of N in $P_n(N)$ enters the limiting expansion. Indeed, notice that the coefficient of v^8 in Equation (23.9) can be written

$$4\frac{1}{2} = 7 - 5/2 = p_8 + p_{4,4} \quad (23.12)$$

If we identify the "number of two separated squares per site" as

$$p_{4,4} = (\square, \square) = -5/2; \quad (23.10)$$

In other words if we take just the coefficient of N in the expression $\frac{1}{2}N(N-5)$ for the total contribution of two squares. It is evident from this example that separated configurations make a negative contribution to the limiting expansion. (Furthermore the separated contributions can only be "eliminated" at the cost of introducing into the expansion more complicated graphs than polygons.)

24. Lattice Constants

The numbers $p_4, p_6, p_8, \dots, p_{4,4}$ and so on, which enter into the calculation of the partition function have been called "lattice constants" by Domb and Sykes (Phil. Mag. 2, 733(1957)) since they characterize the lattice in question and, indeed, will enter into any statistical (or combinatorial) problem specified on a lattice. Generally, given a lattice L , which need only be specified topologically, that is as a connected set of N^* bonds and N vertices, we may define the lattice constant of the finite graph G_V^l , of v vertices and l lines, as the number of ways of embedding G_V^l in L subject to the rules: (a) each vertex of G_V^l must lie on a distinct site of L , and (b) each line of G_V^l must lie on a distinct bond of L . If the total number of embeddings is P , the lattice constant per site of a connected graph is defined as

$$(G_V^l)^L = P/N. \quad (24.1)$$

In practice the superscript L is dropped when it is clear what lattice is being considered. For disconnected graphs the lattice constant per site is defined in terms of the coefficient of N as explained previously.

For Ising model expansions at low-temperatures and high fields (which proceed by overturning spins in a fully magnetized lattice and are the direct analogue of the familiar Mayer z -expansion for a gas at low density), it proves convenient to define lattice constants with a stronger embedding condition, namely, in addition to (a) and (b) we require: (c) if two vertices of G_V^l lie on two sites of L which are connected by a bond of L then a line of G_V^l must lie on this bond. It turns out that the set of "low-temperature" or "strong embedding" lattice constants" $[G_V^l]_L$ can be expressed generally in terms of the "high-temperature" or "weak embedding" constants $(G_V^l)^L$. For other problems (for example, the "percolation problem") other still more restricted types of lattice constants enter, but again they can be expressed in terms of the $(G_V^l)^L$.

As we have already seen, the calculation of lattice constants for graphs of more than a few lines and vertices is in general rather difficult, especially for three-dimensional lattices. A variety of systematic methods has been developed however (see in particular M. F. Sykes, J. Math. Phys. 1, 52(1961) and the review by Domb), and by now most lattice constants of up to nine or ten lines have been tabulated for the usual lattices. Once the work has been done, of course, we may use these tables like lists of standard integrals!

25. Correlation Functions and Susceptibility

The pair correlation functions in zero field are defined by

$$\langle s_0 s_r \rangle = Z^{-1} \text{tr} \left\{ s_0 s_r e^{K \sum s_i s_j} \right\} \quad (25.1)$$

so that, introducing (22.7)

$$\langle s_0 s_r \rangle = Z^{-1} (\text{ch } K)^{N^*} \text{tr} \left\{ s_0 s_r \prod_{(ij)} (1 + v s_i s_j) \right\}. \quad (25.2)$$

Multiplying out the product and arguing as before we see that the configurations entering the v -expansion of $\langle s_0 s_r \rangle$ are given by the previous rule except that the vertices at the sites 0 and r must be odd rather than even (i. e., an odd number of lines must meet at these two sites). This means that in addition to all possible arrangements of (closed) polygons we must have an (open) chain of bonds running from the site 0 to the site r . In fact, the dominant contribution to the n -th order expansion coefficient will come from the number of non-crossing (or self-avoiding) "walks" of n steps from 0 to r .

The problem of determining the number and properties of self-avoiding walks on a lattice has been much studied in its own right as a model of a polymer molecule with "excluded volume."[†] Clearly it is a special case of the lattice constant problem corresponding to the embedding of a chain of n lines and $n+1$ vertices.

When the spins s_0 and s_r are in the same row (or column), we see that the leading term in the expansion of $\langle s_0 s_r \rangle$ is just v^r . Consequently, above T_c the correlations decay exponentially (to leading order) with a decay parameter, or "inverse range"

$$\kappa a = |\ln v| [1 + O(v)], \quad (25.3)$$

where a is the lattice spacing. This exponential decay can be seen more generally from the expressions for the correlation functions in terms of the transition matrix \underline{M} (see B. Kaufman and L. Onsager, Phys. Rev. 76, 1232(1949) and Onsager's original paper).

To obtain a series for the initial susceptibility we use the general "fluctuation" theorem which relates the susceptibility of a system with Hamiltonian,

$$\mathcal{H} = \mathcal{H}_0 - g\beta_B H \sum_{i=1}^N s_i^z, \quad (25.4)$$

to the corresponding spin-pair correlation functions $\langle S_0^z S_j^z \rangle$. We

[†] See, for example, M. F. Sykes and M. E. Fisher, Phys. Rev. 114, 45(1959) and M. E. Fisher and B. J. Hiley, J. Chem. Phys. 34, 253(1961).

suppose the system is translationally invariant so that the magnetization per spin is

$$\begin{aligned} M(T, H) &= g\beta \langle S_0^Z \rangle \\ &= g\beta Z^{-1} \text{Tr} \left\{ S_0^Z e^{-(\mathcal{H}_0 - g\beta_B H \sum S_i^Z)/kT} \right\}. \end{aligned} \quad (25.5)$$

Now differentiate under the trace with respect to H remembering that $Z = Z(T, H)$. This yields the desired result, namely,

$$\chi(T, H) = \frac{g^2 \beta_B^2}{kT} \sum_{i=1}^N \left(\langle S_0^Z S_i^Z \rangle - \langle S_0^Z \rangle^2 \right). \quad (25.6)$$

In zero field above the Curie point the mean magnetization, and hence $\langle S_0^Z \rangle$, vanishes identically. For an infinite Ising system of spin $\frac{1}{2}$ we may thus rewrite the theorem as

$$\chi_0(T) = \frac{m^2}{kT} \left[1 + \sum_{r \neq 0} \langle s_0 s_r \rangle \right], \quad (T > T_C), \quad (25.6a)$$

where the summation now extends over all lattice sites (excluding the origin). Notice that the prefactor in this equation is just the susceptibility of a free spin (Curie's law) so that Equation (25.6) shows how any deviations from free spin behaviour are directly attributable to the correlations.

There is an analogous fluctuation formula for the compressibility of a gas, namely,

$$K_T = (1/\rho kT) [1 + \rho \int G(\vec{r}) d\vec{r}]. \quad (25.7)$$

As expected, the prefactor is equal to the compressibility of an ideal gas while $G(\vec{r})$ is the net pair correlation function,

$$G(\vec{r}) = g(\vec{r}) - 1 = (n_2(\vec{r}) - \rho^2)/\rho^2 \quad (25.8)$$

in which $n_2(\vec{r})$ is the usual pair distribution function. We might remark that the rigorous proofs of these fluctuation theorems in the thermodynamic limit have not been given[†] although there is no reason

[†]The point at issue is the interchange of the infinite summation or integration over the correlation functions, with the operation of taking the thermodynamic limit for the correlation functions themselves.

to doubt their validity for systems with proper thermodynamic behaviour.

Accepting Equation (25.6), we see that to calculate the high-temperature expansion of the initial susceptibility of the Ising model we need configurations made up of polygons plus a chain of bonds with one end at the origin. The dominant contribution to a_n , the n th coefficient of the susceptibility series, will be the total number of n -step self-avoiding walks c_n . However, the contributions from the polygons will be negative in total so that $a_n \leq c_n$. Even so, the behaviour of the two sets of coefficients is rather similar as we shall indicate.

Chapter VII

26. The Misuse of Power Series

By the methods sketched in the previous sections, power series expansions have been obtained for the specific heats and susceptibilities of the standard plane lattices, the three three-dimensional cubic lattices and, recently, for the tetrahedral (diamond) lattice. In most cases between nine and fifteen coefficients are available (although for the plane honeycomb lattice twenty-four terms of the expansion for $\chi_0(T)$ are known!). By way of example, the expansion of the square net susceptibility is

$$\begin{aligned} kT\chi_0/m^2 = & 1 + 4v + 12v^2 + 36v^3 + 100v^4 \\ & + 276v^5 + 740v^6 + 1972v^7 + \dots \\ & \dots + 1486308v^{14} + 3763460v^{15} + \dots \end{aligned} \quad (26.1)$$

while for the simple cubic lattice, *

$$\begin{aligned} kT\chi_0/m^2 = & 1 + 6v + 30v^2 + 150v^3 + 726v^4 + 3510v^5 \\ & + 16710v^6 + 79494v^7 + 375174v^8 \\ & + 1769686v^9 + 8306862v^{10} + 38975286v^{11} + \dots \end{aligned} \quad (26.2)$$

These series are fine to behold and clearly represent a lot of configurational information! The question is, however, "What good

*The last two coefficients here differ by small corrections from the values published by Domb and Sykes, *J. Math. Phys.*, 2, 63(1961).

are they?—how can they be used?"

One answer to this question, of course, is simply to evaluate the truncated series as it stands for a range of v (i.e., of temperature). We know that this procedure should yield more and more accurate approximations to the true value $\chi_0(T)$ when v is small as we include more terms (see Figure 26.1). However, we are not really interested in small v (which is equivalent to $T/T_C \gg 1$). On the contrary, we wish to study $\chi_0(T)$ for values of v near the critical value v_c where we "know" that $\chi_0(T)$ will diverge to infinity. But by truncating the series we are always left with a polynomial and a polynomial can never take on an infinite value! Consequently, this direct approach will not yield significant information on the critical behaviour even if we do have fifteen or more terms.

A somewhat better approach is to observe that if $\chi_0(T) \rightarrow \infty$, then $1/\chi_0(T) \rightarrow 0$ as $T \rightarrow T_C$. By a little algebra we can invert the series for $\chi_0(T)$ to get one for $1/\chi_0(T)$ and then we can try evaluating this series truncated after $n = 1, 2, 3, \dots$ terms (see Figure 26.2). Now our polynomial approximations to $1/\chi_0$ might cut the $1/\chi_0 = 0$ axis at some point and, if so, we obtain a "Curie point" which should be an approximation to the true Curie point. This could be "improved" by adding a further term to the series although if we are

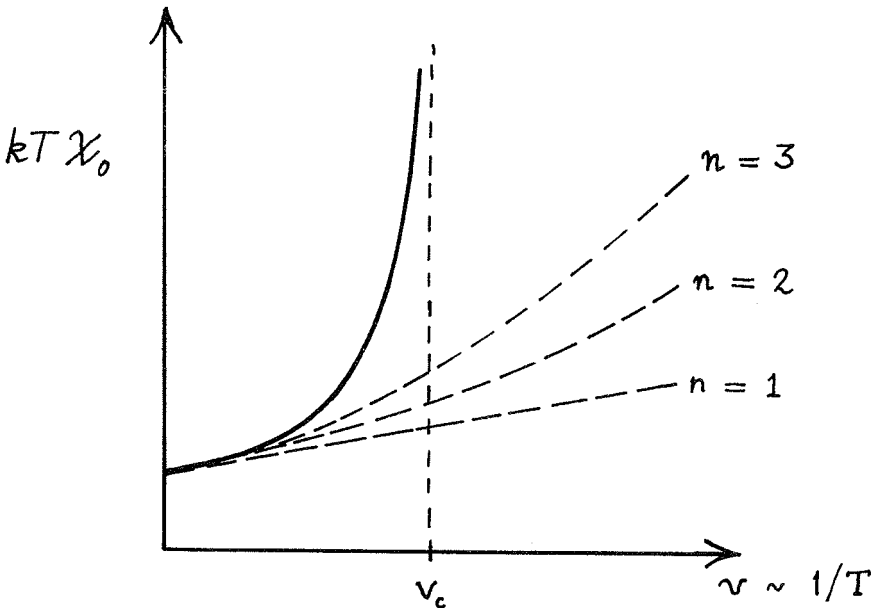


Figure 26.1. Successive approximations based on truncating the series for $\chi_0(T)$ compared with the expected behaviour.

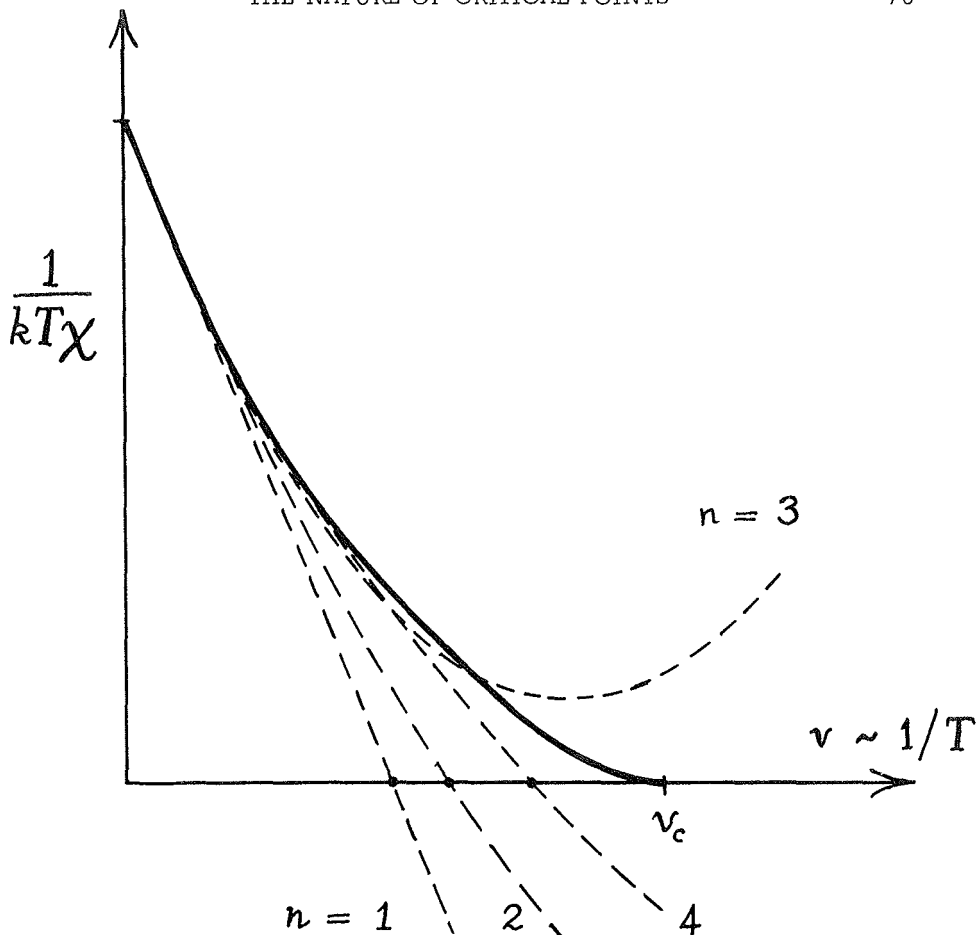


Figure 26.2. Successive approximations based on truncating the series for $1/\chi_0(T)$ compared with the expected behaviour.

unlucky this may cause our truncated function to miss the axis altogether!* (See curve for $n = 3$ in Figure 26.2.) It is, however, reasonable to expect this method to give a sequence of approximations for ν_c which will ultimately approach the correct value as n increases.

This does, in fact, seem to work out in practice except that the rate of convergence is often painfully slow and frequently rather erratic. More important, however, is the conclusion we will draw

*In this case one feels morally bound to compute still one further term before one publishes the result!

about the nature of the divergence of $\chi_0(T)$ at T_C . Since our approximation polynomial will always cut the axis (if it does not miss or just graze it) at a definite slope (and since it is necessarily analytic), we must always conclude,

$$\chi_0(T) \cong \frac{B}{(T - T_C)} \quad (T \rightarrow T_C) \quad (26.3)$$

i. e., the classical Curie-Weiss law! However, what we already know about the experimental results and about the rigorous behaviour of the two-dimensional Ising model should warn us to be prepared for a more general type of singularity of the form, *

$$\chi_0(T) \cong \frac{B}{(T - T_C)^\gamma} \quad (T \rightarrow T_C) \quad (26.4)$$

with, perhaps, $\gamma \neq 1$. It is clear that the methods discussed for handling the series cannot yield an estimate for γ .

27. The Ratio Method

A more purely mathematical approach to the problem may be formulated as follows: We have a function known only through its power series expansion,

$$F(x) = \sum_{n=0}^{\infty} a_n x^n. \quad (27.1)$$

We believe, on physical grounds, that for some real positive $x = x_C$, $F(x)$ diverges to infinity. We may assume the coefficients are positive (compare with (26.1) and (26.2)). It then follows that $F(x)$ has its nearest singularity on the real positive axis and that the position of this singularity determines the radius of convergence of the series. Identifying this singularity with the critical point x_C shows that our task is to estimate the radius of convergence of the series given its coefficients.

For this purpose we might use the general formula

$$\mu = 1/x_C = \lim_{n \rightarrow \infty} |a_n|^{1/n}. \quad (27.2)$$

and attempt to estimate μ by studying the sequence $|a_n|^{1/n}$. However, this expression for μ is really too powerful! It will give the correct answer even for a very erratic sequence a_n but normally

*In writing this asymptotic formula we do not, of course, rule out the possibility of further but weaker singularities coincident with the critical point.

converges only rather slowly. For a smoothly varying sequence (compare Equations (26.1) and (26.2) again) we may also expect the ratios

$$\mu_n = a_n/a_{n-1}, \quad (27.3)$$

to approach μ as $n \rightarrow \infty$.

Some simple examples will illustrate the sort of behaviour to expect. Given the series

$$F(x) = 1 + \mu x + \mu^2 x^2 + \mu^3 x^3 + \mu^4 x^4 + \dots \quad (27.4)$$

we would, making the natural conjecture, have

$$F(x) = 1/(1 - \mu x) \quad (27.5)$$

which has a simple pole at $x = x_C = 1/\mu$. The n th ratio μ_n is in this case just μ . Consider the series

$$1/(1 - \mu x)^2 = 1 + 2\mu x + 3\mu^2 x^2 + \dots + (n+1)\mu^n x^n + \dots \quad (27.6)$$

With a double pole at $x = 1/\mu$ in this case

$$\mu_n = \mu(1 + 1/n) \quad (27.7)$$

so that μ_n approaches μ linearly with $1/n$.

Let us try this procedure on the Ising model susceptibility series. Figure 27.1 shows a plot of the ratios μ_n versus $1/n$ for the triangular and face centered cubic lattice susceptibilities. (This figure is taken from Domb and Sykes (J. Math. Phys. 2, 63(1961)) who are responsible for developing this approach.) For both lattices the ratios rapidly seem to settle down to linear behaviour. If this linear behaviour continues, one should be able to estimate the limit μ by calculating the linear intercept from alternate ratios,* i.e.,

$$\mu_{\text{est}} = \frac{1}{2} [n\mu_n - (n-2)\mu_n]. \quad (27.8)$$

For the triangular lattice twelve coefficients are known and the last eight linear intercepts are found to be

*Alternate ratios are used rather than successive ratios to reduce the effects of small irregularities. See also the behaviour of loose packed lattices (Figure 27.2).

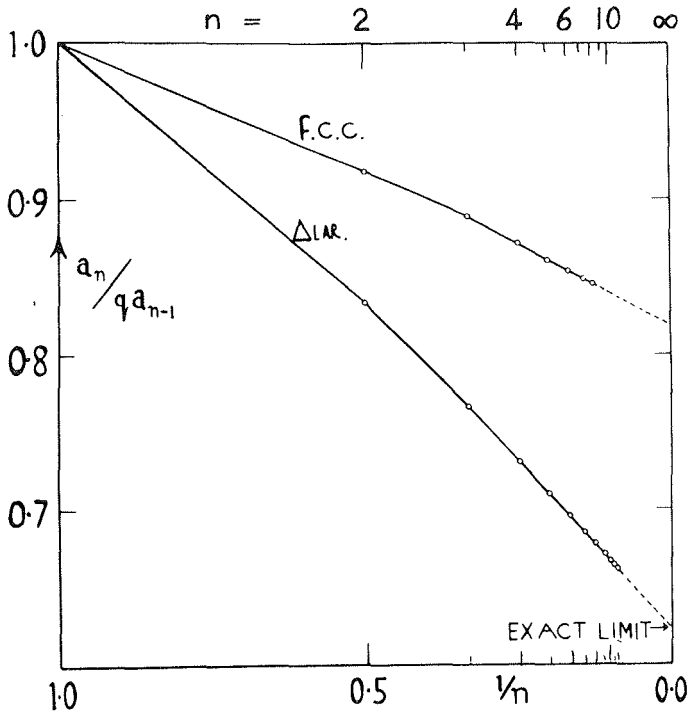


Figure 27.1. Ratios of coefficients of the susceptibility series of the triangular ($q=6$) and f.c.c. ($q=12$) lattices (from C. Domb and M. F. Sykes, *J. Math. Phys.* 2 63(1961)).

3.768,	3.767,	3.753
3.7414,	3.7401,	3.7395,
3.7381,	3.7368,	...

These are falling slightly so we would probably be inclined to make the estimate,

$$\mu = 1/v_c = 3.733 \pm 0.003, \quad (27.9)$$

for the critical point of the triangular lattice. Thanks to Onsager, however, we know the exact result, namely,

$$1/v_c = 2 + \sqrt{3} = 3.73205 \dots \quad (27.10)$$

We see that our estimate is accurate to within three parts in 10^4 !

It is natural to assume that the f.c.c. series will behave similarly—the same sort of configurational information has gone into the series and by the time lattice constants of nine or ten lines are included, one should have "sampled" the lattice quite fully. One may check the procedure for consistency by reexpanding in terms of $K=J/2kT_C$ (rather than v) and taking ratios in this series. One finds from the last six intercepts the estimates

$$\begin{array}{lll} kT_C/qJ = 0.826, & 0.817, & 0.8159 \\ & 0.8158, & 0.81616, & 0.81632. \end{array}$$

These seem to be converging more rapidly than in two dimensions and one might estimate finally

$$kT_C/qJ \cong 0.8162$$

which agrees closely with the v -series estimate.

Figure 27.2 curve (b) illustrates the typical alternating behaviour observed with loose packed lattices (in this case the square net). However, the ratios here are formed from the numbers c_n of n -step self-avoiding walks rather than the susceptibility coefficients! Evidently the linear behaviour of the ratios is not confined to Ising model series.

Our examples (27.5) and (27.6) show that the slope of the $(1/n)$ plot is related to the strength of the critical singularity. More generally suppose that

$$F(x) \approx \frac{A}{(1-\mu x)^\gamma} \{1 + \dots\}, \quad (x \rightarrow 1/\mu). \quad (27.11)$$

Then one has (by the Binomial Theorem)

$$a_n \approx \frac{A}{\Gamma(\gamma)} n^{\gamma-1} \mu^n, \quad (n \rightarrow \infty) \quad (27.12)$$

so that

$$\mu_n \approx \mu \left\{ 1 + \frac{\gamma-1}{n} + O\left(\frac{1}{n^2}\right) \right\}, \quad (n \rightarrow \infty). \quad (27.13)$$

Thus the limiting slope g equals $\gamma - 1$. (Note that a logarithmic singularity $\approx \ln(1 - \mu x)$ corresponds to $\gamma = 0$.)

Given an estimate μ' of μ we may estimate the slope from

$$g_n = n \left(\frac{\mu_n}{\mu'} - 1 \right) \quad (27.14)$$

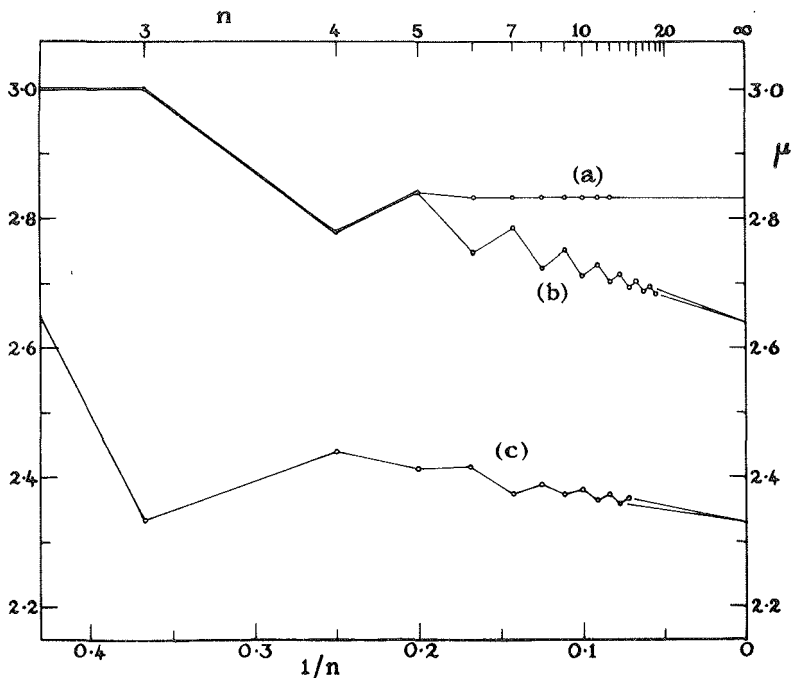


Figure 27.2. Ratios c_n/c_{n-1} for walks on the square lattice (a) with only reversals and squares disallowed, (b) with no self-intersections, (c) with no self-intersections or nearest neighbour contacts. (From M. E. Fisher and B. J. Hiley, *J. Chem. Phys.* 34, 1253(1961).)

and this should approach $g_\infty = \gamma - 1$ linearly with $1/n$ if μ' is sufficiently accurate. In this way one can actually attempt to estimate the nature of the critical singularity!

Let us try the method on the triangular lattice (using the exact critical point). We find from the last eight ratios the estimates for g :

$$\begin{array}{cccc} 0.707, & 0.717, & 0.726, & 0.728 \\ 0.729, & 0.7326, & 0.7344, & 0.7359. \end{array}$$

These are increasing quite linearly with $1/n$ and extrapolation yields the estimate

$$\gamma = 1.749 \pm 0.003. \quad (27.15)$$

Estimates for the square and honeycomb lattices converge more rapidly and also come out close to 1.75 (C. Domb and M. F. Sykes, Proc. Roy. Soc. A240, 214(1957)).* In view of the exact result $\beta = 1/8$ for all lattices, it is natural to conjecture that

$$\gamma = 1 \frac{3}{4} \quad (27.16)$$

for all plane Ising lattices. Once again we have found a large deviation from the classical prediction $\gamma = 1$.

It is hardly necessary to point out that the method leading to this conclusion is not rigorous! We have assumed that the apparent asymptotic behaviour of the first dozen or so coefficients will continue to infinity. Mathematically there is no necessity for this. However, the fact that one obtains good agreement with the exact critical points and that one understands the combinatorial origin of the coefficients gives one confidence in the reasonableness of the procedure. It would, however, be very valuable to have some general theorems assuring us, say, that the asymptotic form (27.12) was generally correct and giving an indication of the rate of convergence to it. Although no such theorems have been proved, one can, at least for the square net, obtain a check on the result $\gamma = 1 \frac{3}{4}$ by analytic arguments. (These are sketched in the next section.) It is also interesting to note that before Yang's result $\beta = 1/8$ was published, Domb (Proc. Roy. Soc. A199, 199(1949)) had suggested $\beta \cong 0.12$ to 0.13 from a study of the first nine nonzero terms of the magnetization series!

Estimates of γ for the three-dimensional lattices (s.c., b.c.c., f.c.c. and tetrahedral) yield

$$\gamma = 1.250 \pm 0.004 \quad (27.17)$$

where the indicated limits represent the uncertainties of the individual extrapolations and the differences between the different lattices. The latter are, in fact, found to be insignificant. It is hard to avoid making the conjecture that

$$\gamma = 1 \frac{1}{4} \quad (27.18)$$

is exact for all three-dimensional Ising lattices!

Actually, Domb and Sykes (Phys. Rev. 128, 168(1962)) have shown that, to within somewhat lower accuracy, this result also holds for Ising models of arbitrary spin (up to $S = \infty$, in fact). They

*The reader with access to a desk calculator might like to try the procedure for himself on the series (26.1)!

also examined the high-temperature series for the Heisenberg model by the same method. As explained, fewer terms are available for the Heisenberg model and their behaviour, especially for low spin, is not as regular. From the series for $S = \infty$, however, one can conclude that

$$1.33 \leq \gamma \leq 1.34 \quad (27.19)$$

which actually represents a larger departure from the classical prediction $\gamma=1$ than in the case of the Ising model.[†] Domb and Sykes showed that this result again seemed to be independent of lattice structure and of spin, and they suggested that the exact value might be $\gamma = 4/3$. We will describe an experimental test of this four-thirds law in the following sections.

28. Extensions

As a refinement of the ratio method let us note that if one has an estimate g' for the slope, a more rapidly convergent sequence of estimates for the critical point will be obtained from

$$\mu_n^* = \frac{na_n}{(n+g')a_{n-1}} = \mu \{1 + \underline{O}(1/n^2)\}. \quad (28.1)$$

If g' differs slightly from g the only effect will be to retard the convergence somewhat by adding a term $(g-g')/n$.

Figure 28.1 shows the behaviour of these estimates versus $1/n$ for (A) the square lattice, where the exact limit is indicated, and (B) and (C) for the simple and body-centered cubic lattices. (The reduced ratios $\beta_n = \mu_n^*/g$ are plotted.) The horizontal lines labelled β^+ and β^- represent $\frac{1}{2}$ per cent deviations above and below the estimated limits. It is interesting that the convergence is more regular in three dimensions than in two.

In this way a set of best estimates of the critical points is obtained.[‡] For the simple cubic lattice the result is

$$v_C = \tanh(J/2kT_C) = 0.21815 = 1/4.5840. \quad (28.2)$$

[†] One might remark that for self-avoiding walks in two and three dimensions the corresponding exponents are found to be $\gamma = 4/3$ and $7/6$ respectively to within about ± 0.005 .

[‡] The best estimates of the critical points and other critical parameters have been tabulated by M. E. Fisher, *J. Math. Phys.* 4, 278 (1963). Note, however, that the entropy estimates for the simple cubic lattice should be altered to $S_C \cong 0.560$, $S_\infty - S_C \cong 0.133$.

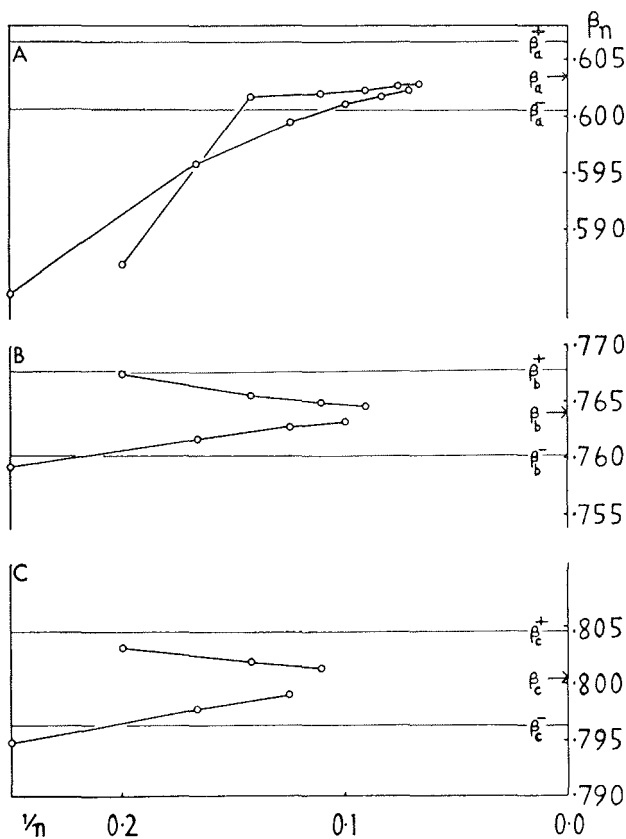


Figure 28.1. Plot of the refined critical point estimates $\beta_n = \mu_n^*/q$ for (A) the square lattice, (B) the simple cubic lattice, and (C) the body-centered cubic-lattice (from Domb and Sykes *loc. cit.*).

There seems little doubt that this is accurate to better than one part in 10^3 and probably to about one part in 10^4 . (As we will see, estimates based on quite a different procedure agree to this extent.)

If we have accurate estimates for the critical point μ and the exponent γ we may estimate the amplitude of the singularity (see Equations (27.11) and (27.12)) from the sequences

$$A_n = a_n \Gamma(\gamma) / n^{\gamma-1} \mu^n, \quad (28.3)$$

or

$$A_n^* = a_n / \binom{n+\gamma-1}{n} \mu^n. \quad (28.4)$$

This latter expression, in terms of the binomial coefficient, is usually more convenient to calculate and often converges more rapidly. Slight errors in the estimates for μ and γ will become amplified in estimating A so that only lower accuracy is attainable. (This provides one justification for obtaining the estimate of μ to as high an accuracy as possible.)

Having obtained estimates for μ , γ and A , one is in a position to write an extrapolation formula for the numerical evaluation of the function $F(x)$ when only the first N coefficients are known exactly. Thus

$$F(x) \cong \sum_{n=0}^N a_n x^n + R_N(x) \quad (28.5)$$

where for the remainder we may most conveniently take

$$\begin{aligned} R_N(x) &= \sum_{n=N+1}^{\infty} A \binom{n+\gamma-1}{n} \mu^n x^n \\ &= A(1-\mu x)^{-\gamma} - \sum_{n=0}^N a_n x^n. \end{aligned} \quad (28.6)$$

More elaborate forms of remainder may be justified if the behaviour of the coefficients a_n is sufficiently regular and is analyzed in more detail. The extrapolation formula (28.5) may, of course, be evaluated for any real or complex x . However, one can expect it to be accurate only close to the positive real axis from $x=0$ to $x=x_C = 1/\mu$, the dominant singularity of the true function.

Figure 28.2 is a plot of the reciprocal initial susceptibilities of two- and three-dimensional Ising lattices calculated by the above procedures. The Weiss mean field prediction is shown for comparison. Note that since $\gamma > 1$ in two and three dimensions, the curves for these lattices actually come into the origin with zero slope although this is not very apparent from the figure.

Let us stress again that all the evidence indicates that the critical point behaviour is independent of the lattice structure and also independent of spin (although strongly dependent on dimensionality).

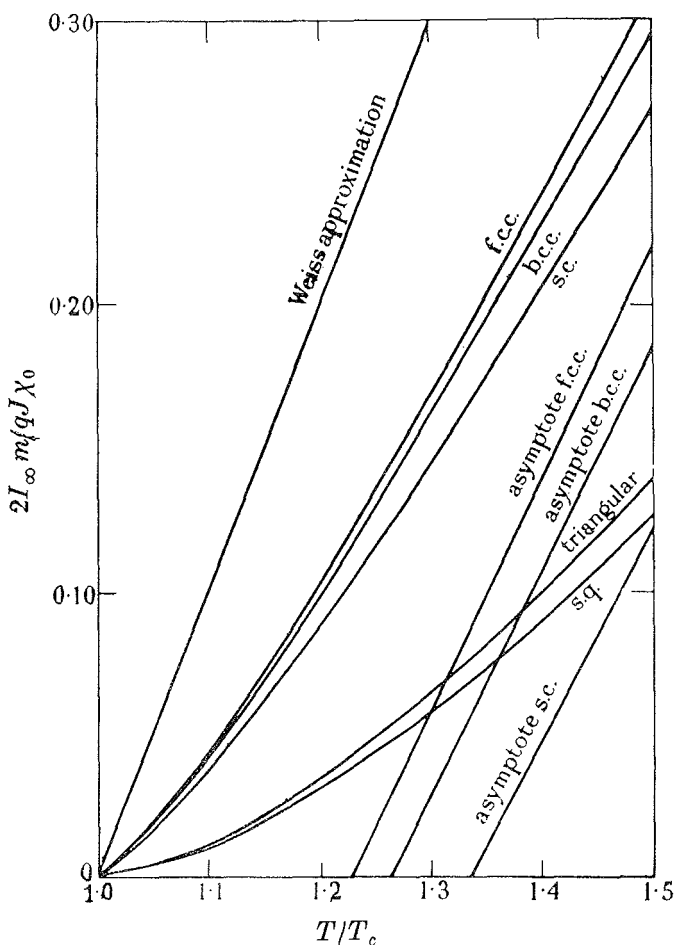


Figure 28.2. Reciprocal susceptibilities of two- and three-dimensional Ising models compared with the Weiss mean field prediction (from C. Domb and M. F. Sykes, Proc. Roy. Soc. A240, 214(1957)).

29. Ferromagnetic Susceptibility of the Square Lattice

Before confronting the nonclassical laws for the susceptibility with experiment let us briefly sketch the analytical arguments leading to the result $\gamma = 7/4$ for the square net.*

*See M. E. Fisher, *Physica* 25, 521(1959); 28, 172(1962); *J. Math. Phys.* 5, 944(1964).

From the fluctuation theorem (25.6) we see that the divergence of $\chi_0(T)$ as $T \rightarrow T_C$ must come from the increasingly slow decay of the correlation functions $\langle s_0 s_r \rangle$ for large r , and the consequent slow convergence of the sum over r . Now, as we pointed out in Section 26, the correlation functions decay, to leading order, exponentially with distance. We may thus write

$$\omega_r(T) = \langle s_0 s_r \rangle = e^{-\kappa r} W_r(T) \quad (29.1)$$

where $W_r(T)$ does not vary exponentially fast with r as $r \rightarrow \infty$. The inverse range of correlation κ will depend on temperature[†] and will approach zero as $T \rightarrow T_C$ corresponding to the correlations becoming "long-ranged." In fact Onsager, in his original paper, showed that as $T \rightarrow T_C$

$$\kappa(T) = c(T - T_C). \quad (29.2)$$

(κ is proportional to the logarithm of the ratio of the largest eigenvalue of M to the second largest eigenvalue but these eigenvalues become degenerate at T_C .)

At the critical point we thus have

$$\omega_r(T_C) = W_r(T_C). \quad (29.3)$$

We now appeal to Onsager and Kaufman's evaluation of the correlation functions. Their general result expresses $\omega_r(T)$ as a complicated determinant (of order proportional to r) and is quite intractable. At the critical point, however, Onsager was able to evaluate the determinant explicitly as a product of gamma functions. Asymptotic analysis of this formula yields the striking result[‡]

$$\omega_r(T_C) = \frac{A}{r^{\frac{1}{4}}} \{1 + O(1/r^2)\}, \quad (r \rightarrow \infty), \quad (29.4)$$

where the correction term is already quite small at the nearest neighbour distance. Comparing with (29.3) gives an expression for $W_r(T_C)$. We might now ignore the dependence of $W_r(T)$ on T near T_C but a more careful analysis of the expression for the correlation functions in terms of the transition matrix and its spectrum shows that this is not quite correct. For large r and T near T_C we may, however, write

[†] Actually there is also a slight dependence on direction which becomes negligible near T_C and which does not in any case affect the general argument.

[‡] We again neglect a slight and unimportant dependence on angle.

$$W_r(T) = (A/r^{3/4}) [1 + Q(\kappa r)] \quad (29.5)$$

where $Q(t) \rightarrow 0$ as $t \rightarrow 0$ and, as before, $Q(\kappa r)$ cannot vary exponentially fast as $t \rightarrow \infty$. Substituting in (29.1) and in the fluctuation theorem (25.6) yields,

$$kT\chi_0(T)/m^2 \approx 1 + \sum_r (Ae^{-\kappa r}/r^{3/4}) [1 + Q(\kappa r)]. \quad (29.6)$$

Near T_C where the sum is diverging, we may safely replace it by an integral,

$$\sum_r \rightarrow 2\pi \int_0^\infty r dr.$$

Making the change of variable $\kappa r = t$ we then obtain

$$kT\chi_0(T)/m^2 \approx 2\pi A\kappa^{-7/4} \int_0^\infty e^{-t} t^{3/4} [t + Q(t)] dt. \quad (29.7)$$

The integral here is a pure number, say I , so that, substituting with (29.2) we finally obtain, as $T \rightarrow T_C$,

$$\chi_0(T) \approx (m^2/kT)(2\pi AI/c^{7/4})/(T - T_C)^{7/4}. \quad (29.8)$$

This confirms the result $\gamma = 7/4$.

Chapter VIII

We will now turn again to experiment and discuss the compressibilities, susceptibilities, critical isotherms and specific heats in the light of our theory.

30. Compressibilities and Susceptibilities

Our prediction $\gamma > 1$ shows that a plot of reciprocal compressibility or susceptibility near T_C should be significantly curved (see Figure 28.2). Consequently if a straight line is fitted to the data above T_C (as has often been done by experimentalists in virtue of the classical result $1/\chi_0 \cong a(T - T_C)$) it should cut the axis at an apparent Curie point greater than the true transition point.

Figure 30.1 shows a plot of the reciprocal compressibility of Xenon, suitably normalized, above T_C at densities close to critical (prepared from the data of H. W. Habgood and W. G. Schneider, Can. J. Chem. 32, 98(1954)). The data (open circles) lie on a curve so that $\gamma > 1$ is definitely indicated. The solid line, following the law

$A[(T/T_C) - 1]^{5/4}$, is based on the lattice gas prediction (with A chosen to fit the data near T_C). In the conventional phrase, "the theoretical curve gives a very good fit to the data" (some deviations away from T_C must be expected since the $\gamma = 5/4$ law is only asymptotic as $T \rightarrow T_C$).

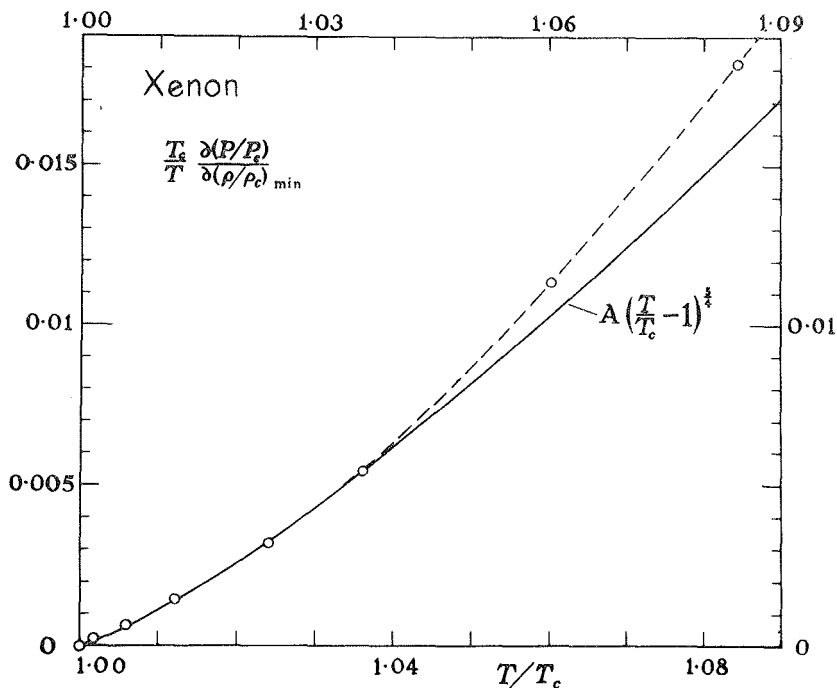


Figure 30.1. Reciprocal compressibility of Xenon above T_C (from M. E. Fisher, *J. Math. Phys.* 5 (July 1964)).

Despite the "good fit" one should not be too impressed! If one looks more closely at the data (especially near T_C , where the experiments are most difficult and the errors introduced by the numerical differentiation involved in deriving K_T from the data), one finds they are somewhat irregular. One may, preferably, attempt to calculate a value of γ directly from the data. Although one can conclude with reasonable confidence that $\gamma_{\text{Xenon}} > 1.1$, the results prove rather indeterminate and one must conclude that more experimental data are needed. One may hope that these will be forthcoming.

Some of the best experiments on a ferromagnet near its Curie point are those made by Weiss and Forrer on nickel in 1926 (*Ann.*

physique 5, 153). Recently Dr. J. S. Kouvel and I[†] have re-analyzed these data in the light of the general prediction

$$\chi_0(T) = \frac{B}{(T-T_C)^\gamma} \{1 + \dots\}, \quad (T \rightarrow T_C). \quad (30.1)$$

To determine the true initial (zero field) susceptibility from the finite field measurements one may plot M^2 versus H/M at fixed temperature.[‡] According to classical theory this should yield a set of straight lines near T_C (see Equation (16.4)). One finds, however, a set of nearly parallel curves. Extrapolation to zero magnetization is easily performed and this yields accurate values for

$$\chi_0(T) = \lim_{M^2 \rightarrow 0} (H/M). \quad (30.2)$$

Rather than attempt some sort of least-squares fit, a more sensitive method of finding γ is to form (by numerical differentiation)

$$\frac{\partial}{\partial T} \ln \chi_0^{-1}(T) = \frac{\gamma}{T - T_C} + \dots \quad (30.3)$$

where the expected behaviour follows from (30.1). Consequently,

$$X(T) = 1/(\partial/\partial T) \ln \chi_0^{-1} = (1/\gamma)(T - T_C) \{1 + o(T - T_C)\}, \quad (30.4)$$

so that a plot of $X(T)$ versus T near T_C should be substantially linear, whatever the value of γ . This is found to be so and an accurate estimate of T_C can hence be found by extrapolation to $X=0$.

Now to estimate the ideal value of γ consider the temperature dependent "effective exponent"

$$\gamma^*(T) = (T - T_C)(\partial/\partial T) \ln \chi_0^{-1}. \quad (30.4a)$$

As $T \rightarrow \infty$, $\gamma^*(T)$ approaches the Curie-Weiss value unity but as $T \rightarrow T_C$

$$\gamma^*(T) = \gamma - a(T - T_C) + \dots \quad (30.5)$$

(Although it is conceivable that the true correction term is somewhat sharper than $(T - T_C)$.) A plot of $\gamma^*(T)$ versus T for nickel in the range $\Delta T/T_C = \frac{1}{2}$ per cent to 12 per cent is shown in Figure 30.2. (The indicated uncertainties arise largely from the numerical

[†]Phys. Rev. 136, A1626 (1964).

[‡]This method is due to Belov and Goryaga and to Kouvel.

differentiation.) The result,

$$\gamma_{\text{nickel}} = 1.35 \pm 0.02, \quad (30.6)$$

is clearly indicated!

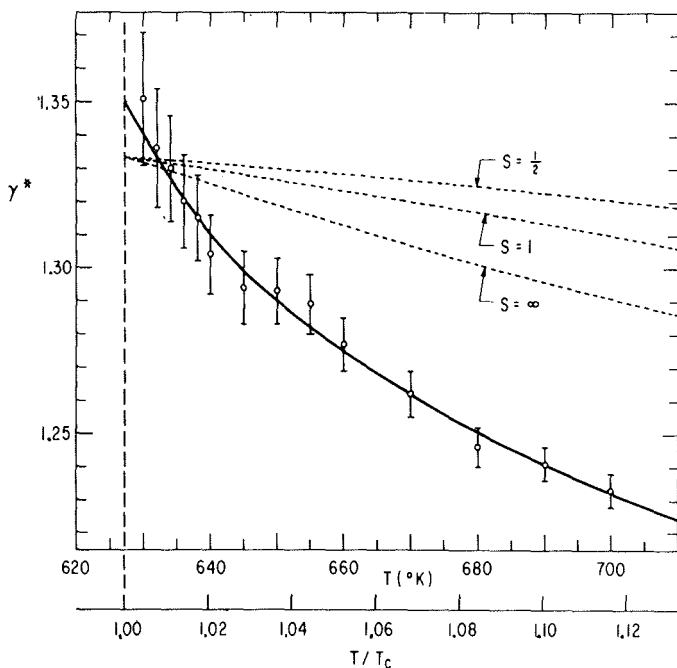


Figure 30.2. Plot of the effective exponent $\gamma^*(T)$ for nickel (from J. S. Kouvel and M. E. Fisher, Phys. Rev. 136, A1626 (1964)).

This value of γ lies well above, not only its classical prediction, but also above the value $\gamma = 1.25$ for the three-dimensional Ising model. All the more surprizingly, it agrees closely (to within its theoretical and experimental uncertainties) with the prediction $\gamma \cong 4/3$ for the nearest neighbour Heisenberg model! As we explained, it is difficult to believe that the localized spin Heisenberg picture is a realistic model for nickel. We thus seem forced to conclude that the behaviour close to T_C is insensitive to the details of the true Hamiltonian. Only the general statistical features notably the dimensionality and the, presumably, finite ranged and isotropic

Interactions seem to determine the nature of the singularity.

We should mention that in experiments on iron very close to T_C Noakes and Arrott (J. Appl. Phys. 35, 931 (1964)) found from a least squares fit $\gamma = 1.37 \pm 0.04$. Miedema, Van Kempen and Huiskamp (Physica 29, 1266 (1963)) observed that $\chi_0(T)$ for the ferromagnetic salts $\text{CuK}_2\text{Cl}_4 \cdot 2\text{H}_2\text{O}$ and $\text{Cu}(\text{NH}_4)_2\text{Cl}_4 \cdot 2\text{H}_2\text{O}$ could be fitted quite well, from about 4 per cent above T_C to about 50 per cent above T_C , by $\gamma = 1.36$ and 1.37 , respectively.

The dashed lines in Figure 30.2 are the theoretical predictions of $\gamma^*(T)$ for the nearest neighbour f.c.c. Heisenberg lattice for various spins. The deviations from the experiments might represent the effects of nonlocalization of the spins. They can also be interpreted, however, as due to the effects of longer range interactions or a slowly changing effective magnetic moment of the spins in nickel.

31. Critical Isotherms

Widom and Rice (J. Chem. Phys. 23, 1250 (1955)) analyzed the critical isotherms of xenon, hydrogen and carbon dioxide and concluded that they were significantly flatter than the Van der Waals prediction (15.4). They found the data were best represented by the power law

$$p - p_C \cong a(\rho - \rho_C)^\delta \quad (31.1)$$

with $\delta = 4.2$ rather than $\delta = 3$.

Figure 31.1 shows a plot of M^3 versus H at the Curie point of nickel, derived again from the measurements of Weiss and Forrer. (In the figure, σ denotes the magnetization density M .) At these relatively very small fields) classical theory would lead one to expect an accurate straight line. If the data are analyzed, in analogy with the susceptibility, in terms of a relation

$$H = aM^\delta + \dots, \quad (31.2)$$

one finds $\delta = 4.22 \pm 0.05$. The dashed line in Figure 31.1 corresponds to $\delta = 4.22$ and agrees closely with the experimental data.

We notice once again the close similarity between the critical behaviour of a fluid and a ferromagnet. As yet no theoretical estimates have been made for the exponent δ , although for the Ising model the necessary series are available and estimates should be forthcoming soon.†

†Note added in proof. The results are $\delta = 15.00 \pm 0.08$ and 5.20 ± 0.15 in two and three dimensions respectively. See D. S. Gaunt, M. E. Fisher, M. F. Sykes and J. W. Essam; Phys. Rev. Letters 13, 713 (1964).

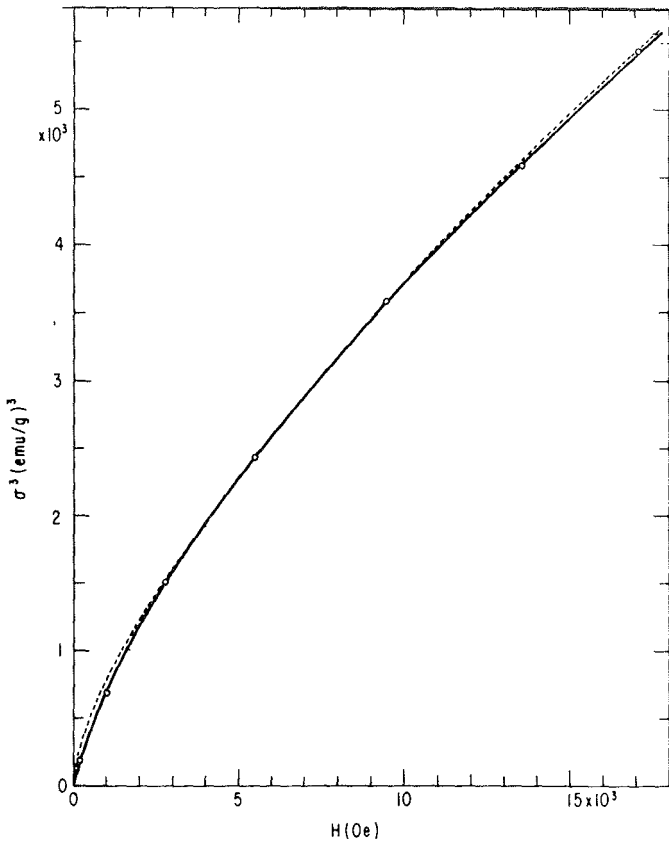


Figure 31.1. Critical isotherm for nickel (from J. S. Kouvel and M. E. Fisher, loc. cit.).

32. Specific Heats

The high-temperature specific heat series for the Ising model are relatively short (since on loose packed lattices alternate terms are missing), the coefficients do not increase very rapidly and they vary less smoothly than the susceptibility coefficients. (These latter facts essentially reflect the much weaker nature of the specific heat singularities.) However, the series appear to converge up to the critical point and they may be analyzed by the ratio method.

One can conclude with confidence that

$$C(T) \rightarrow \infty \quad \text{as} \quad T \rightarrow T_C +, \quad (32.1)$$

for all the three-dimensional models. The series are not inconsistent

with a logarithmic divergence (as in two-dimensions); but, if we write, as $T \rightarrow T_C \pm$,

$$C(T) = \frac{D^\pm}{\alpha} [|1 - (T/T_C)|^{-\alpha} - 1] + \dots, \quad (32.2)$$

a careful analysis indicates $\alpha \cong 0.2$, that is, a sharper singularity. (Note Equation (32.2) yields a logarithmic singularity in the limit $\alpha \rightarrow 0$.) The amplitudes D^+ for the various lattices are, however, about one half of the two-dimensional values.

Below T_C the series cannot be handled directly by the ratio method (except in the case of the tetrahedral lattice—for the methods used, see later sections) but again the specific heat appears to diverge at T_C . The present, somewhat uncertain, numerical evidence suggests that this divergence is not sharper than logarithmic, so that we may take $\alpha' = 0$ in Equation (32.2) (using the prime to denote values of the exponent below T_C).

One may, however, calculate quite accurate numerical values for $C(T)$ except very close to T_C . Figure 32.1 shows the estimated variation[†] of the specific heat of the f.c.c. Ising lattice and approximations to it. Notice that the approximate theories, although still misleading, are more accurate than in two dimensions (compare with Figure 19.2). It is gratifying that the theoretical curve now reproduces the characteristic asymmetry about T_C noticed in the experimental results (compare with Figures 2.5 and 5.2). If, for the sake of the comparison, one fits the series to $\alpha = \alpha' = 0$, one finds the ratio D^+/D^- lies between 2.3 and 2.6 in contrast to the two-dimensional result $D^+ = D^-$.

In the case of argon a more detailed comparison with experiment is justified.[‡] To compare the experimental $C_V(T)$ data with the specific heat per site of the Ising model, we first calculate the configurational specific heat per atom from

$$\frac{C_{\text{config}}}{k} = \frac{[C_V - (3/2)Nk]}{Nk} \quad (32.3)$$

and then the reduced specific heat density

$$C^*(T) = \frac{\rho_C}{\rho_{\text{max}}} C_{\text{config}}(T). \quad (32.4)$$

[†]To within graphical accuracy this estimated curve (solid line) should be essentially exact.

[‡]The following discussion is based on a forthcoming paper: M. E. Fisher, Phys. Rev. 136, A1599 (1964).

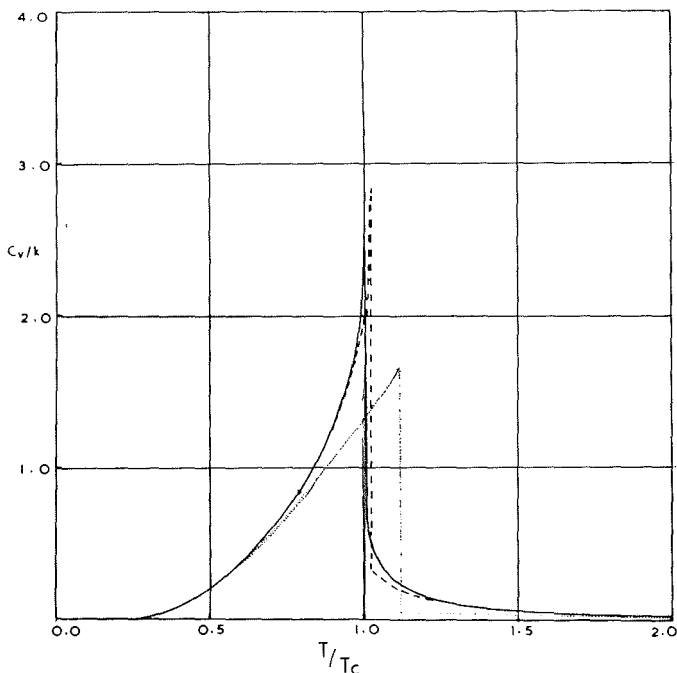


Figure 32.1. Specific heat of the f.c.c. Ising lattice from series estimates (solid curve), from the Kikuchi (dashed curve) and Bethe (dotted curve) approximations. (From C. Domb, *Adv. in Phys.* 9, Nos. 34, 35(1960).)

(For argon $\rho_C/\rho_{\max} \cong 1/3.3$.) Figure 32.2 shows a plot of $C^*(T)$ for argon versus $\ln |1 - (T/T_C)|$. The experimental data are shown by the open and shaded circles (corresponding to the experimental uncertainty in T_C), except that below $0.99 T_C$ the points crowd so closely to the line a that they are not shown. The upper curve (corresponding to $T < T_C$) is a good straight line so that we may conclude that $\alpha'_{\text{argon}} \cong 0$ and probably α' does not exceed 0.1. A similar behaviour is found for some magnetic specific heats (notably for $\text{NiCl}_2 \cdot 6\text{M}_2\text{O}$; see Figure 5.2).

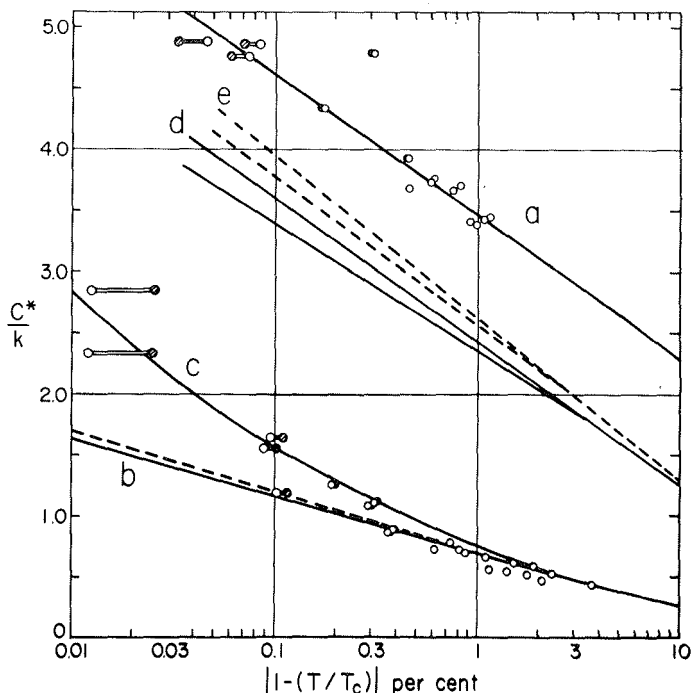


Figure 32.2. Logarithmic plot of the reduced configurational specific heat of argon (circles and line a) compared with Ising model predictions (curves b, c, d and e). (From M. E. Fisher, *Phys. Rev.* 136, A1599 (1964)).

Above T_c (lower curves) the data seem not to lie on a straight line, although they might do so close to T_c .^{*} The solid curve c is calculated for the f.c.c. Ising lattice with the preferred exponent $\alpha = 0.2$ (and fitted only to the critical point). The agreement is surprisingly good. (Curves b show the consequences of assuming $\alpha = 0$ for f.c.c. and s.c. lattices.)

^{*}The famous measurements of Fairbanks on the lambda anomaly in liquid helium revealed an accurately logarithmic singularity over four decades in $|T - T_c|$ both above and below T_c . (See M. J. Buckingham and W. M. Fairbanks, in *Progress in Low Temperature Physics III* (North Holland Publishing Company, 1961).) The behaviour of helium, however, is presumably determined essentially by quantum mechanics and it is not clear how far one should expect an analogy with the "classical" critical points.

The curves \underline{d} and \underline{e} are calculated for the f.c.c. and s.c. lattices below T_C . (The spread of the curves indicates the theoretical uncertainties.) The strength of the singularity, as represented by the slope of the lines, agrees quite well with the experimental results but the actual magnitude of $C^*(T)$ is too small by an almost constant amount (equivalent to 6.9 cal/mole °K for argon). This seems to be the main deficiency of the lattice gas description of the critical specific heat. Quite probably it is associated rather directly with the over-simple representation of the hard core by a single lattice site but further calculations are needed to confirm this.

Chapter IX

33. Low-Temperature Behaviour

In the previous sections we have seen how the nature of the critical singularities of the Ising model, as T approaches T_C from above, can be elucidated by a numerical study of the high-temperature series expansions. Can the same be done at low-temperatures and, in particular, can we estimate the spontaneous magnetization-coexistence exponent β for the three-dimensional models?

Low-temperature power series expansions of the free energy in the two variables x and y (see Equation (10.8)) can be derived by overturning spins in a fully magnetized lattice ($y = 0, H = \infty$). By differentiation a series for the magnetization is obtained, and on setting $y = 0$ (i.e., taking the limit $H \rightarrow 0$) one obtains an expansion for the spontaneous magnetization in powers of x . (The procedure can, of course, be checked in two dimensions.) For the f.c.c. lattice many terms have been calculated and, writing $u = x^2$, we find

$$\begin{aligned}
 M_0(T) = & 1 - 2u^6 - 24u^{11} + 26u^{12} + 0 + 0 \\
 & - 48u^{15} - 252u^{16} + 720u^{17} - 438u^{18} \\
 & - 192u^{19} - 984u^{20} - 1008u^{21} + 12924u^{22} \\
 & - 19536u^{23} + 3062u^{24} - 8280u^{25} \\
 & + 26694u^{26} + 153536u^{27} - 507948u^{28} \\
 & + \dots
 \end{aligned} \tag{33.1}$$

A quick glance at this series shows that the ratio method is quite inapplicable; the magnitudes of the coefficients go up and down in an erratic fashion and the signs also seem quite random! What does this mean? The answer is more immediately obvious if we look

at the series for the simple cubic lattice. This is found to have smoothly increasing coefficients but the signs alternate regularly. Clearly, this means that the nearest singularity of the function $M_0(u)$ lies on the negative u axis (corresponding to a complex temperature) rather than on the real positive u axis where we expect to find the singularity corresponding to the critical point! Since the "nonphysical" singularity lies nearer the origin than the physical singularity, it dominates the behaviour of the coefficients and determines the radius of convergence. The more complicated behaviour of the f.c.c. coefficients evidently means that the dominant singularities lie in the complex u -plane away from the axes (see Figure 33.1). In fact, it transpires that two or more pairs of complex nonphysical singularities intervene between the origin and the critical singularity u_c . The radius of convergence is determined by the nearest pair of singularities (see Figure 33.1) and is appreciably less than u_c .*

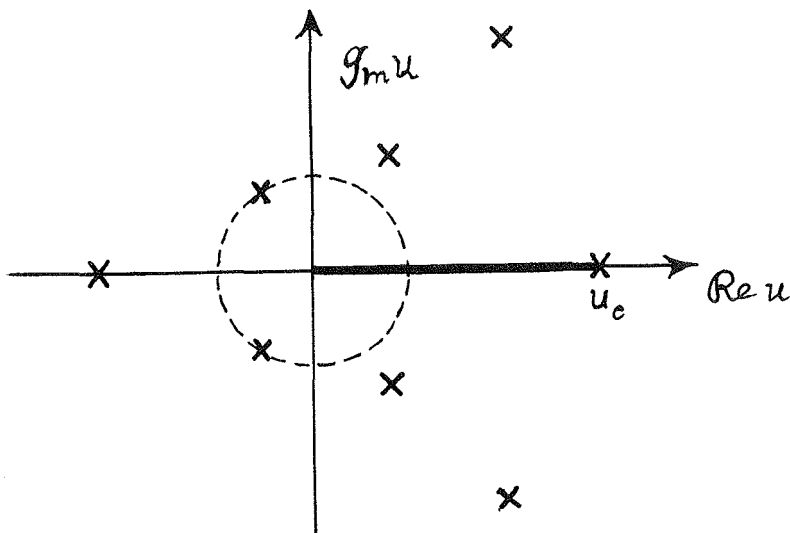


Figure 33.1. Complex u plane illustrating the physical region on the real positive axis, and interfering singularities which limit the radius of convergence.

To overcome the difficulty, various methods of grouping terms corresponding to a fixed number of overturned spins were tried (the "metastable method"). Although reasonably accurate numerical values could be calculated below T_c , little significant information

*It might be mentioned that low-temperature series for the two-dimensional lattice converge up to the physical critical point.

was gained regarding the critical singularities. Real progress was made only with the application of the Padé approximant method, introduced into physics by Baker and Gammel (J. Math. Anal. and Appl. 2, 21(1961) and G. A. Baker, Jr., J. L. Gammel and J. G. Wills, ibid., p. 405) and first applied to the Ising model by Baker (Phys. Rev. 124, 768(1961)).

34. Padé Approximants

Our mathematical task, as before, is given a function $F(x)$ in terms of its Taylor series expansion coefficients to study its behaviour near one of its singularities. In this case, however, the singularity of interest lies beyond the radius of convergence of the power series so that the function must be analytically continued. In principal, if one has a complete convergent power series expansion, a function can be analytically continued up to and around all its singularities, the process stopping only at a natural barrier of the function (beyond which it remains undefined). What we require, therefore, is a practical method of approximate analytical continuation.

We pointed out the deficiencies of approximating $F(x)$ by a polynomial (straight truncation) or by a reciprocal polynomial (truncation of the series for $1/F(x)$) but let us consider, more generally, approximation by a ratio of polynomials

$$F(x) \cong \frac{P_L(x)}{Q_M(x)} = \frac{p_0 + p_1x + \dots + p_Lx^L}{q_0 + q_1x + \dots + q_Mx^M}. \quad (34.1)$$

We may clearly choose

$$q_0 = 1$$

with no loss of generality. To choose the remaining $L+M+1$ coefficients $p_0, p_1, \dots, p_L, q_1, q_2, \dots, q_M$, let us demand that the power series expansion of $P_L(x)/Q_M(x)$ agree with the first $N+1$ exactly known coefficients a_0, a_1, \dots, a_N of the expansion of $F(x)$. Clearly we must, in general, choose $L+M = N$ in order to have sufficient relations to determine the p_i and q_j .

To see what is involved in calculating the coefficients of such an $[L, M]$ Padé approximant, cross-multiply in (33.1) to obtain

$$\left(\sum_{n=0}^N a_n x^n \right) \left(\sum_{i=0}^M q_i x^i \right) \cong \sum_{j=0}^L p_j x^j \quad (34.2)$$

and require that this relation be an identity in the first N powers of x . Equating coefficients of x^0 to x^L (and recalling $q_0 = 1$) yields $a_0 = p_0$ and

$$\begin{bmatrix} a_1 \\ a_2 \\ a_3 \\ \vdots \\ \vdots \\ \vdots \\ a_L \end{bmatrix} + \begin{bmatrix} a_0 & & & & \\ a_1 & a_0 & & & \\ a_2 & a_1 & a_0 & & \\ \vdots & \vdots & \vdots & \vdots & \\ \vdots & \vdots & \vdots & \vdots & \\ \vdots & \vdots & \vdots & \vdots & \\ a_{L-1} & a_{L-2} & a_{L-3} & \dots & a_0 \end{bmatrix} \begin{bmatrix} q_1 \\ q_2 \\ q_3 \\ \vdots \\ \vdots \\ \vdots \\ q_L \end{bmatrix} = \begin{bmatrix} p_1 \\ p_2 \\ p_3 \\ \vdots \\ \vdots \\ \vdots \\ p_L \end{bmatrix} \quad (34.3)$$

where, if $M < L$, we set $q_{M+1}, q_{M+2}, \dots, q_L$ equal to zero. From the coefficients of x^{L+1} to x^{L+M} we get

$$\begin{bmatrix} a_{L+1} \\ a_{L+2} \\ \vdots \\ \vdots \\ \vdots \\ a_{L+M} \end{bmatrix} + \begin{bmatrix} a_L & a_{L-1} & \dots & a_{L-M+1} \\ a_{L+1} & a_L & \dots & a_{L-M+2} \\ \vdots & \vdots & \vdots & \vdots \\ \vdots & \vdots & \vdots & \vdots \\ \vdots & \vdots & \vdots & \vdots \\ a_{L+M-1} & a_{L+M-2} & \dots & a_L \end{bmatrix} \begin{bmatrix} q_1 \\ q_2 \\ \vdots \\ \vdots \\ \vdots \\ q_M \end{bmatrix} = 0 \quad (36.4)$$

where, if $L < M$, we set $a_{-1}, a_{-2} \dots$ equal to zero. This latter equation is a set of M linear equations for the denominator coefficients. The solution, in an obvious matrix notation, is

$$q = -A_2^{-1} a_2, \quad (34.5)$$

and substitution in (34.3) then yields the numerator coefficients,

$$p = a_1 + A_1 q = a_1 + A_1 A_2^{-1} a_2. \quad (34.6)$$

Calculation of the coefficients is therefore a routine matter readily performed with the aid of an electronic digital computer. In practice, the Equations (34.4) are often rather "ill-conditioned" (i.e., the determinant of A_2 is small) so that precautions must be taken to prevent the build-up of round-off errors. If $\det A_2$ vanishes identically, a Padé approximant of the form sought does not exist. We might remark that Padé approximants are equivalent to a certain class of continued fractions and an alternative sequential method for the calculation of approximants of the form $[M+l, M] \quad M=1, 2, 3 \dots$ can be based on this approach.

35. Analytical Character

The advantage of using an $[L, M]$ Padé approximant is that it has both zeros and poles (i.e., the zeros of $P_L(x)$ and the zeros of $Q_M(x)$). Thus if $F(x)$ is meromorphic inside some circle (i.e., has only poles), we might hope for rapid convergence of the approximants throughout the circle, and in particular beyond the nearest pole to the origin.* In fact, it is clear that if $F(x)$ consists of a sum of m poles of different amplitudes, we will obtain the exact answer from the sequence of "diagonal approximants" $[M, M]$ once $M \geq m$. Practical numerical experiments show that in such a case convergence in the vicinity of the nearer poles is extraordinarily rapid even when $M \ll m$. This rapid convergence may be understood by noting that diagonal approximants are invariant under the Euler transformation

$$x = \frac{cw}{1 + \lambda w}, \quad (35.1)$$

which is often used to hasten the convergence of power series. We thus see that in a certain sense the diagonal approximants are at least as effective as the best Euler transformation. In practice, the near-diagonal sequences $[M \pm \ell, M]$ are observed to converge equally rapidly.

Suppose now that our function $F(x)$ has branch points rather than merely poles, for example,

$$F(x) = (1 + 2x)^{\frac{1}{2}} (1 + x)^{-\frac{1}{2}}, \quad (35.2)$$

or

$$F(x) = -(1/x) \ln(1 - x). \quad (35.3)$$

What will the Padé approximants do? First, let us note that a Padé approximant is a single-valued function throughout the complex x -plane whereas functions with branch points are many-valued. Consequently, we could at best hope for the approximants to converge to $F(x)$ in a suitably cut plane. In practice this is just what seems to happen!

The Padé approximants "select" a particular set of branch cuts and "place" a series of alternating zeros and poles along the

*There are relatively few rigorous theorems on the convergence of Padé approximants but it has, for example, been proved that if $F(x)$ is analytic for $|x| \leq R$ except for m poles within this circle, then the sequence $[M, m]$ converges uniformly to $F(x)$ as $M \rightarrow \infty$ throughout the circle except for points within small circles surrounding the m poles. (See Baker, Gammel and Wills, loc. cit.)

cut.* For example, the $[1,1]$ approximant to (35.2) is

$$\frac{1 + (7/4)x}{1 + (5/4)x}$$

so that the zero and pole lie at $x = -4/7$ and $-4/5$ on the "obvious" choice of cut from $x = -\frac{1}{2}$ to $x = 1$! (See Figure 35.1.) For (35.3) the $[1,1]$ approximant is $(1 - x/6)/(1 - 2x/3)$ and the zero and pole lie at $x = 6$ and $x = 1\frac{1}{2}$ on the cut from $x = +1$ to $+\infty$. As we increase the order of the approximants the zeros and poles on the cuts close up to form, in an electrostatic analogy, a "dipolar layer" of strength just sufficient to give the discontinuity in $F(x)$ that must occur when one crosses a cut. Except in the vicinity of the cuts, the approximants still converge rapidly and may be used to compute $F(x)$ far outside the circle of convergence of the original power series.

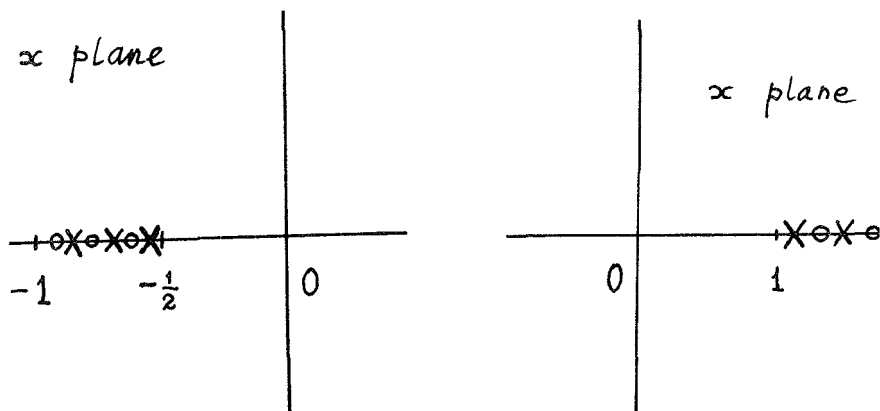


Figure 35.1. Illustrating the distribution of zeros and poles of the Padé approximants to the functions of Equations (35.2) and (35.3).

However, if we know or suspect that our function has an algebraic branch point at a "critical point" x_c , so that

$$F(x) = A(x - x_c)^{\delta} \{1 + O(x - x_c)\}, \quad (x \rightarrow x_c), \quad (35.4)$$

*Although in simple examples it is easy to guess which cuts will be selected, no criteria are known for deciding this point in general.

we will do better by studying the series for $D(x)$, the logarithmic derivative of $F(x)$ (compare with Section 30). Since

$$\frac{\partial}{\partial x} \ln F(x) = \frac{\delta}{(x - x_C)} + O(1); \quad (x \rightarrow x_C), \quad (35.5)$$

this function will have only a simple pole at $x = x_C$. Consequently, we can expect the approximants to $D(x)$ to converge rapidly in the vicinity of the original branch point. Furthermore, the position of the pole in the approximant which will appear in the neighbourhood of x_C will give an estimate of the true critical point x_C and, more importantly, the residue at this pole will represent an approximation to the critical exponent δ .

Notice that if our function $F(x)$ were simply a product of algebraic factors like (35.2), for which

$$D(x) = \frac{(\frac{1}{2})}{\frac{1}{2} + x} + \frac{(-\frac{1}{2})}{1 + x}, \quad (35.6)$$

our technique would eventually yield the exact result! (This would happen with the spontaneous magnetization series of the two-dimensional Ising lattices.)

If we have an exact value or a good estimate for x_C a more accurate method of estimating the exponent δ will be to form the series for

$$\delta^*(x) = (x - x_C) \frac{\partial}{\partial x} \ln F(x) = \delta + O(x - x_C) \quad (35.7)$$

(as in Section 30) and to evaluate the approximants to this series at $x = x_C$, which will be an analytic point of $\delta^*(x)$.

Conversely if we know, or have a good estimate for, δ a refined estimate of x_C will be obtained by locating the appropriate pole in the approximants to the series for

$$[F(x)]^{-1/\delta} = \frac{B}{(x - x_C)} + O(1), \quad (35.8)$$

since this function has a simple pole and convergence should be rapid. Given accurate values of δ and x_C we can evaluate $F(x)$ itself accurately in the neighbourhood of x_C by writing,

$$F(x) = A(x) (x - x_C)^\delta, \quad (35.9)$$

forming the series for $A(x)$ and evaluating the approximants to $A(x)$ at the points of interest.

The above procedures are based on the supposition that $F(x)$ has a pure algebraic branch point at x_c . We might hope, however, that they would still work moderately well if any other coincident singularities were sufficiently weak. Logarithmic singularities like (35.3) present more difficulty since the logarithmic derivative will still contain a logarithmic branch point. Similarly the derivative $F'(x)$ will in general contain both a pole and a logarithmic singularity. For example, from (35.3),

$$F'(x) = \frac{1}{(1-x)} + x^{-1} [1 + x^{-1} \ln(1-x)]. \quad (35.10)$$

Although in particular cases the pole will now dominate, it is clear that we must be prepared for slower convergence near the critical point and branch cut.

36. Applications to the Ising Model

Let us, following Baker, first try these techniques on the Ising model high-temperature susceptibility series. Estimating the critical point and the exponent γ from the poles and residues of the $[M, M]$ approximants to the logarithmic derivative (Equation (35.5)) yields, for the plane square lattice,

$M = 2$	$v_c \cong 0.4111$	$\gamma \cong 1.654$
3	0.4093	1.626
4	0.4164	1.797
5	0.4121	1.682
6	0.41412	1.746
7	0.4142106	1.7496.

The last estimate of v_c agrees with the exact result, 0.4142135..., to the first five decimal places! The corresponding estimate for γ deviates from $7/4$ by only 0.0004. Results for the honeycomb and triangular lattices are equally encouraging. For the simple cubic lattice one similarly finds

$M = 2$	$v_c \cong 0.2151$	$\gamma \cong 1.205$
3	0.2189	1.281
4	0.21815	1.2505
5	0.21818	1.2518.

The agreement with the estimates $v_c = 0.21815$ and $\gamma = 1\frac{1}{4}$ based on the ratio method is astonishingly close and increases one's confidence in the reliability and accuracy of both methods. (The results for the f.c.c. and b.c.c. lattices are quite comparable.)

Using the exact critical points in two dimensions, let us estimate γ by forming the approximants to $\gamma^*(v_C)$ as in Equation (35.7). For the square net the last four estimates are

$$\gamma \cong 1.728, \quad 1.7516, \quad 1.7499, \quad 1.7498$$

while for the honeycomb lattices, where twenty-four terms are available, one finds for the last five estimates

$$\gamma = 1.754, \quad 1.7503, \quad 1.75019, \quad 1.75019, \quad 1.75009.$$

In three dimensions, adopting Baker's estimates

$$v_C \cong 0.101767, \quad (\text{f.c.c.})$$

and

$$\cong 0.218156, \quad (\text{s.c.})$$

which differ by only one or two parts in 10^4 from the ratio method estimates, one computes from $\gamma^*(v_C)$ the estimates

$$\begin{aligned} \gamma \cong 1.259, \quad 1.2498 \quad 1.2498 \quad (\text{f.c.c.}) \\ \cong 1.22, \quad 1.30, \quad 1.2502, \quad 1.2507, \quad 1.2505 \quad (\text{s.c.}). \end{aligned}$$

There thus seems little doubt that the result $\gamma = 1\frac{1}{4}$, based on the ratio method, is exact! (It should be noticed that changes in the last two places of the estimates for v_C only produce changes in the fourth place of the γ estimates.)

So far we have merely reconfirmed the conclusions of the ratio method. Let us now examine the magnetization series[†] (e.g., Equation (33.1)). Using the estimates of the critical points obtained from the high temperature susceptibility series, we find from the evaluation of the approximants to β^* the estimates

[†]This analysis was first performed by Baker who concluded $\beta \cong 0.30$, but Fisher and Essam (J. Chem. Phys. 38, 802(1963)) restudied the problem using longer series with the results presented here.

M	s.c.		f.c.c.	
4	0.303	0.304	0.282	0.238
5	0.312	0.304	0.305	0.296
6	0.322	0.278	0.297	0.293
7	0.3133	0.3141	0.303	0.314
8		0.3144	0.316	0.307
9			0.309	0.308
10			0.307	0.307
11			0.312	0.306
12				0.306

where the two columns for each lattice represent two different diagonal sequences $[M+m, M]$. These figures (and those for the b.c.c. lattice) certainly suggest that β is the same for all the lattices and yield the estimate

$$0.303 \leq \beta \leq 0.318. \quad (36.1)$$

This is consistent with the conjecture

$$\beta = \frac{5}{16} = 0.312500 \quad (36.2)$$

which is rather natural in view of the inverse powers of 2 occurring in the already established values of γ and β .

It will be noticed that the sequence of estimates is somewhat "noisy" and shows no very steady trends. Considering the complicated series from which the estimates came, this is perhaps not very surprising. This characteristic does, however, seem to be fairly typical of the behaviour of Padé approximants to functions with a number of singularities. Whereas the ratio method, when it is applicable, focuses more and more attention on the closest singularity as one studies higher and higher terms, the Padé approximants attempt also to improve the representation of the other singularities, even if at a slight cost to the accuracy near the singularity of interest.

This point is borne out by the magnetization series for the tetrahedral lattices derived by Essam and Sykes (*Physica* 29, 378 (1963)). For a three-dimensional lattice the coordination number, $q=4$, is anomalously low and apparently for this reason the low temperature series are found to have coefficients of one sign and hence to converge up to the critical point. The ratio method may thus be used and leads to a steadily increasing sequence of estimates β_n which yield the estimate $\beta=0.312 \pm 0.002$ thereby confirming the conjecture (36.2) more closely.

A further check on the consistency of $\beta = 5/16$ is obtained by estimating the critical points from $[M_0(T)]^{-1/\beta}$ as in Equation (35.8). This yields values in good agreement with the high temperature estimates whereas less satisfactory agreement is obtained if one assumes $\beta = 3/10$.

37. Physical Conclusions

The reader will, of course, have noticed, without at this stage much surprize, that the result $\beta \cong 5/16$ is seriously at variance with the classical approximate result $\beta = \frac{1}{2}$. Much more surprizing, however, is the fact that such a simplified model of a magnet or a gas could lead to a result for the exponent β so close to the experimentally observed one third laws described in the first chapter. Again the conclusion is forced on us that the detailed properties of the Hamiltonian become relatively unimportant in the critical region, whereas the dimensionality becomes a prime factor. Figure 37.1, which shows the exact and estimated spontaneous magnetization curves for various two- and three-dimensional lattices,* illustrates this point as far as the effects of lattice structure go.

One might indeed ask whether the difference between the theoretical result $\beta \cong 0.312$ and the experimental results $\beta \cong 0.33$ is significant in view of the uncertainties involved in both cases. Although for some physical systems (e.g., binary fluid solutions) this point may still be open to doubt, the high accuracy of the measurements on xenon (Section 2), on europium sulphide (Section 3) and on manganese fluoride (Section 3) seem to place the experimental values at least 0.015 above the theoretical value. The artificial nature of the Ising model does therefore make itself felt, but, as in the case of the specific heats and the susceptibilities, to a much smaller extent than might have been guessed. An outstanding theoretical task is to characterize just which relevant features of real systems are oversimplified by the model.

Unfortunately, there seems no way at present in which one might seek to estimate β for the Heisenberg model. The low-temperature behaviour in that case is given by the spin wave expansion and its correction terms which have proved exceedingly difficult to calculate. There are, however, good reasons for believing that the spin wave approach yields only an asymptotic series (terms like $e^{-J/kT}$ are neglected) so that even the complete series might not describe the critical point behaviour.

*This figure is based on earlier numerical work by D. M. Burley (Phil. Mag. 5, 909(1960)) which lead only to the rough estimate $0.25 \leq \beta \leq 0.50$. To graphical accuracy, however, Burley's actual numerical results are confirmed by the Padé approximant studies.

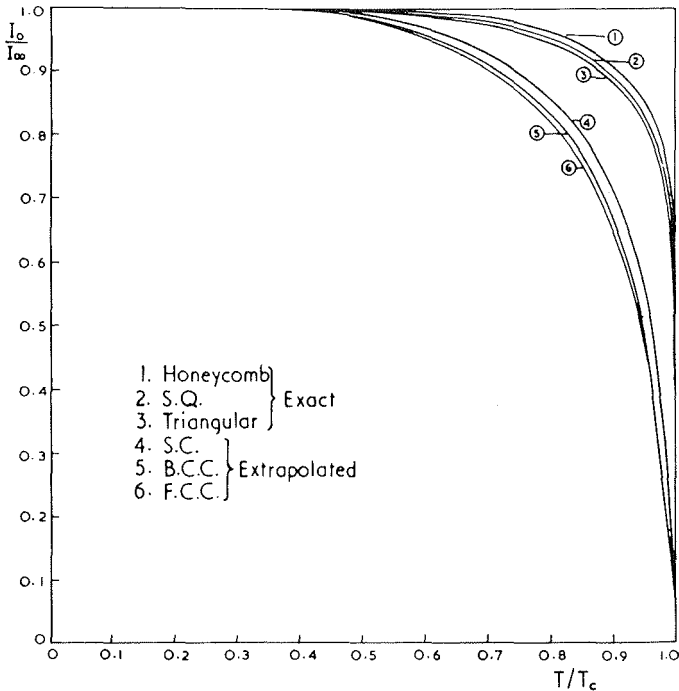


Figure 37.1. Spontaneous magnetization of two- and three-dimensional Ising lattices (from D. M. Burley, *Phil. Mag.* 5, 909(1960)).

38. Further Applications

The Padé approximant technique may also be used to study the low-temperature zero field susceptibilities.* If γ' is the exponent for the divergence of $\chi_0(T)$ as $T \rightarrow T_c^-$, one finds in two-dimensions $\gamma' = 1.75$, that is, the same value as above T_c . The amplitude of the singularity below T_c is, however, much smaller being given by

$$\frac{B^-}{B^+} \cong \frac{1}{37} \quad (38.1)$$

*J. W. Essam and M. E. Fisher, *J. Chem. Phys.* 38, 802(1963).

for all the plane lattices.

For the three-dimensional lattices the extrapolations are somewhat less certain but it appears again that $\gamma' = \gamma = 1.25$. At present, however, the uncertainties might allow γ' to be somewhat higher although it seems unlikely that γ' exceeds 1.30. The symmetry $\gamma' = \gamma$ is rather appealing theoretically and, if one accepts it provisionally (and more recent work seems to confirm it), one finds for the amplitudes above and below T_C ,

$$\frac{B^-}{B^+} \cong \frac{1}{5.2} \quad , \quad (38.2)$$

for the three cubic lattices. Recall that the mean-field prediction for the ratio is $\frac{1}{2}$. (Detailed estimates of the amplitudes B^+ , B^- and other critical parameters have been tabulated in M. E. Fisher, J. Math. Phys. 4, 278(1963).)

The specific heat series may also be studied with Padé approximants.* Below T_C the series are found to be quite consistent with a logarithmic singularity so that, as mentioned, $\alpha' \cong 0$. Above T_C the approximants prove appreciably less informative than the ratio method, as might have been anticipated in view of the weak (near logarithmic) nature of the singularity and our remarks at the end of Sections 35 and 36.

Subsequent to Domb and Sykes' work on the Heisenberg model susceptibility above T_C leading to the conclusion $\gamma \cong 4/3$ (Section 27), Gammel, Marshall and Morgan (Proc. Roy. Soc. A275, 257(1963)) made an extensive Padé approximant study of the three cubic Heisenberg lattices for spins $1/2$, 1 , $3/2$, 2 , $5/2$, 3 , 10 and ∞ . By way of example estimates of γ , using successively more terms, for $S = \infty$ were

b. c. c.			f. c. c.		
1.01			1.27		
1.71	1.23		1.31,	1.35	
1.01,	1.31,	1.33	1.334,	1.364,	1.364
1.336,	1.345		1.351,	1.355.	

These and the results for other spin values support the conclusion $1.32 \cong \gamma \cong 1.36$.

It is worth mentioning that the Padé approximant and ratio technique have been used successfully on a number of other physical problems. In later sections we will outline the application to anti-ferromagnetic susceptibilities. However, the approach has also been

*G. A. Baker, Jr., Phys. Rev. 129, 99(1963).

used in percolation problems, for hard "sphere" lattice gases, binary mixtures of "Gaussian molecules," in lattice dynamics, in many-body perturbation theory and the calculation of Regge poles in scattering theory.

Chapter X

I will now take up a few topics concerning the general behaviour and interrelations of the various critical exponents: α and α' for the specific heats above and below T_C , β for the spontaneous magnetization, γ and γ' for the susceptibility above and below T_C and δ for the critical isotherm (Section 31).

39. Dependence on Dimensionality

Table I summarizes the information gained from theory and experiment on the values of the critical exponents. (The queries ? and (?) indicate greater and lesser degrees of uncertainty! The experimental entries for γ' will be explained in Section 41.)

Inspection of Table I shows that the trend towards classical behaviour with increase in dimensionality is quite rapid; the discrepancies between the three-dimensional and classical values being a half to a third of the corresponding discrepancies in two dimensions.

Table I. Critical Exponents.

Temperatures	$T \leq T_C$			$T = T_C$	$T \geq T_C$	
	α'	β	γ'	δ	α	γ
Classical Theory	$0_{\text{discont.}}$	$\frac{1}{2}$	1	3	$0_{\text{discont.}}$	1
Ising $d = 2$	$0_{\text{log.}}$	$\frac{1}{8}$	$1\frac{3}{4}$	15	0_{log}	$1\frac{3}{4}$
Ising $d = 3$	$\cong 0$	$\cong \frac{5}{16}$	$\cong 1\frac{1}{4}(?)$	$\cong 5.2$	$\cong 0.2$	$1\frac{1}{4}$
Heisenberg $d = 3$?	?	?	?	$\cong 0?$	$\cong 1\frac{1}{3}$
Experiment Magnets	$\cong 0_{\text{log}} ?$	0.33	$\cong 1.22$	$\cong 4.22$	$\cong 0.1?$	$\cong 1.35$
Experiment Fluids	$\cong 0_{\text{log}}$	0.33-0.36	$\cong 1.18$	$\cong 4.2$	$\cong 0.1?$	$> 1.1(?)$

To see if this trend continued to higher dimensions, Dr. D. S. Gaunt and I (Phys. Rev. 133, A224(1964)) calculated the high-temperature susceptibility expansion of a d -dimensional "simple" cubic lattice. Eleven coefficients, $a_n(d)$, for general d were obtained and analyzed by the ratio and Padé techniques. Up to six dimensions accurate values of the critical points were obtained and thence estimates for the exponents γ . Our results may be written

$$\gamma - 1 = \frac{3}{4'} \frac{3}{12'} \frac{3}{32 \pm 1'} \frac{3}{80 \pm 2'} \frac{3}{188 \pm 12'} \dots \quad (39.1)$$

as $d=2, 3, 4, 5, 6, \dots$. Evidently the rapid approach to classical behaviour continues at an exponential rate. It is possible that for some $d = d_0 \geq 6$, the classical value $\gamma=1$ is actually attained (although weaker singularities might remain at T_C), but our series are not long enough to decide this rather academic question!

If we use the definition of the critical point as the radius of convergence of the susceptibility series, i.e.,

$$\ln v_C(d) = -\lim_{n \rightarrow \infty} (1/n) \ln a_n(d), \quad (39.2)$$

it proves possible to obtain a series expansion for the critical point v_C ! By formally taking the logarithm of the expression for $a_n(d)$ we find the dependence on n drops out for large enough n and in terms of the coordination number q , which for these lattices is just $2d$, we find

$$\begin{aligned} \frac{kT_C}{\frac{1}{2}qJ} &= 1 - (1/q) - 1\frac{1}{3}(1/q^2) - 4\frac{1}{3}(1/q^3) \\ &\quad - 21 \frac{34}{45}(1/q^4) - 133 \frac{14}{15}(1/q^5) - \dots \end{aligned} \quad (39.3)$$

As we might have anticipated the leading term, corresponding to $(1/q) \rightarrow 0$ or $d \rightarrow \infty$, represents just the classical or mean field prediction for the critical point! The first two terms constitute essentially the Bethe approximation. Examination of the origin of the series and the behaviour of its coefficients (which go approximately as $(n-1)!$) indicates that the series is only asymptotic. However, truncation of the series at the smallest numerical term yields a value for $kT_C/\frac{1}{2}qJ$ accurate to 1 per cent even in three dimensions!

Extrapolation of the corresponding specific heat series suggests that for $d \geq 4$ the specific heat remains finite as $T \rightarrow T_C+$. In four, five and six dimensions, however, its slope probably becomes

infinite at T_c so that the critical point remains an analytic singularity of the free energy.

40. Droplet Model of Condensation

A model of condensation in many ways complementary to the Van der Waals picture is the "droplet" model originally introduced by Bijl, Frenkel and Band and since discussed by Fierz and De Boer.[†] By extending the theory slightly we can, in a heuristic way, derive from the model a relation between the low-temperature critical exponents α' , β and γ' .[‡]

The basic idea of the approach is that in a gas of molecules with short-range attractive forces and repulsive cores, the typical configuration at low temperatures and densities will consist of well separated coherent clusters of molecules. Each cluster will be, in effect, a small droplet of the liquid at the same temperature. Of course these droplets will be in dynamic equilibrium and will grow by coalescence or shrink by evaporation if the conditions of pressure or temperature change. Condensation on this picture corresponds to the growth of a macroscopic droplet of liquid.

To make a more formal theory let us, in first approximation, neglect the volume excluded by the droplets. At low temperatures this should be an excellent approximation since condensation occurs at very low densities. (The important results of the theory are not altered by taking account of the excluded volume to first order but taking the effect into account more rigorously seems difficult.)

The grand partition function for a domain of volume V is then given by

$$\ln \Xi = \frac{pV}{kT} = \sum_{\ell=1}^{\infty} q_{\ell} z^{\ell}, \quad (40.1)$$

where $q_{\ell} = q_{\ell}(V, T)$ is the configurational partition function for all possible clusters of ℓ molecules (see, for example, De Boer).

The centre of each cluster is free to move through the volume so that q_{ℓ} is simply proportional to V . Now the energy of a cluster

[†]A. Bijl, "Discontinuities in the Energy and Specific Heat," Doctoral Dissertation, Leiden 29 April 1938.

J. Frenkel, J. Chem. Phys. 7, 200; 538(1939); "Kinetic Theory of Liquids," Chap. VII (Oxford, 1946).

W. Band, J. Chem. Phys. 7, 324; 927(1939).

M. Fierz, Helv. Phys. Acta. 24, 357(1951).

J. De Boer in "Changement de Phases," Comptes Rendus 2^e Réunion de Chimie Physique, p. 8 (Paris, June, 1952).

[‡]The argument was first presented in J. W. Essam and M. E. Fisher, J. Chem. Phys. 38, 802(1963).

will be made up of (a) a "bulk term" $-\ell\epsilon$, where ϵ is the binding energy per molecule in the fluid; and (b) a "surface term" $+ws$ where s is the surface area (or perimeter in two dimensions) and w is the "surface tension," arising, of course, from a loss of part of the bulk binding energy ϵ , by molecules in the surface of the cluster. One expects that the mean surface of a cluster of ℓ molecules will, for large ℓ , vary as a power of ℓ , that is,

$$\bar{s}(\ell) = A\ell^\eta, \quad (\ell \rightarrow \infty). \quad (40.2)$$

Traditionally one expects $\eta=2/3$ in three dimensions and $\eta=1/2$ in two dimensions. Let us not, however, make this assumption but rather just assume that there is some "effective mean surface area" with $\eta < 1$ such that we may write

$$q_\ell(V, T) \cong V \nu(\bar{s}) e^{\ell\beta\epsilon} e^{-\beta w \bar{s}(\ell)}, \quad (40.3)$$

where $\nu(\bar{s})$ is proportional to the number of distinct clusters of perimeter $\bar{s}(\ell)$ (and size ℓ). The definition of $\nu(\bar{s})$ may be made more concrete by considering a lattice gas; in two dimensions $\nu(\bar{s})$ is then the number of polygons of perimeter $\bar{s}(\ell)$ (and area ℓ). On general grounds we thus expect*

$$\nu(\bar{s}) \cong B\lambda^{\bar{s}}/\bar{s}^\phi, \quad (\bar{s} \rightarrow \infty) \quad (40.4)$$

where B is constant. Recall for example that the number of closed \underline{s} -step random walks on a lattice varies as $Bq^{\underline{s}}/s^{d/2}$ for large s .

Combining these results leads to the approximation

$$\frac{p}{kT} = BA^{-\phi} \sum_{\ell=1}^{\infty} \ell^{-\eta\phi} (\lambda e^{-\beta w})^{A\ell^\eta} (e^{\beta\epsilon} z)^\ell. \quad (40.5)$$

For a simple lattice gas one sees directly that

$$e^{-\beta\epsilon} = x^q \quad (40.6)$$

so that, by Equation (10.22),

$$e^{\beta\epsilon} z = y, \quad (40.7)$$

and

$$e^{-\beta w} = x \quad (40.8)$$

* The introduction of the factor $\bar{s}^{-\phi}$ seems to be new.

if the perimeter and surface area are measured in terms of the number of "wrong bonds." We can, with no loss of generality, thus rewrite (40.5) as

$$\pi(x, y) = \frac{p}{kT} = C \sum_{\ell=1}^{\infty} \ell^{-\eta\phi} (\lambda x)^{A\ell^\eta} y^\ell, \quad (40.9)$$

where C is constant.

Let us consider briefly some of the consequences of this approximation, which should be good at low temperatures. (One may in fact derive (40.9) by keeping only the dominant low temperature behaviour of each of the Mayer $b_\ell(T)$ coefficients.) The radius of convergence of the series in y is

$$y_0 = \lim_{\ell \rightarrow \infty} |\ell^{\eta\phi} (\lambda x)^{-A\ell^\eta}|^{1/\ell} = 1 \quad (40.10)$$

since $\eta < 1$. One easily sees that for $y > 1$ infinitely large clusters can appear. Consequently, $y = y_0 = 1$ is the condensation point. (For the lattice gases we know, of course, that this result is exact since $y=1$ corresponds to $H=0$.)

Since the coefficients of y^ℓ are all positive the condensation point is evidently a singularity of $\pi(y)$ and hence of the pressure, density and higher derivatives. The nature of this singularity does not seem to have been generally recognized. To determine it, consider the k th derivatives of $\pi(x, y)$ at the condensation point $y=1$. We have

$$\pi^{(k)}(x) = \left(y \frac{\partial}{\partial y} \right)^k \pi(x, y) \Big|_{y=1} = C \sum_{\ell=1}^{\infty} \ell^{k-\eta\phi} (\lambda x)^{A\ell^\eta}. \quad (40.11)$$

This series converges for all $x < \lambda$ whatever the value of k . In other words, $\pi^{(0)}$ or the pressure, $\pi^{(1)}$ or the density, $\pi^{(2)}$ or the compressibility and all higher derivatives have definite finite values at the condensation point. This means that the condensation point is an essential singularity of $p(z)$, $\rho(z)$, etc. Although all the derivatives exist at condensation, they cannot be used to construct a convergent Taylor series since the n th derivative is essentially of order $(n!)^{1+\zeta}$ with $\zeta > 0$.

We will not discuss this point and its implications for the theory of metastability further in these lectures; rather let us notice that we may regard the divergence of the condensation-point or zero-field series (40.11), at $x = x_c = 1/\lambda$, as locating the critical point of the system. Of course, this is pushing the model well beyond the low temperature region in which it may be expected to be valid. Optimistically, however, we might hope that deviations from the low

temperature behaviour could be absorbed into "effective values" for the basic exponents η and ϕ .

Accepting this interpretation, the behaviour of p , ρ , K_T , etc., at the critical point is then determined by the asymptotic behaviour of the terms in Equation (40.11). In this way one finds that as $x \rightarrow x_C$ (i.e., $T \rightarrow T_C$) the dominant singularities are

$$\begin{aligned} \pi^{(k)}(x) &\approx D_k [1 - (x/x_C)]^{\delta(k)} + \dots \\ &\approx D'_k [1 - (T/T_C)]^{\delta(k)} + \dots \end{aligned} \quad (40.12)$$

where the critical point exponents are given in terms of η and ϕ by

$$\delta(k) = \phi - \frac{k+1}{\eta}. \quad (40.13)$$

To identify these exponents with those previously introduced, recall that to calculate the specific heat the free energy (or the pressure) must be differentiated twice with respect to T . Thus

$$\alpha' = 2 - \delta(0). \quad (40.14)$$

The coexistence curve and variation of the compressibility correspond directly to $k = 1$ and $k = 2$ so that

$$\beta = \delta(1), \quad \alpha' = -\delta(2). \quad (40.15)$$

An extension of the argument yields the exponents above T_C .

41. Relation for the Critical Exponents

We notice that the sequence of critical exponents $\delta(k)$ depends on only the two basic parameters ϕ and η . Thus given, say, $\delta(0)$ and $\delta(1)$, all other $\delta(k)$ are determined. In terms of α' and β we find

$$\frac{1}{\eta} = 2 - \alpha' - \beta, \quad (41.1)$$

$$\phi = 4 - 2\alpha' - \beta, \quad (41.2)$$

from which follows the relation

$$\alpha' + 2\beta + \gamma' = 2 \quad (41.3)$$

which is independent of η or ϕ .

Of course, our arguments for this relation are purely heuristic. Let us accept it as a conjecture and test it against the known results

listed in Table I. For the two-dimensional Ising model the left hand side is

$$0 + 2(1/8) + 7/4 = 2$$

so the identity is verified! For the classical theories (interpreting a discontinuity as $\alpha' = 0$, as one should—see also below), we have

$$0 + 2(\frac{1}{2}) + 1 = 2$$

and the relation is again correct. The expression (40.13) for $\delta(k)$ may also be checked against the higher derivatives in the classical case and, by extrapolation, the prediction $\delta(3) = -3.750$ for the two-dimensional Ising model is found to be correct within uncertainties of ± 0.05 .

Before considering the implications of the relation (41.3) for the three-dimensional models and for experiments, we will show by an argument of Rushbrooke's (J. Chem. Phys. 39, 842(1963)) that it can be derived by purely thermodynamic arguments as an inequality with the "=" replaced by " \geq ".

42. A Thermodynamic Inequality

Let us first give a more precise mathematical definition of a critical exponent which agrees with the usage we have made of the concept. Thus we will write

$$F(T) \sim |T_C - T|^\lambda, \quad T \rightarrow T_C^- \quad (42.1)$$

if the limit

$$\lambda = \lim_{T \rightarrow T_C^-} \left\{ \frac{\ln F(T)}{\ln |T_C - T|} \right\} \quad (42.2)$$

exists. Note that $\lambda = 0$ if $F(T)$ has a logarithmic singularity or if $F(T_C^-)$ is finite.

Now a specific heat is defined thermodynamically by

$$C_0 = T \left(\frac{\partial S}{\partial T} \right)_0 \quad (42.3)$$

where the subscript zero denotes the conditions under which it is measured. Let us, in particular, consider a ferromagnet. Then quite generally one has

$$\left(\frac{\partial S}{\partial T}\right)_0 = \left(\frac{\partial S}{\partial T}\right)_H + \left(\frac{\partial S}{\partial H}\right)_T \left(\frac{\partial H}{\partial T}\right)_0 \quad (42.4)$$

and since

$$S = -\left(\frac{\partial F}{\partial T}\right)_H, \quad M = -\left(\frac{\partial F}{\partial H}\right)_T, \quad (42.5)$$

one can prove the "Maxwell relation"

$$\left(\frac{\partial S}{\partial H}\right)_T = -\frac{\partial^2 F}{\partial T \partial H} = \left(\frac{\partial M}{\partial T}\right)_H. \quad (42.6)$$

Furthermore,

$$\left(\frac{\partial H}{\partial T}\right)_M \left(\frac{\partial T}{\partial M}\right)_H \left(\frac{\partial M}{\partial H}\right)_T = -1. \quad (42.7)$$

Now let the zero subscript denote constant magnetization, multiply (42.4) by T and substitute in the last term with (42.6) and (42.7). We then obtain

$$C_M = C_H - T \left(\frac{(\partial M / \partial T)_H^2}{(\partial M / \partial H)_T} \right), \quad (42.8)$$

which is simply the magnetic analogue of the well known relation between C_V and C_p .

If we let H approach zero at temperatures below the critical point, M becomes the spontaneous magnetization, and $(\partial M / \partial H)_T$ the zero field susceptibility, and so

$$C_{H=0}(T) = C_M(T) + T \left(\frac{(\partial M_0 / \partial T)^2}{\chi_0(T)} \right), \quad (H=0). \quad (42.9)$$

Now the specific heat $C_M(T)$ is essentially a mean square energy fluctuation and hence is never negative. (This result follows equivalently from the convexity of the free energy as a function of temperature at fixed magnetization.) Consequently we have the inequality

$$C_{H=0}(T) \geq T \left(\frac{(\partial M_0 / \partial T)^2}{\chi_0(T)} \right) \quad (42.10)$$

To use the definition (42.2) for α' and the other exponents, take

logarithms and divide by $|\ln(T_C - T)|$. On taking the limit $T \rightarrow T_C^-$, we obtain

$$\alpha' \geq 2(1 - \beta) - \gamma' \quad (42.11)$$

which may be written

$$\alpha' + 2\beta + \gamma' \geq 2, \quad (42.12)$$

for comparison with (41.3). (Note that if we could prove that $C_H(T)/C_M(T) > 1 + \epsilon$ ($\epsilon > 0$) as $T \rightarrow T_C$, we would have the equality in (42.11).)

This inequality can also be proved for the specific heat at constant volume in the two-phase region of a fluid by a similar but more complicated argument.*

We have already seen that the case of equality occurs for the classical theories and for the two-dimensional Ising model. Indeed, in the latter case we could have rigorously concluded $\gamma' \geq 7/4$ from the exact results $\alpha' = 0$, $\beta = 1/8$. In the case of the three-dimensional Ising model, if we use $\beta = 5/16$ and accept $\gamma' = \gamma = 1\frac{1}{4}$ we conclude from (42.11) that $\alpha' \geq 1/8$. This implies a significantly sharper singularity than the logarithmic form ($\alpha' = 0$) which was found by the numerical studies to be consistent with the series. Conversely, as we observed, the series for $\chi_0(T)$ might be consistent with a value of γ' as large as 1.30 or 1.32 in which case $\alpha' = 0.06$ or 0.07 would be possible. At present we are unable to decide unequivocally between these alternatives. My own guess is that the specific heat singularity, being the weakest and hence the most difficult singularity to study numerically, will prove sharper as T approaches closely to T_C and that the symmetry $\gamma' = \gamma$ will be confirmed.

For the Heisenberg model only pure speculation is possible! If we assume $\gamma' = \gamma$ and accept the estimate $\gamma = 4/3$, we obtain $\beta \geq \frac{1}{3} - \frac{1}{2}\alpha'$. If $\alpha' = 0$ this would be consistent with the one-third law $\beta = \frac{1}{3}$! So far, however, nobody has suggested how either one of these assumptions could be substantiated!

In the experimental situation we learn something new. Thus for the ferromagnet EuS we have $\beta \cong 0.33 \pm 0.01$ and to judge from other magnetic specific heats $\alpha' < 0.1$. This enables us to conclude that the initial susceptibility below T_C , which is not easily measured, is characterized by an exponent $\gamma' \cong 1.22$. This suggests that in the experimental case γ' might equal γ .

For gases we have $\beta = 0.33$ to 0.36 and, judging by argon, α'

*See M. E. Fisher, *J. Math. Phys.* 4, 944 (1964).

approximately zero and almost certainly less than 0.1. Consequently, we can conclude $\gamma' \geq 1.18$ and possibly $\gamma' \geq 1.3$. This is a valuable result since, as yet, there are no good measurements on fluid compressibilities that clearly yield a nonclassical exponent.

Finally let us raise the problem of whether one could also find thermodynamic inequalities for the behaviour of higher derivatives of the pressure and the free energy which might match the more general exponent relation (40.13) (which was found to be valid classically and in two dimensions).[†]

Chapter XI

43. The Theory of Antiferromagnets

So far in our detailed discussion of critical point behaviour we have considered only systems in which the dominant interactions are of the "like-attracts-like" class. Let us turn now to systems where the repulsive interactions dominate and, in particular, to antiferromagnets where the coupling between spins tends to align neighbouring spins in opposite senses. (As we explained, binary alloys which undergo order-disorder transitions also belong to this class but, since their properties are less accessible experimentally, we will not discuss them explicitly.)

Antiferromagnetic crystals generally display significant magnetic anisotropy. In the simplest, uniaxial case the crystal has a single preferred axis of easy spin alignment (the "parallel" axis) and two unfavourable ("perpendicular") axes. For a single crystal specimen we must therefore distinguish between the parallel susceptibility χ_{\parallel} and the perpendicular susceptibility χ_{\perp} . The parallel susceptibility may be considered the more fundamental quantity and we will sometimes denote it just by χ . If experiments are made on a polycrystalline powder the observed susceptibility is

$$\chi_{\text{powder}} = \frac{1}{3}\chi_{\parallel} + \frac{2}{3}\chi_{\perp} \quad (43.1)$$

At high temperatures χ_{\parallel} and χ_{\perp} are normally indistinguishable and vary approximately as $1/(T + \Theta)$, the positive sign of the parameter Θ being an indication of the antiferromagnetic coupling between neighbouring spins. (Compare with the Curie-Weiss law $1/(T - T_C)$ for ferromagnets.) As the temperature is lowered χ_{\parallel} and χ_{\perp} go through a maximum (see Figure 43.1) in the vicinity of which one observes a typical lambda anomaly in the specific heat. Usually the

[†]Note added in proof. Attention should be drawn to recent work by R. B. Griffiths (Phys. Rev. Letters 14, 623 (1965) and a forthcoming paper) who proves $\alpha' + (1 + \delta)\beta \geq 2$.

difference between χ_{\parallel} and χ_{\perp} can be detected at the maximum. As T falls below the transition temperature T_c (often called the Néel point) χ_{\parallel} drops rapidly but χ_{\perp} remains more or less constant (see Figure 43.1).

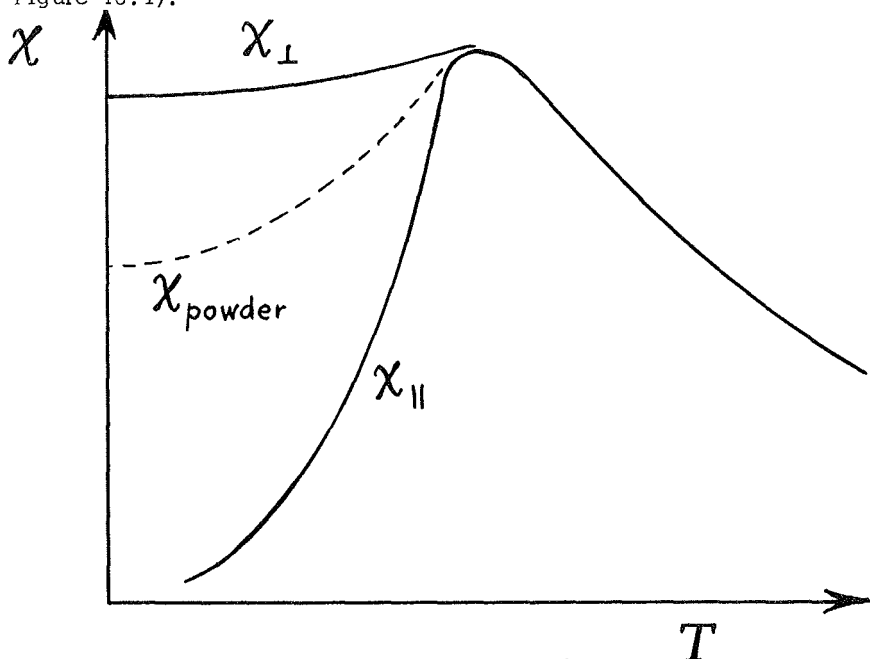


Figure 43.1. Temperature variation of the susceptibilities of a typical antiferromagnetic material.

Below T_c the spins are predominantly aligned on two interpenetrating sublattices of "up spins" and "down spins." (We will not consider the intricate spiral and related spin structures which have been found in certain materials.) The simplest theoretical account of this situation is given by mean field theory (see, for example, Kittel "Introduction to Solid State Physics," John Wiley). The two sublattices are treated effectively as two macroscopic spins coupled together. This yields equations of the form

$$M_a = f \left\{ \frac{H - \lambda M_b}{kT} \right\}$$

$$M_b = f \left\{ \frac{H - \lambda M_a}{kT} \right\} \quad (43.2)$$

where $f(H/kT)$ is the magnetization of an isolated spin in a field H

and M_a and M_b are the magnetizations of the two sublattices.

The predicted variation of specific heat and susceptibilities is shown in Figure 43.2. The specific heat rises to a finite peak and

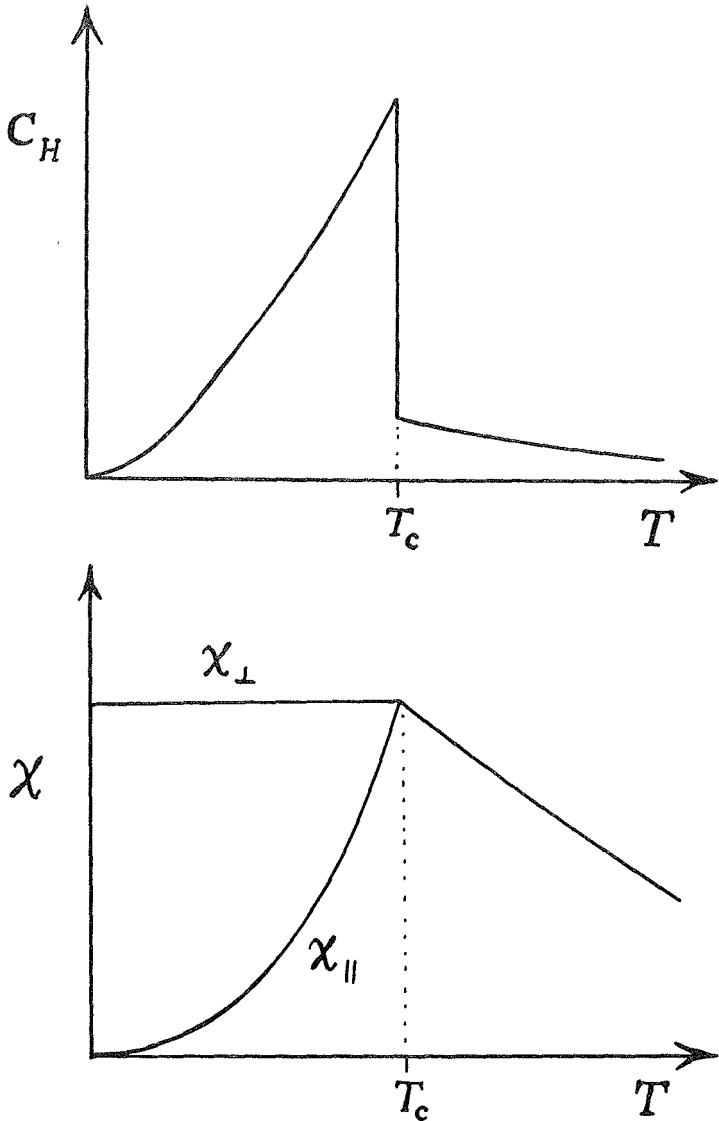


Figure 43.2. Behaviour of the specific heat and susceptibilities of an antiferromagnet according to the mean field and related approximations. Note that the peaks in $C(T)$ and in $\chi(T)$ occur at the same temperature.

drops discontinuously at T_C (as in all mean field theories). The parallel susceptibility rises to a sharp peak at T_C where the gradient abruptly changes sign. Above T_C one gets $\chi_{\perp} = \chi_{\parallel}$ but below T_C the perpendicular susceptibility remains constant at its critical value. The Bethe and related approximations make similar predictions—in particular these approximate theories all predict that the maximum in the susceptibility should occur at the same temperature as the specific heat peak. The earlier measurements, taken at somewhat coarse temperature intervals, were generally held to be in agreement with the theory. Nevertheless, a closer examination shows that the " T_C " as determined from thermal experiments often appeared to be from 2 to 6 per cent lower than the " T_C " found from magnetic experiments! We will discuss the validity of the simple theories in the transition region* and show how this apparent discrepancy can be understood.

One remark we may make immediately. Consider a system of spins with nearest neighbour coupling on a "loose-packed" lattice which admits antiferromagnetic ordering. By changing the sign of the exchange constant J we go from ferromagnet to antiferromagnet. In general this transformation will change the partition function of the system. However, for (a) Ising coupling and any value of the spin S or (b) Heisenberg coupling and $S = \infty$, the partition function in zero magnetic field is left invariant. This follows since the effect of the change $J \rightarrow -J$ can be precisely compensated by reversing the signs of the spin variables on one sublattice (which is allowed as these variables are equivalent to dummy summation indices). Consequently, the thermodynamic behaviour of such ferromagnets and antiferromagnets in zero field will be identical. In particular the specific heat singularities will be the same. We may therefore take over our previous discussions which showed that logarithmic or near logarithmic specific heat singularities should be expected both above and below T_C . (Although the Heisenberg model of finite spin is not exactly symmetric in $\pm J$, it seems quite likely that the specific heat singularities will not depend very strongly on the sign of J .)

The prediction that antiferromagnets should display very sharp singularities is well borne out by experiment (see, for example, Figures 52.1 and 52.3 below). In particular, in a recent experiment by Friedberg and Skalyo (Phys. Rev. Letters 13, 133(1964)) the specific heat of $\text{CoCl}_2 \cdot 6\text{H}_2\text{O}$ was observed to be quite accurately logarithmic from about 10 per cent above and below T_C to within 0.3 per cent of $T_C = 2.289^\circ\text{K}$. (Closer to T_C the specific heat was rounded

*At low temperatures quantum mechanical effects become important and more sophisticated theories allowing antiferromagnetic spin waves must be used.

off, this probably being due to imperfections and strains in the multi-crystalline specimens.)

These considerations show that the standard approximate treatments of antiferromagnets cannot be relied on in the transition region so that we must find a better approach to calculating the susceptibilities near T_C .

44. Exactly Soluble Antiferromagnetic Model

As a first step in elucidating the transition point behaviour we will show that there are certain two-dimensional Ising lattices of antiferromagnetic character which can be solved rigorously even in the presence of a magnetic field. We will then go on to discuss how far the properties of these rather special models are typical of more realistic systems.

Consider a simple $S = \frac{1}{2}$ Ising lattice with nearest neighbour interactions in a magnetic field H . We can "decorate" such a lattice by replacing some or all of the direct interaction bonds by a "decorated bond" consisting of an arbitrary physical system which interacts with the two spins s_1 and s_2 at the ends of the bond (see Figure 44.1)*

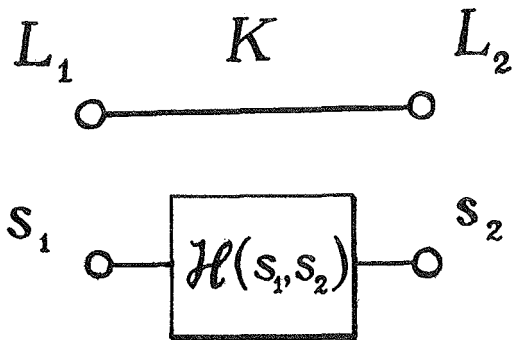


Figure 44.1. Bond transformation.

In the expression for the partition function, $Z(T, H)$, of the basic, or undecorated, lattice there will be a factor

$$f = \exp[Ks_1s_2 + L_1s_1 + L_2s_2] \quad (44.1)$$

for the bond between spins s_1 and s_2 , where

*The decoration of bonds by single spins seems to have been first used by S. Naya, Progr. Theoret. Phys. (Japan) 11, 53(1954). The general transformation theory was given by M. E. Fisher, Phys. Rev. 113, 969(1959).

$$K = \frac{J}{2kT}, \quad L_i = m_i \frac{H}{kT} \quad (i = 1, 2), \quad (44.2)$$

and where m_1 and m_2 are the, possibly different, magnetic moments of these spins. Now suppose $\mathcal{H} = \mathcal{H}(s_1, s_2)$ is the hamiltonian of the decorating system. In general this will depend not only on the variables s_1 and s_2 but also on a set of internal variables and on external variables like the magnetic field. The partition function, $Z^*(T, H)$, of the decorated system will then contain the factor

$$f^* = \text{Tr} \left\{ \exp \left[\frac{-\mathcal{H}(s_1, s_2)}{kT} \right] \right\} \exp [L_1 s_1 + L_2 s_2] \quad (44.3)$$

for the corresponding bond, where the trace is taken over the internal variables of the decorating hamiltonian.

Now let us try to represent the decorated bond in terms of an equivalent undecorated bond by writing

$$f^* = g \exp [K' s_1 s_2 + L'_1 s_1 + L'_2 s_2]. \quad (44.4)$$

where the prefactor g does not depend on the spin variables. In other words, we try to impose the identity

$$\begin{aligned} \psi(s_1, s_2) &= \text{Tr} \left\{ \exp \left[\frac{-\mathcal{H}(s_1, s_2)}{kT} \right] \right\} = \sum_n \exp \left[\frac{-E_n(s_1, s_2)}{kT} \right] \\ &\equiv g \exp [K' s_1 s_2 + \delta L_1 s_1 + \delta L_2 s_2] \end{aligned} \quad (44.5)$$

where

$$\delta L_i = \delta m_i \frac{H}{kT}, \quad (i = 1, 2), \quad (44.6)$$

in which the δm_i are increments to the magnetic moments of the spins s_1 and s_2 arising from the removal of the decorating system. (The E_n are the eigenvalues of \mathcal{H} .)

Recall now, as in Section 22, that the spin variables only take the values ± 1 so that the identity (44.5) need only hold for the four cases $s_1, s_2 = \pm 1$. There are four disposable parameters, g , K' , δL_1 and δL_2 and we may thus solve to find the transformation equations

$$4K' = 4K'(T, H) = \ln \left(\frac{\psi_{++}\psi_{--}}{\psi_{+-}\psi_{-+}} \right) \quad (44.7)$$

$$g^4 = \psi_{++}\psi_{+-}\psi_{-+}\psi_{--}, \quad (44.8)$$

and

$$4\delta L_1 = \ell n \left(\frac{\psi_{++}}{\psi_{--}} \right) + \ell n \left(\frac{\psi_{+-}}{\psi_{-+}} \right), \quad (44.9a)$$

$$4\delta L_2 = \ell n \left(\frac{\psi_{++}}{\psi_{--}} \right) + \ell n \left(\frac{\psi_{-+}}{\psi_{+-}} \right), \quad (44.9b)$$

where

$$\psi_{\pm\pm} = \psi(\pm 1, \pm 1).$$

Considering the form of (44.4) we see that the problem of the decorated lattice has been reduced to that of an equivalent undecorated lattice with modified magnetic moments and a transformed temperature

$$kT' = kT'(T, H) = \frac{J}{2K'(T, H)}. \quad (44.10)$$

The total increment to i th magnetic moment is $\Delta m_i = \sum \delta m_i$ where the sum runs over all the decorated bonds meeting at spin i . If $m_i = m$ and $\Delta m_i = \Delta m$ (constant), we may introduce a transformed magnetic field through

$$mH' = mH'(T, H) = (m + \Delta m)H, \quad (44.11)$$

and then the partition function for a lattice with M decorated bonds is just

$$Z^*(T, H) = g^M Z(T', H'). \quad (44.12)$$

One of the simplest decorating systems we can choose is a single extra spin coupled to s_1 and s_2 and so having the hamiltonian

$$\mathcal{H}(s_1, s_2) = -J(S_0^Z s_1 + S_0^Z s_2) - m\vec{H} \cdot \vec{S}_0. \quad (44.13)$$

In the special case of $S = \frac{1}{2}$ and \vec{H} parallel to the z -axis, this yields

$$\psi(s_1, s_2) = 2 \cosh [K(s_1 + s_2) + L]. \quad (44.14)$$

For this case the increment to the magnetic moments are then given

by

$$\delta L = \delta L(K, L) = \ell n \left[\frac{\cosh(L+2K)}{\cosh(L-2K)} \right] \quad (44.15)$$

Now notice that changing the sign of J , and hence of K , merely changes the sign of δL . The same conclusion follows for the general hamiltonian (44.13) as a consequence of its invariance under the transformation $(\vec{S}, s_1, s_2, H) \rightarrow (-\vec{S}, -s_1, -s_2, -H)$. This simple observation allows us to introduce a class of antiferromagnetic decorated lattices in which the total increment to the magnetic moments is zero.

Consider the decorated square lattice shown in Figure 44.2. The N spins on the vertical bonds are coupled ferromagnetically to the N vertex spins of the basic lattice, while the N spins on the horizontal bonds are coupled antiferromagnetically (but with the same value $|J|$). At absolute zero the $2N$ bond spins will order in an antiferromagnetic array as indicated by the arrows in the figure. Consequently, if we suppose that the vertex spins have zero (or negligible) magnetic moments, the whole system will behave magnetically as an antiferromagnet, the "magnetic" spins lying on a square lattice rotated by $\pi/4$ with respect to the original square lattice and of relative lattice spacing $1/\sqrt{2}$. If, indeed, we forget about the nonmagnetic vertex spins altogether, we may regard the magnetic spins as

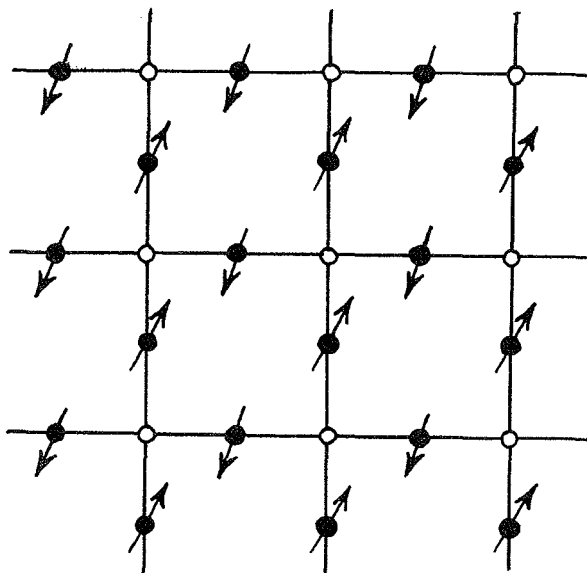


Figure 44.2. Decorated square lattice.

interacting antiferromagnetically with one another by a type of "superexchange" coupling transmitted through the vertices.*

To compute the properties of this superexchange lattice we need (a) the transformed temperature which, for $S = \frac{1}{2}$ and a parallel field, is given by

$$K'(T, H) = \frac{1}{4} \ln \operatorname{ch}(2K+L) + \frac{1}{4} \ln \operatorname{ch}(2K-L) - \frac{1}{2} \ln \operatorname{ch} L, \quad (44.16)$$

and (b) the total increments to the magnetic moments which, by our previous remarks, is

$$\begin{aligned} \Delta L &= 2\delta L_{\text{vertical}} + 2\delta L_{\text{horizontal}} \\ &= 2\delta L(K, L) + 2\delta L(-K, L) \equiv 0. \end{aligned} \quad (44.17)$$

Since the vertex spins are nonmagnetic the total magnetic moments on the equivalent (modified) square lattice will thus also be zero and the transformed field H' in (44.11) will vanish. Consequently, the properties of the superexchange model in an arbitrary field follow directly from Onsager's zero field solution for the square lattice! Explicitly we have

$$Z_{\text{superex.}}(T, H) = g^{2N}(T, H) Z_{\text{square}}(T', 0), \quad (44.18)$$

where T' follows from (44.16) and $g(T, H)$ is given by (44.8) with (44.14).

A variety of other such superexchange lattices can easily be constructed in two and three dimensions. In the latter case, however, the required zero field undecorated partition functions would have to be calculated from the series expansions.

45. Properties of the Superexchange Model

Let us examine the thermal and magnetic behaviour of the plane square superexchange lattice.† The critical temperature in zero field is given by

*This mechanism is similar to the usual superexchange coupling in spirit only! The effective coupling can be reexpressed as a sum of pair terms between the four bond spins around each vertex plus a smaller but temperature dependent, four-spin coupling term.

† Detailed formulas and derivations are given in M. E. Fisher, Proc. Roy. Soc. A254, 66(1960), A256, 502(1960).

$$K_C = \frac{J}{2kT_C} = \frac{1}{2} \cosh^{-1}(1 + \sqrt{2}) = 0.7649 . \quad (45.1)$$

As the field increases from zero, however, the transition temperature drops, $[T_C - T_t(H)]$ varying quadratically with H (see Figure 45.1). As the field increases further the transition temperature becomes linear with H and finally vanishes at the critical field

$$H_C = \frac{J}{m} , \quad (45.2)$$

as indicated in Figure 45.1. At $H/H_C = \frac{1}{2}$ the transition temperature has dropped by 19.5 per cent.

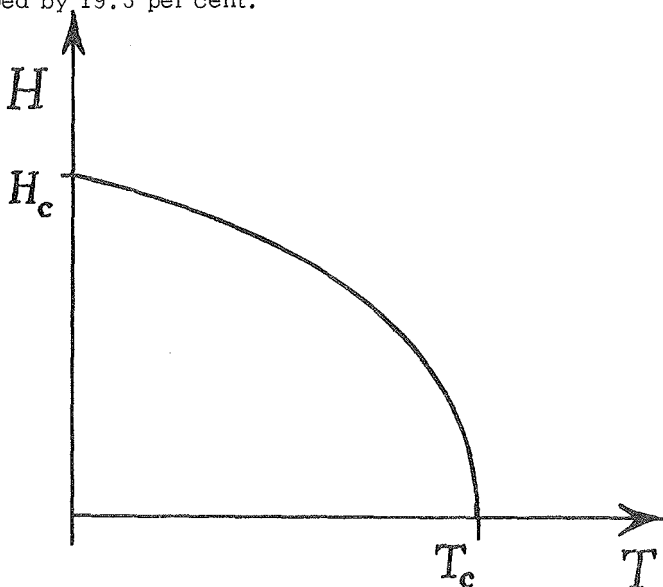


Figure 45.1. Sketch of the transition curve for the plane superexchange model.

On the "inside" of the transition curve (low fields and low temperatures) the magnetic spins display long-range antiferromagnetic order. At fixed field and at fixed temperature, the sublattice magnetization (or "long-range order") vanishes as

$$M_0 \approx D_H [T_t(H) - T]^{1/8} \quad \text{and} \quad D_T [H_t(T) - H]^{1/8} , \quad (45.3)$$

respectively, where $H_t(T)$ is the transition field.

As might be anticipated, the specific heat in zero field displays a symmetric logarithmic singularity. More generally in a

fixed field one finds

$$C_H(T) \approx A(H) |\ln |T - T_t(H)|| + \dots \tag{45.4}$$

as $T \rightarrow T_t(H)$. Thus the singularity remains even in a field (in contrast to a ferromagnet) although it moves to lower temperatures. Furthermore, its amplitude $A(H)$ drops as H increases, and goes to zero as $H \rightarrow H_C$ and $T_t \rightarrow 0$. These general features of the specific heat are observed in real antiferromagnetic systems, at least for relatively small fields. The experimental singularities, however, are typically asymmetric about T_t which, as we have seen, should be expected for three-dimensional systems.

As shown in Figure 45.2, the magnetization curves at fixed temperature are found to be continuous (except at zero temperature where a discontinuity occurs at $H = H_C$). As the transition field is approached, however, the magnetization varies as

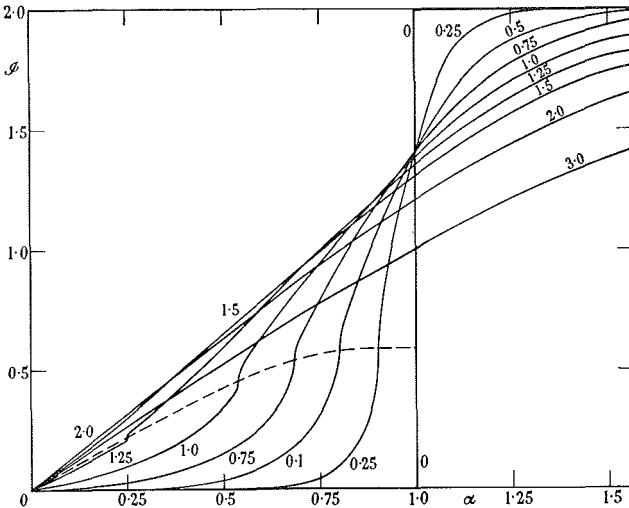


Figure 45.2. Constant temperature magnetization curves for the superexchange model. Note $\phi = 2M/M_{\max}$ and $\alpha = H/H_C$. (From M. E. Fisher, Proc. Roy. Soc. A254, 66 (1960).)

$$M(H) \approx M_t + c(H - H_t) \ln |H - H_t| + \dots \quad (45.5)$$

so that the differential susceptibility, $\chi(H) = \partial M / \partial H$, becomes infinite on the transition curve below T_C . (The simple approximate theories predict a change in gradient of the magnetization curve with $\chi(H)$ remaining finite.)

Finally, the zero field parallel susceptibility is found to vary as shown in Figure 45.3 (solid curve). The curve rises as the temperature drops, displays a rather rounded maximum and then falls quite sharply to zero. The important feature to notice, however, is that the maximum in $\chi_{||}(T)$ occurs well above the critical temperature T_C ! In fact, $T_{\max} / T_C \cong 1.40$. In the immediate critical region the susceptibility varies as

$$\chi_{||}(T) = \frac{m^2}{kT} \{ \xi_C + B(T - T_C) \ln |T - T_C| \}, \quad (H = 0). \quad (45.6)$$

Consequently, the true transition point is marked by an infinite slope in the $\chi(T)$ curve rather than by the maximum (see Figure 45.3 where the true critical point is marked on the $T \sim K^{-1}$ axis).

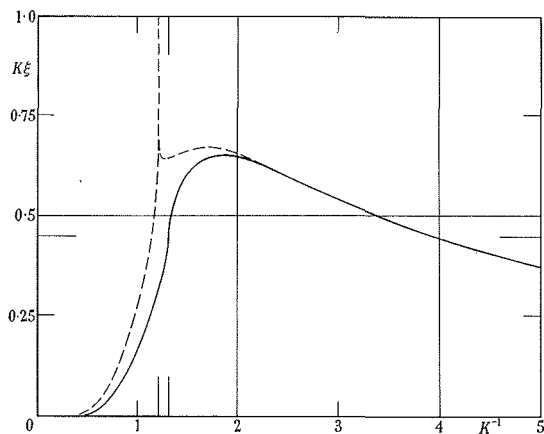


Figure 45.3. Parallel susceptibility of the superexchange model versus temperature in zero field (solid line) and in a field $H = \frac{1}{4}H_C$ (dashed curve). (From M. E. Fisher, Proc. Roy. Soc. A254, 66(1960).)

Although the difference found between T_{\max} and T_C is rather large, the rigorous result that the maximum in $\chi(T)$ lies above T_C does throw light on the apparent "anomaly" noted in Section 43: namely, that the critical points deduced experimentally from the peaks in $\chi(T)$ and in $C(T)$ differ by some 2 to 6 per cent. Related to the large difference between T_{\max} and T_C is the fact that the maximum in $\chi(T)$ for the model is much broader and less sharp than observed experimentally. We may anticipate, however, and will show below, that this feature is largely a reflection of the two-dimensionality of the model.

In a nonzero magnetic field the critical temperature T_C in the formula (45.6) for the susceptibility must be replaced by $T_t(H)$ and an additional term proportional for small fields, to $H^2 |\ln |T - T_t||$, appears. As illustrated by the dashed curve in Figure 45.3, this term leads to a weak but infinite logarithmic singularity in $\chi(T, H)$ at T_t . Although at first sight unexpected, the presence of this singularity is merely a consequence of the finite slope of the transition curve in a nonzero field and the behaviour of $M(H)$ near T_t (see Equation (45.5)). Since the strength of the singularity is proportional to H^2 , it will probably prove difficult to detect experimentally, but there are some indications of its existence. The overall increase in χ , even above T_C , as H increases from zero is observed in real materials.

As a final observation on the susceptibility of the model, we will record the following relation which is found to hold, namely, between the susceptibility and the energy in zero field,

$$\xi(T) = kT \chi/m^2 = 1 - (\tanh 2K) \left[\frac{U(T)}{U(0)} \right]. \quad (45.7)$$

Here $U(T)$ is the configurational energy per spin which goes to zero as $T \rightarrow \infty$ and to $U(0) < 0$, as $T \rightarrow 0$. Since $\tanh 2K$ is a slowly varying function of T and since, by virtue of the specific heat singularity, $U(T)$ must vary as $U_C + A(T - T_C) \ln |T - T_C|$ near T_C , the relation shows why the susceptibility has a singularity of the form (45.6). Since $\chi(T)$ rises as T increases from zero and has a positively infinite slope at T_C but nevertheless has to decay as $1/T$ when $T \rightarrow \infty$ it necessarily follows that its maximum lies above T_C . If we ignored the variation of $\tanh 2K$ in (45.7) we would conclude that $\xi(T)$, or $T\chi(T)$, should be rather similar to $1 - [U(T)/U(0)]$. A comparison of these two functions in Figure 45.4 shows indeed that they are strikingly alike! Within the context of this special superexchange model, it is by no means clear that this relationship should have any special significance. However, we will show that such a relation between the energy and the susceptibility of an antiferromagnet should hold under rather general circumstances.

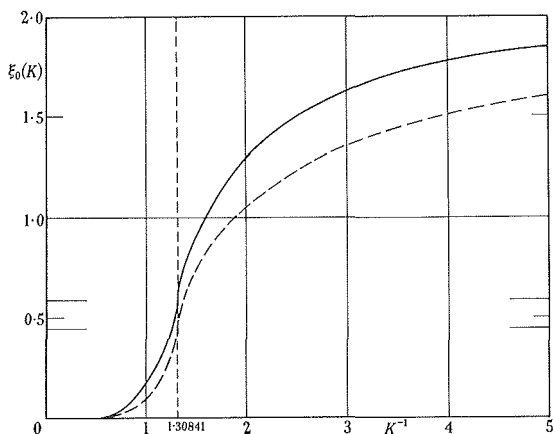


Figure 45.4. Comparison of the reduced susceptibility $\xi(T) = kT \chi/m^2$ and the function $1 - [U(T)/U(0)]$. Note that the scale of ordinates has been doubled and that K^{-1} is proportional to T . (From M. E. Fisher, Proc. Roy. Soc. A254, 66(1960).)

46. Perpendicular Susceptibility of the Ising Model

The behaviour of the superexchange models in a perpendicular (or in a skew field) can be found by calculating the full expression for the transformation function $\psi(s_1, s_2)$ using Equations (44.5) and (44.13). In place of (44.14) one finds

$$\psi(s_1, s_2) = 2 \cosh \left\{ [K(s_1 + s_2) + L_z]^2 + L_x^2 \right\}^{\frac{1}{2}} \quad (46.1)$$

where L_z and L_x refer to the parallel and perpendicular components of the field. The (zero field) perpendicular susceptibility derived from (46.1) is shown in Figure 46.1 (curve b) together with the parallel susceptibility (curve c). The behaviour of $\chi_{\perp}(T)$ in the critical region is strikingly different from the mean field predictions. In particular a maximum occurs just above T_C (at $T_{\max}/T_C = 1.043$) and the critical point (marked by an open circle) is again characterized by an infinite slope. In fact, the behaviour close to T_C is of the same form, $\xi_C + B(T - T_C)^{\ln} |T - T_C|$, found for $\chi_{\parallel}(T)$.

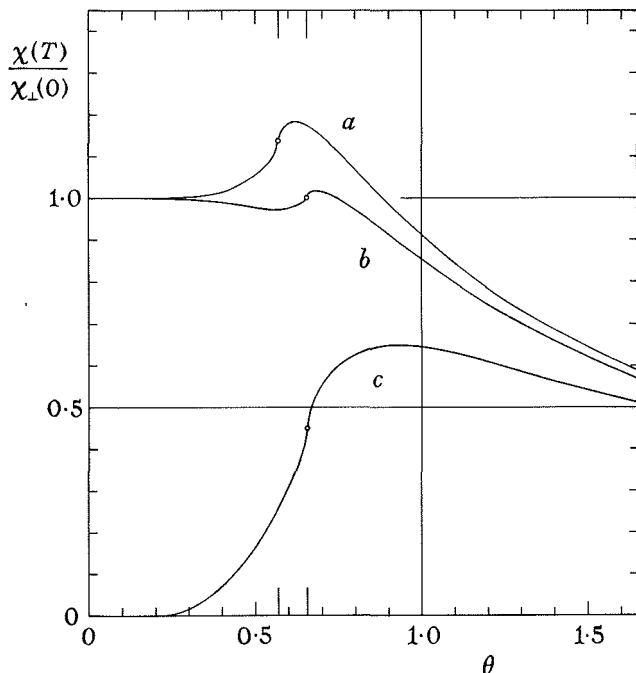


Figure 46.1. Perpendicular susceptibility of (a) the plane square Ising lattice, (b) the square superexchange lattice compared with (c) the parallel susceptibility of the superexchange model. (From M. E. Fisher, *J. Math. Phys.* 4, 124 (1963).)

The difference between χ_{\perp} and χ_{\parallel} above T_C is vastly greater than observed in most real antiferromagnetic crystals. It is clear, however, that this is merely a consequence of the extreme anisotropy of the Ising exchange interaction. With Ising coupling, a spin pointing perpendicular to the z-axis becomes, essentially, uncoupled from its neighbours whereas in a real material such a spin would still feel an appreciable antiferromagnetic interaction. Thus in an Ising antiferromagnet χ_{\perp} is closer to the free spin susceptibility than to χ_{\parallel} while in real antiferromagnets the reverse is the case.

It turns out that the perpendicular susceptibility (in zero field) can also be calculated exactly for the standard Ising lattices with hamiltonian

$$\mathcal{H} = -J \sum_{ij} S_i^z S_j^z - g\beta H_{\perp} \sum S_i^x. \quad (46.2)$$

This is achieved by extending the transformation theory, along the lines expounded for the general bond decoration process, to calculate the partition function of a lattice in which one or more spins have been replaced by an arbitrary interacting system. If the inserted system is chosen to be just a spin in a perpendicular field, one can obtain an expression for the total perpendicular susceptibility of the original lattice as a linear combination of the pair, quadruplet (and possibly higher order) spin correlation functions between the spins neighbouring the single spin in the unperturbed lattice.[†] For the plane honeycomb lattice one finds

$$\chi_{\perp}(T) = (g^2\beta^2/6J) \tanh K [3 + (\tanh K)^2 - 3 \tanh K \langle s_0 s_1 \rangle], \quad (46.3)$$

where $\langle s_0 s_1 \rangle$ is the nearest neighbour pair correlation function. Since the interactions are between nearest neighbours this correlation function is simply proportional to configurational energy; explicitly,

$$\langle s_0 s_1 \rangle = \omega_1(T) = \frac{U(T)}{U(0)}. \quad (46.4)$$

The formula (46.3) is thus very similar to the relation (45.7) between the parallel susceptibility and energy of the superexchange model! As before, it follows from the existence of the logarithmic specific heat singularity that the gradient of the susceptibility becomes logarithmically infinite at T_C .

The expressions corresponding to (46.3) for the square and triangular lattice involve quadruplet and further pair correlation functions, but these can be evaluated explicitly in terms of elliptic integrals and they all have the same type of singularity at T_C . The perpendicular susceptibility of the standard square lattice Ising model is shown in Figure 46.1 (curve a). The results for the honeycomb and triangular lattices are very similar.

Experimental measurements of χ_{\perp} (notably for $\text{MnCl}_2 \cdot 4\text{H}_2\text{O}$ by M. A. Lasheen, J. Van den Broek and C. J. Gorter, *Physica* 24, 1061(1958)) do indicate a small but distinct maximum in the critical region in qualitative agreement with the exact theoretical results.

Chapter XII

47. Counting Theorem for the Susceptibility

To examine the critical behaviour of the susceptibility for three-dimensional Ising models (and for the orthodox two-dimensional models) we must have recourse to the series expansions. In

[†] For the details of the theory see M. E. Fisher, *J. Math. Phys.* 4, 124(1963) and *Physica* 26, 816, 1028(1960).

Sections 22 to 25 we sketched the derivation and calculation of the high temperature expansions in powers of the variable $v = \tanh(J/2kT)$. The practical calculation of the coefficients is appreciably simplified by a configurational "counting theorem" discovered by Sykes[†] which, for a lattice of coordination number q , may be written

$$\xi(v) = \frac{kTX}{\frac{1}{4}g^2\beta^2} = \frac{[1 - (q-2)v + v^2 - qv\omega_1(v) + G(v)]}{[1 - (q-1)v]^2}. \quad (47.1)$$

In this expression $\omega_1 = U(T)/U(0)$ is again the nearest neighbour correlation function or the reduced energy, and the "residual function" is given by

$$G(v) = 8(1+v)^2 \sum_{n=3}^{\infty} g_n v^n \quad (47.2)$$

where the coefficients g_n are weighted sums of certain, relatively few, closed lattice constants of n lines. (On most lattices $g_3 = \dots = g_6 = 0$.)

For a ferromagnet J is positive and thus so is v . In this case the denominator in (47.1) gives rise to a spurious singularity at the Bethe approximation critical point $v_B = 1/(q-1)$. This singularity must in reality be exactly cancelled by a coincident double zero of the complete numerator.[‡] Clearly, however, if the numerator is known only as a truncated series the formula will not be useful as an approximation (although, of course, the correct expansion coefficients for χ may be derived from it). For an antiferromagnet, on the other hand, J and v are negative and the spurious singularity does not arise. In this case we may introduce an "energetic approximation" to the susceptibility by ignoring the residual function $G(v)$ in (47.1). Numerically this approximation is rather good since, as one may estimate from the series expansion, $G(v)$ amounts only to between 2 and 5 per cent of the numerator for two-dimensional lattices, and to less than 0.5 per cent for three-dimensional lattices even at the critical point.

This energetic approximation is very similar to the exact relation (45.7) noted for the superexchange model. It leads again to the

[†]See M. F. Sykes and M. E. Fisher, Phys. Rev. Letters 1, 321 (1958) and M. F. Sykes, J. Math. Phys. 2, 52(1961).

[‡]Notice that for a Bethe lattice, with no closed circuits, $G(v) \equiv 0$ and $\omega_1 = v$ for $T \geq T_C$. The numerator then has a simple zero at $v = v_B$ and the expression (47.1) reduces to the correct expression for the Bethe lattice susceptibility (Firgau formula) which diverges at v_B .

conclusion that the critical behaviour of the susceptibility matches that of the energy and, hence, in two dimensions is of the form $\xi_C + B(T - T_C) \ln |T - T_C|$. In three-dimensions our study of the specific heat singularity (Section 32) indicates a similar or slightly sharper singularity with, however, a smaller amplitude above T_C than below. Actually, as the considerations of the next section show, it appears that $G(v)$ does make some contribution to the singularity in $\chi(T)$ but its inclusion does not change the general behaviour.

48. Extrapolation to the Antiferromagnetic Singularity

It will be recalled that the high-temperature susceptibility series for χ (or ξ) has positive coefficients and that the dominant singularity lies on the positive v -axis at the ferromagnetic critical point $v_{\text{ferro}} = +v_C$ where χ diverges as $[1 - (v/v_C)]^{-\gamma}$. The antiferromagnet corresponds to negative v , the critical point being at $v_{\text{anti}} = -v_C$ where χ is expected to have only a mild singularity (neither a zero nor an infinity). The series to be summed for the antiferromagnetic susceptibility thus consists of numerically large coefficients with alternating signs. At first sight, there thus seems little chance of detecting the singularity at v_{anti} .

This difficulty may be overcome, however, by factoring off the dominant ferromagnetic singularity by writing

$$\ln \xi(v) = -\gamma \ln [1 - (v/v_C)] + \ln \phi(v) \quad (48.1)$$

and calculating the coefficients c_n of the expansion of $\ln \phi(v)$.[†] In two dimensions, of course, $\gamma = 7/4$ and the exact values of v_C are known. In three dimensions one may set $\gamma = 5/4$ and the most accurate estimates for v_C must be used. For the honeycomb lattice it even proves necessary to factor off two further dominant singularities on the circle of convergence of the form $(1 \pm iv)^{1/8}$. After these manipulations, it is found that the coefficients c_n alternate regularly in sign indicating that the dominant singularity of $\phi(v)$ is at the antiferromagnetic critical point. The nature of the singularity and the numerical values of the susceptibility may now be estimated by the ratio method (and the Padé approximant procedure may also be used).[‡]

The coefficients for both two- and three-dimensional lattices appear to vary as $A(-v_C)^{-n}/n(n+1)$ as would, in fact, be expected for a $[1 - (v/v_C)] \ln [1 - (v/v_C)]$ singularity. To test this we may calculate the sequences

$$A_n = c_n(-v_C)^n n(n+1). \quad (48.2)$$

[†]See M. E. Fisher and M. F. Sykes, *Physica* 28, 919, 939(1962).

[‡]Although various special techniques must be adopted because of the weak near-logarithmic nature of the expected singularity.

For the square lattice one finds, for $n = 8$ to 16 ,

$$A_n = 2.02, 1.98, 1.97, 1.96, 1.98, 1.99, \\ 2.015, 2.016, 2.022, \dots \quad (48.3)$$

and for the simple cubic lattice, for $n = 4$ to 11 ,

$$A_n = 0.271, 0.344, 0.330, 0.334, 0.335, \\ 0.341, 0.332, 0.346, \dots \quad (48.4)$$

The constancy of these values (to within 3 per cent for the square lattice) confirms the logarithmic or near logarithmic nature of the singularity. (The slight tendency for the A_n for the simple cubic lattice to increase may indicate a slightly sharper singularity.) The magnitudes of the A_n yield estimates of the strength of the singularity. By comparison with the energetic approximation one finds that the residual function $G(v)$ contributes about 30 per cent of the amplitude in two dimensions but only 10 per cent in three dimensions.

The low-temperature series for the two-dimensional antiferromagnets converge up to the critical point but are not very regular. Extrapolation leaves no doubt, however, that $\chi(T)$ is continuous and indicates a symmetric (or almost symmetric[†]) logarithmic singularity as expected on the basis of the exact results for the superexchange model. The three-dimensional low-temperature series for the cubic lattices do not converge up to the critical point so that metastable or Padé approximant techniques must be used. The series are consistent with the same type of singularity but with an amplitude of from two and a half to three times larger than above T_C (as observed also in the specific heats).

The best estimate for the critical behaviour of the simple cubic lattice may be written

$$\chi_{||}(T) = \frac{g^2 \beta^2}{4kT} \{0.340 + B_{\pm} [1 - (T/T_C)]^{\ell_n} |1 - (T/T_C)| + \dots\} \quad (48.5)$$

where $B_+ \cong 0.11$ and $B_- \cong 0.29$. The parameters for the body centred lattice are $\xi_C \cong 0.369$, $B_+ \cong 0.11$ and $B_- \cong 0.31$.

[†]The original, tentative, estimates from the low temperature series yielded amplitudes some 40 per cent lower than above T_C . However, more recent Padé approximant studies by Marshall et al. indicate a symmetric singularity.

49. Comparison with Experiment

The variation of $\chi_{||}(T)$ for the s.c. and b.c.c. Ising lattices in the critical region is shown in Figure 49.1. The maximum above T_C is much less broad than in two dimensions and it lies closer to T_C . In fact the shapes of the curves compare quite surprisingly well with those observed in sufficiently detailed and accurate experiments. The theory taken together with modern experiments leaves no doubt that the critical point corresponds to the steepest point of the $\chi_{||}(T)$ curve while the maximum lies somewhat above T_C .

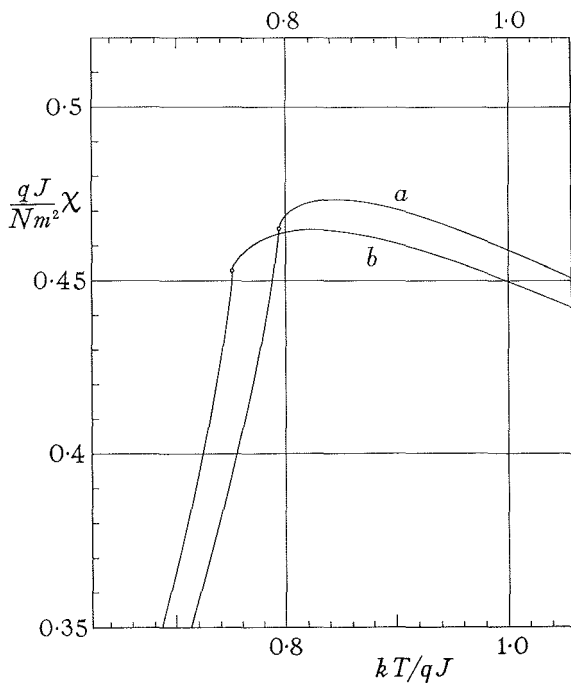


Figure 49.1. Parallel susceptibilities of (a) the body centred cubic ($q=8$) and (b) the simple cubic ($q=6$) Ising lattices near the antiferromagnetic critical point which is marked by a circle. (From M. F. Sykes and M. E. Fisher, *Physica* 28, 930(1962).)

A more stringent test of the fit in the critical region may be made by comparison with the measurements of Gorter and coworkers on $\text{MnCl}_2 \cdot \text{H}_2\text{O}$ (*Physica* 24, 1061(1958)). Thus we find

Spin	Ising s. c. 1/2	Ising b. c. c. 1/2	MnCl ₂ ·4H ₂ O 5/2
$(T_{\max} - T_C)/T_C$	0.098	0.065	0.050
χ_{\max}/χ_C	1.28	1.17	1.19
$\chi(2T_C)/\chi_{\max}$	1.24	1.27	1.30
$(T_1 - T_C)/T_C$	0.285	0.197	0.180

where T_1 is the temperature at which $\chi_{\parallel}(T)$ falls again to its critical value, i. e., $\chi_{\parallel}(T_1) = \chi_C$ so that $(T_1 - T_C)/T_C$ measures the width of the susceptibility peak. It is evident that the differences between "theory" and "experiment" are no greater than the differences between the two models of different lattice structure. Bearing in mind also that the real material has a spin of 5/2 and is not so extremely anisotropic as the Ising model, it seems probable that the critical behaviour is not very sensitive to lattice structure, magnitude of spin or form of interaction. Once again dimensionality and the finite range of the interaction seem to be the dominant factors. As yet, however, calculations for higher spin values and for the Heisenberg model have not been undertaken to test this surmise numerically.

50. Relation to Correlation Functions

The detailed numerical calculations for the Ising models in two and three dimensions have confirmed the expectations based on the soluble but special, superexchange model. How far, however, can one understand the critical behaviour in more general terms? What can be said for the Heisenberg and other models and for real antiferromagnetic systems? To answer this question we recall the general theorem enunciated in Section 25 which relates the susceptibility to the spin pair correlation functions.

For a spin system in a field H parallel to an axis α the hamiltonian may be written generally as

$$\mathcal{H} = \mathcal{H}_0 - g\beta H \sum_i S_i^\alpha, \quad (50.1)$$

where \mathcal{H}_0 is the interaction hamiltonian. If the system is translationally invariant, so that the spins are all equivalent, the magnetization per spin is

$$M^\alpha = g\beta \langle S_0^\alpha \rangle. \quad (50.2)$$

The susceptibility per spin can thence be expressed as

$$\chi^\alpha(T) = \left(\frac{g^2 \beta^2}{kT} \right) \sum_r \left[\langle S_0^\alpha S_r^\alpha \rangle - \langle S_0^\alpha \rangle^2 \right] \quad (50.3)$$

where the subscripts 0 and r denote the lattice sites at the origin and at \vec{r} . With our previous convention we have $\chi^Z = \chi_{\parallel}$ and $\chi^X = \chi_{\perp}$.

In zero field the magnetization of an antiferromagnet always vanishes so that $\langle S_0^\alpha \rangle = 0$ and we may write

$$\chi_{\parallel}(T) = \left[\frac{1}{3} g^2 \beta^2 S(S+1) / kT \right] \xi(T), \quad (50.4)$$

where

$$\xi(T) = \sum_r \omega_r(T), \quad (50.5)$$

in which the reduced correlation functions are

$$\omega_r(T) = \frac{\langle S_0^Z S_r^Z \rangle}{\frac{1}{3} S(S+1)}. \quad (50.6)$$

This agrees with our previous definition

$$\omega_r(T) = \langle s_0 s_r \rangle \quad (50.7)$$

for an Ising $S = \frac{1}{2}$ system.

These formulae show that we can understand the behaviour of the susceptibility in terms of the temperature variation of the spin pair correlation functions if we can perform the summation (50.5).[†]

We must, therefore, consider the behaviour of the correlation functions in more detail. Notice first that as $T \rightarrow \infty$ the individual spins become independent so that

$$\omega_r(T) \rightarrow 0, \quad (r \neq 0) \quad (50.8)$$

whereas

$$\omega_0(T) \rightarrow 1, \quad (50.9)$$

and so

$$\xi(T) \rightarrow 1, \quad (50.10)$$

[†] The analysis that follows is based on M. E. Fisher, *Phil. Mag.* 7, 1731 (1962).

which means that $\chi_{||}$ approaches the susceptibility for a free spin. Using (50.10) we may rewrite (50.4) as

$$\xi(T) = \frac{\langle TX \rangle}{\langle TX \rangle_{\infty}} \quad (50.11)$$

where

$$\langle TX \rangle_{\infty} = \lim_{T \rightarrow \infty} \langle TX \rangle. \quad (50.12)$$

For a spin $\frac{1}{2}$ system the self-correlation function $\omega_0(T)$ must be identically unity and so is certainly temperature independent. The same conclusion follows for general S in a fully isotropic system since, in that case,

$$\begin{aligned} \langle (S_0^Z)^2 \rangle &= \langle (S_0^Y)^2 \rangle = \langle (S_0^X)^2 \rangle \\ &= \frac{1}{3} \langle \vec{S} \cdot \vec{S} \rangle = \frac{1}{3} S(S+1). \end{aligned} \quad (50.13)$$

If $S \geq 1$ and the system is anisotropic, the self-correlation function may vary with temperature but we expect it to vary only slowly and to differ relatively little from unity. †

51. Correlations in a Simple Antiferromagnet

To make further progress let us specify the nature of our system more closely. We will assume that the interaction hamiltonian \mathcal{H}_0 is "essentially antiferromagnetic," in the sense that the spins always tend to orient themselves in opposite senses on two similar interpenetrating sublattices. ‡ We will suppose that the "dominant" spin interactions are bilinear and of short range. In such a simple antiferromagnet any terms opposing the regular ordering will be relatively small and should play only a minor role in the critical behaviour, although they may provide a "background."

With these rather general assumptions we can immediately say quite a lot about the correlation functions. First, in view of the dominant antiferromagnetic coupling, $\omega_r(T)$ will alternate in sign as

† Except, perhaps, at temperatures well below T_C . Notice that in any case ω_0 cannot exceed $3S/(S+1)$. The possibility that ω_0 might vary with temperature was overlooked in the reference cited in the previous footnote.

‡ We assume each spin has q nearest neighbours on the opposite sublattice. It is possible, however, to allow for four or more sublattices.

\vec{r} varies, being positive on the sublattice containing the origin and negative on the other sublattice. Below T_C long-range order is present so that, as $r \rightarrow \infty$,

$$|\omega_r(T)| \rightarrow \omega_\infty(T). \quad (51.1)$$

The long-range correlation function, $\omega_\infty(T)$, is proportional to the square of the sublattice magnetization and hence may be expected to vary as $(T_C - T)^{2\beta}$ as $T \rightarrow T_C$ (with $\beta \cong 0.3$ to 0.35 , say, in three dimensions). Except close to T_C , the decay of the correlations to their limiting value will be quite rapid (probably exponential) so that the functions $|\omega_r(T)|$ will, for all r , be very similar to $\omega_\infty(T)$.

Above T_C there is no long-range order so the correlations must decay to zero as $r \rightarrow \infty$. In fact the decay will be dominated by an exponential,

$$|\omega_r(T)| \sim e^{-\kappa r}, \quad (r \rightarrow \infty), \quad (51.2)$$

as can be seen by making a high temperature expansion. (If J is the dominant nearest neighbour exchange integral, the inverse range of correlation along an axis is given roughly by $\kappa = (1/a) \ln(kT/J)$, when $T \gg T_C$, where a is the lattice spacing.) As the critical temperature is approached, however, the decay of the correlations becomes less rapid in anticipation of the onset of long-range order at T_C . Thus as $T \rightarrow T_C$ we will have $\kappa(T) \rightarrow 0$; at T_C we may expect a relatively slow decay such as an inverse power law. Increasing the temperature will weaken the effects of the interactions so that the correlations will be monotonic functions of T at fixed r .

From these considerations it follows that the general behaviour of the correlations must be as sketched in Figure 51.1. (As previously, ω_1 denotes the nearest neighbour correlation; the dashed curves denote successively more distant correlation functions.) The qualitative correctness of this picture is borne out by the rigorous calculations of Kaufman and Onsager (Phys. Rev. 79, 350(1949)) for the plane square $S = \frac{1}{2}$ Ising lattice with nearest neighbour interactions. In that case $\omega_0 = 1$, $\omega_\infty \sim (T_C - T)^{\frac{1}{4}}$, and $\omega_1(T)$ and all further correlation functions have singularities at the critical point of the form $\omega_r(T_C) + B_r(T - T_C)^{\ln |T - T_C|}$. Above T_C the correlations decay, to leading order, exponentially with r with a range parameter $\kappa(T)$ which varies as $|T - T_C|$ near T_C . Below T_C the "net correlation functions," $[|\omega_r(T)| - \omega_\infty(T)]$, decay in the same way. At T_C , however, an inverse power law takes over and one has[†]

[†]See M. E. Fisher, *Physica* 25, 521 (1959); 28, 172 (1962); *J. Math. Phys.* 5, 944 (1964).

$$|\omega_r(T_C)| = A/r^{\frac{1}{2}} [1 + O(r^{-2})]. \quad (51.3)$$

Throughout the critical region the correlation function for the site at \vec{r} is very similar to those at $\vec{r} + \vec{\delta}$ where $\vec{\delta}$ is a nearest neighbour lattice vector.

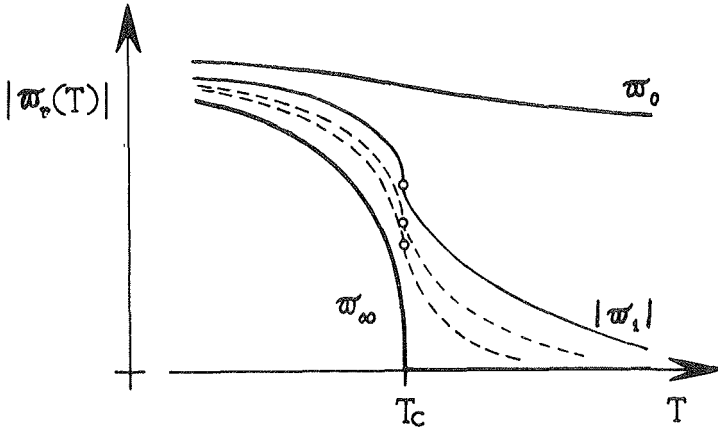


Figure 51.1. Qualitative behaviour of the correlation functions of a simple antiferromagnet.

The temperature variation of the correlation functions in the critical region can be understood by recalling that for an Ising model with nearest neighbour interactions $\omega_1(T)$ is directly proportional to $U(T)$, the magnetic energy per spin measured relative to $U(\infty) = 0$. The same conclusion is true for a fully isotropic Heisenberg model with nearest neighbour interactions since then

$$\langle S_0^Z S_1^Z \rangle = \frac{1}{3} \langle \vec{S}_0 \cdot \vec{S}_1 \rangle. \quad (51.4)$$

Combining both cases we may write, for all S ,

$$\omega_1(T) = \frac{bU(T)}{q|J|S(S+1)} \quad (51.5)$$

where $b = 1$ for the Heisenberg model and $b = 3$ for Ising interactions.

For real antiferromagnets with relatively small anisotropy the Heisenberg limit should be the more appropriate in the critical region. In reality, however, we must also recognize the existence of further neighbour interactions, dipolar forces, biquadratic exchange and other forms of interaction. To the extent that the system corresponds

to our ideal of a simple antiferromagnet, the contributions of these further interaction terms to the mean total energy $U(T)$ (i.e., their thermodynamic expectation values) may be expected to mirror the nearest neighbour contributions plus, possibly, a slowly varying background. Thus, for example, a second neighbour bilinear term would contribute an energy proportional to $J_2\omega_2(T)$, but, as we have seen, to a reasonable approximation this in turn is proportional to $\omega_1(T)$! We may, therefore, hope to allow for the extra terms in \mathcal{H}_0 by taking J to be an effective or equivalent nearest neighbour exchange constant, and by recognizing that b in (51.5) will be a slowly varying function of T (although it should remain of order unity in the critical region).

Accepting (51.5) generally, we thus see that the nearest neighbour correlation function will always reflect the behaviour of the magnetic specific heat which is, of course, just the derivative of $U(T)$. In particular, if $C_{\text{mag}}(T)$ approaches infinity at T_C then $\omega_1(T)$ should have a vertical tangent (infinite gradient) at T_C . By analogy with the plane Ising model it seems likely that the further correlation functions will be similarly "infected."

52. Energy-Susceptibility Relation

Having discovered the general nature of the correlation functions our task is to perform the sum (50.5) to find $\xi(T)$. We have seen that the terms in the sum alternate regularly in sign but their magnitudes vary slowly in the critical region. Consequently, the sum itself will converge only slowly.[†] This difficulty may be overcome by the device of grouping terms. Thus we rewrite (50.5) as

$$\xi(T) = \sum_{\underline{r}}^0 \left\{ \omega_{\underline{r}}(T) - q^{-1} \sum_{\underline{\delta}} |\omega_{\underline{r}+\underline{\delta}}(T)| \right\}, \quad (52.1)$$

where the zero on the leading sum denotes that \underline{r} runs only over the sublattice containing the origin. All the $\omega_{\underline{r}}$ on this sublattice are positive. In the second summation $\underline{\delta}$ runs over the q nearest neighbour lattice vectors. Each negative correlation function thus appears q times with coefficient $1/q$ and so is included correctly.

Now, since the origin has q similar neighbours, the leading term in (52.1) is simply

$$\xi(T) = [\omega_0 - |\omega_1|] + \dots \cong 1 - |\omega_1| + \dots \quad (52.2)$$

[†]For an Ising model or Heisenberg model with $S=\infty$ the convergence must be only conditional at T_C since the ferromagnetic susceptibility, for which all the signs in the sum are positive, diverges at T_C .

All the higher order terms have the form of a finite difference approximation to the Laplacian of a smoothly varying function[†] $\Omega(\underline{r}) \cong \omega_{\underline{r}}$ and hence their sum is, to a good approximation, proportional to the gradient of $\Omega(\underline{r})$ at the second neighbour shell. This, in turn, is essentially proportional to $|\omega_1| - \omega_2$ which by the last section is small and approximately proportional to $|\omega_1|$. (These conclusions can be verified explicitly from the exact results for the plane square Ising lattice.) In total, therefore, we may sum (52.1) approximately as

$$\xi(T) \cong 1 - p(T)|\omega_1(T)|, \quad (52.3)$$

where the function $p(T)$ is of order unity and varies only slowly in the critical region. (From the high temperature expansions one can see that $p(T)$ rises to a value of order q as $T \rightarrow \infty$.)

Combining this result with (50.11) and (51.5) finally yields a fundamental, although approximate relation between the susceptibility and energy of a simple antiferromagnet, which may be written

$$\frac{TX(T)}{(TX)_{\infty}} \cong 1 - \frac{U(T)}{f(T)U_0}, \quad (52.4)$$

where

$$f(T) = b/p \quad (52.5)$$

is a slowly varying function of magnitude near unity in the critical region, and

$$U_0 = qJS(S+1), \quad (52.6)$$

which is approximately equal to the zero point energy, $U(0)$.[‡]

Notice the similarity of this result to the special relation (45.7) for the superexchange model, to the expressions for χ_{\perp} for the Ising model, such as (46.3), and to the energetic approximation:

[†]For a Bravais lattice of spacing \underline{a} and dimensionality \underline{d} one has, correct to second order in \underline{a} ,

$$\begin{aligned} \nabla^2 \Omega &= (d/q) \sum_{\underline{\delta}} \left[\Omega(\underline{r} + \underline{\delta}) - 2\Omega(\underline{r}) + \Omega(\underline{r} - \underline{\delta}) \right] / a^2 \\ &= -2(d/a^2) \left[\Omega(\underline{r}) - (1/q) \sum_{\underline{\delta}} \Omega(\underline{r} + \underline{\delta}) \right] \end{aligned}$$

[‡]Note that J , U_0 , $U(0)$ and $U(T)$ are all negative.

Equation (47.1) with $G(v) \equiv 0$. As in those cases a lambda anomaly in the specific heat implies an infinite slope in $u(T)$ and hence in $TX(T)$. This in turn means that $\chi(T)$ has a vertical tangent at T_C and a maximum above T_C . The distance of the maximum from T_C depends on the rate at which $C_{\text{mag}}(T)$ drops as T increases from T_C . The more rapidly the short-range order disappears above the transition, the closer is T_{max} to T_C .

If we neglect the variation of $f(T)$ near T_C we may differentiate (52.4) to obtain

$$C_{\text{mag}}(T) \cong 2kT_C f \frac{\partial}{\partial T} \left[\frac{TX(T)}{(TX)_{\infty}} \right], \quad (52.7)$$

where we have used the approximation

$$kT_C \cong \frac{1}{2} q |J| S(S+1) = \frac{1}{2} |U_0|, \quad (52.8)$$

which is moderately accurate for the nearest neighbour Heisenberg model. This formula shows explicitly that it is the gradient $\partial(TX)/\partial T$ which should match the specific heat. Indeed it is interesting that the relation is followed even by the approximate theories. Thus the break in the slope of $\chi(T)$ at T_C predicted by the mean field or Bethe approximations corresponds to the discontinuity in $C(T)$ predicted on the same basis! (See Figure 43, 2.)

An experimental test of (52.7) for the long-known antiferromagnetic crystals MnF_2 and MnO is shown in Figure 52.1. (The former material has a b.c.c. structure; the face centred structure of MnO may be regarded magnetically as four interpenetrating, but effectively independent, simple cubic lattices which order antiferromagnetically.) The specific heats and differentiated susceptibilities are very similar (notice the vertical displacement of the two scales) and differences between the two materials are reflected in both quantities. Both C_{mag} and $\partial(TX)/\partial T$ seem to become "infinite" as $T \rightarrow T_C \pm$ but the (relatively old) data used to prepare the curves are not sufficient to reveal the behaviour very close to T_C as accurately as might be desired. Numerical comparison of the two sets of curves confirms that $f(T)$ is close to unity in the critical region ($f \cong 1.1$).

A more accurate test of the theory has been made recently by Wolf and Wyatt (Phys. Rev. Letters, 13, 368 (1964)) who measured $C(T)$ and $\chi_{||}(T)$ for dysprosium aluminium garnet (DAG). This material orders at 2.49 °K which implies relatively weak spin coupling. Consequently, long-range dipole-dipole interactions play an important role. Wolf and Wyatt show how the observed, shape dependent, susceptibility may be simply corrected in order to effect a proper comparison with (52.4) and (52.7) (in the derivation of which dominant long-range

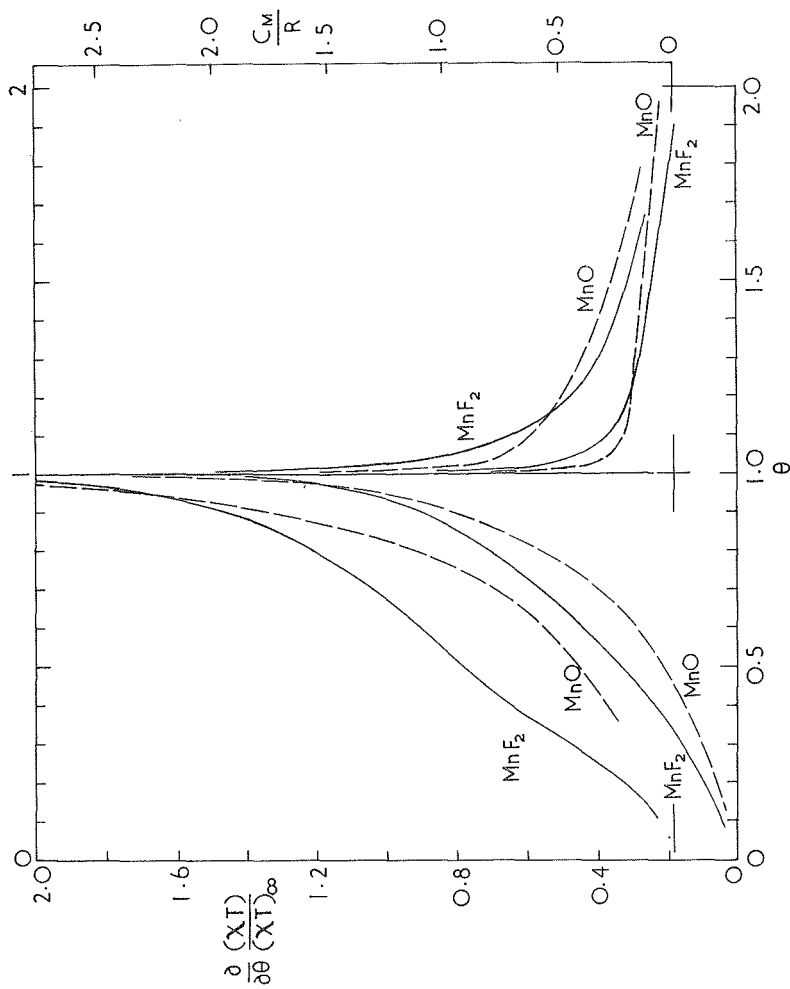


Figure 52.1. Comparison of the magnetic specific heats (upper pair of curves and right hand scale) with the susceptibility gradients (lower pair of curves and left hand scale) versus $\theta = T/T_C$ for MnF_2 solid curves and MnO (broken curves). Note the different zero levels of the two vertical scales. (From M. E. Fisher, Phil. Mag. Z, 1731(1962).)

forces were excluded). Their results are shown in Figures 52.2 and 52.3. The similarity of energy and $T\chi$ and of specific heat and $\partial(T\chi)/\partial T$ is very close. The numerical agreement of the thermal and magnetic curves again indicates that f is close to unity. (The deviation for large T in Figure 52.2 can be understood in terms of the special structure of DAG.)

53. Other Properties

To discuss the perpendicular susceptibility, we need to consider the transverse correlation functions

$$\omega_r^\perp(T) = \langle S_0^X S_r^X \rangle. \quad (53.1)$$

The general behaviour of the transverse correlation will, however, be quite similar to that of the parallel correlations from high temperatures down to, say, $0.9 T_C$ where the anisotropy becomes dominant. Indeed, in a system with small anisotropy the actual magnitudes of the parallel and transverse functions will be almost equal in this range. (At lower temperatures, however, $\xi_\perp(T)$ will vanish only as fast as T since χ_\perp approaches a positive value as $T \rightarrow 0$ where $\xi_\parallel(T)$ vanishes more rapidly.) Consequently, the behaviour of $T\chi_\perp(T)$ should be similar to that of $T\chi_\parallel(T)$ in the critical region as, in fact, we discovered in the plane Ising lattices and as is confirmed by accurate experimentation.

The behaviour of the susceptibility in a small nonzero field near T_C can be investigated by noting that the magnetization M will be roughly proportional to $H\chi(T)$ except that we must allow for a change of transition temperature with field. If we assume the transition curve varies as

$$T_t(H) = T_C - \delta |H|^\epsilon \quad (H \rightarrow 0) \quad (53.2)$$

with positive δ and ϵ , we can thus write

$$M(T, H) \cong H(T\chi)_\infty \xi(T + \delta |H|^\epsilon) / T, \quad (53.3)$$

$$\cong H(T\chi)_\infty [1 - p|\omega_1(T + \delta |H|^\epsilon)] / T, \quad (53.4)$$

where we have used (50.11) and (52.3). Differentiation with respect to H at constant T now yields an expression for $\chi(T, H)$ which will clearly contain a term proportional to $-p\delta\epsilon |H|^{\epsilon-1} (\partial |\omega_1| / \partial T)$. But, as we have seen, the derivative $\partial |\omega_1| / \partial T$ is essentially proportional to the magnetic specific heat. Consequently, if $C_{\text{mag}}(T)$ has a lambda anomaly, a similar sharp peak should be observed in χ at the transition point when $H \neq 0$. As we commented before, however, the

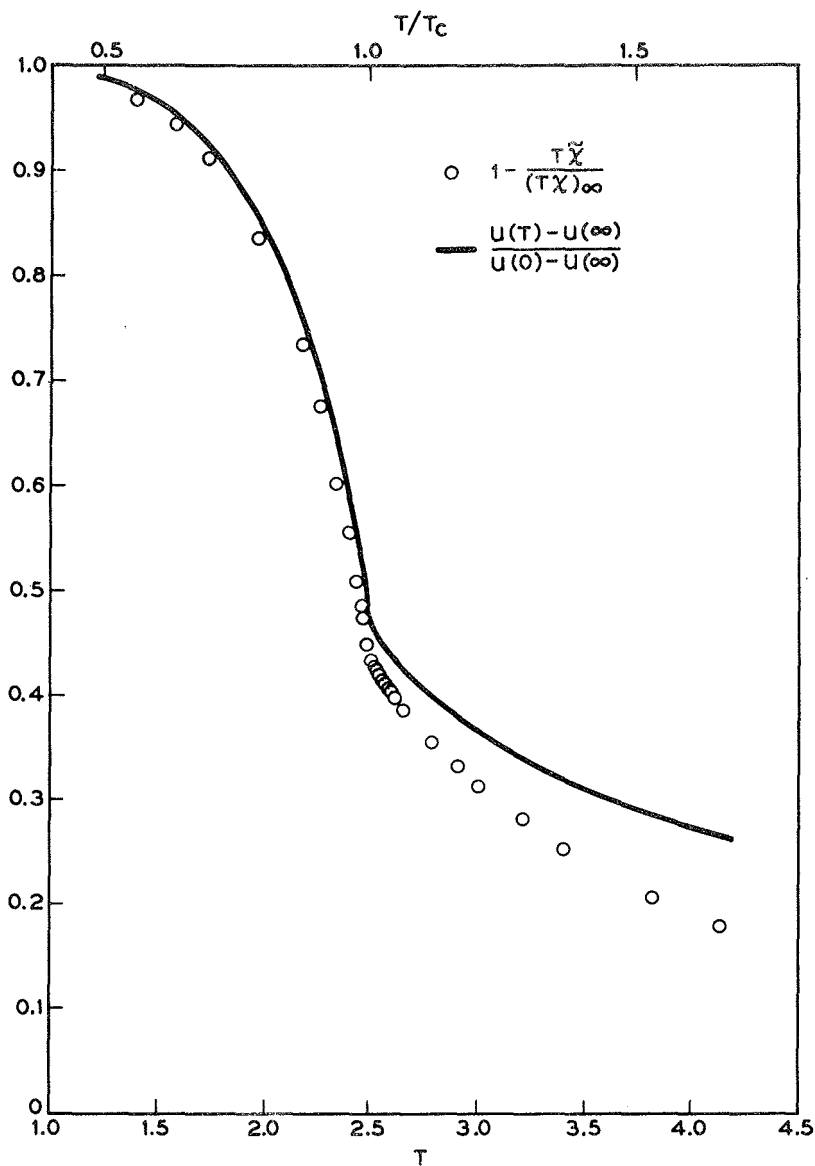


Figure 52.2. Comparison between the magnetic energy and the susceptibility for dysprosium aluminium garnet. The critical point is at 2.49 °K. (From W. P. Wolf and A. F. G. Wyatt, Phys. Rev. Letters 13, 368 (1964).)

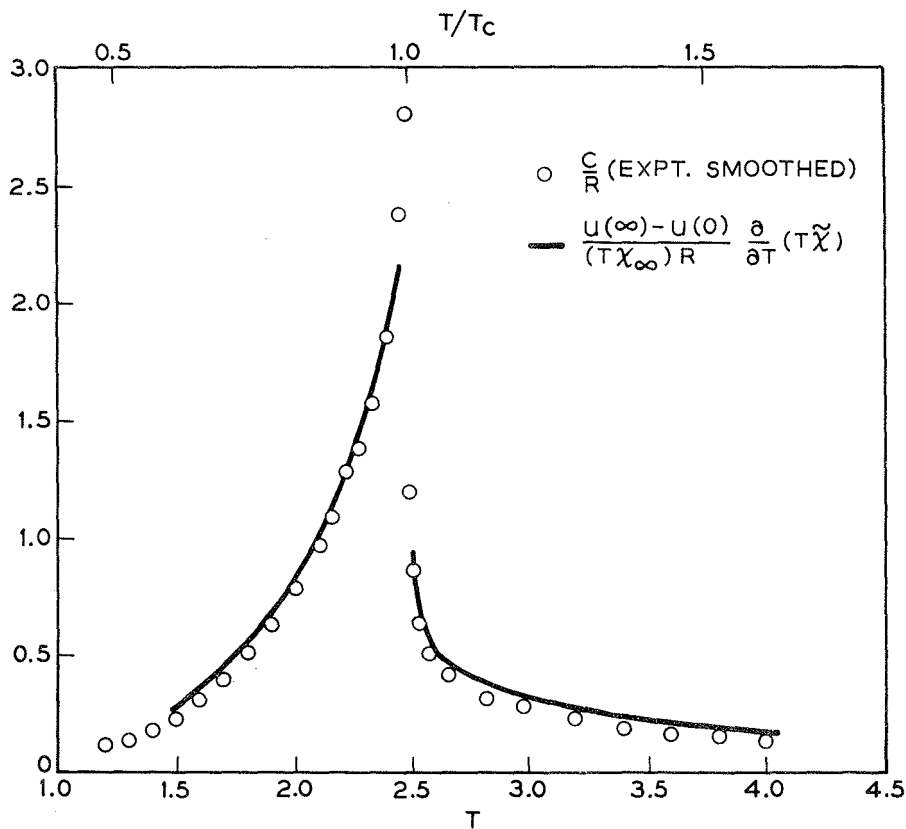


Figure 52.3. Comparison of the specific heat of DAG with the gradient $\partial(T\chi)/\partial T$ normalized by a factor corresponding to $F(T) = 1$ in Equation (52.4). (From W. P. Wolf and A. F. G. Wyatt, *Phys. Rev. Letters* 13, 368(1964).)

amplitude $\delta\epsilon|H|^{\epsilon}$ will normally be rather small so that the anomaly may be difficult to detect experimentally.

In larger fields and at lower temperatures the mean field approximation and the simple spin wave theory suggest that an intermediate transition should take place in an anisotropic antiferromagnet (see Figure 5.4). This is the "spin flopping" transition from the ordered antiferromagnetic state with spins aligned parallel to the easy axis to a new state in which there is still antiferromagnetic order but where the spins are mainly aligned perpendicular to the easy axis. The occurrence of some such transition is confirmed by experiment but its nature has not yet been investigated theoretically in any detail.

Chapter XIII

54. Critical Scattering

In our investigation of the nature of critical points we have, so far, considered only the macroscopic thermodynamic and magnetic properties. We have seen that insight into the behaviour of these properties may be gained by considering the microscopic correlation functions for the system. However, the correlation functions themselves are accessible to direct experimental study, since any scattering experiment on a system measures, in effect, the spatial Fourier transform of the pair correlation function. Thus if light, X-rays or neutrons of wavelength λ are scattered elastically† at angle θ from a fluid, the intensity is given (in the absence of multiple scattering) by

$$\frac{I(\vec{k})}{I_0(\vec{k})} = 1 + \rho \int d^3\vec{r} e^{i\vec{k}\cdot\vec{r}} G(\vec{r}), \quad (54.1)$$

where \vec{k} is the change in wave vector,

$$k = (4\pi/\lambda)\sin\frac{1}{2}\theta \quad (54.2)$$

and where $I_0(\vec{k})$ is the form factor for the scattering centres (i.e., the scattering intensity that would be observed for an isolated particle). The pair correlation function is defined as before (Section 25) by

$$G(\vec{r}) = \left[\frac{n_2(\vec{r})}{\rho^2} \right] - 1, \quad (54.3)$$

where $n_2(\vec{r})$ is the pair distribution function.

† More precisely, quasielastically.

A relation quite analogous to (54.1) holds for the elastic scattering of neutrons from magnetic systems if $G(\vec{r})$ is replaced by the spin pair correlation function

$$\Gamma^{\alpha\beta}(\vec{r}) = \langle S_0^\alpha S_r^\beta \rangle. \quad (54.4)$$

In fact, for elastic scattering from a polycrystal with isotropic spin hamiltonian the scattered intensity is simply proportional to the Fourier transform

$$\hat{\Gamma}(\vec{k}) = \sum_{\vec{r}} e^{i\vec{k}\cdot\vec{r}} \langle S_0^z S_r^z \rangle, \quad (54.5)$$

(See L. Van Hove, Phys. Rev. 95, 1374(1954).)

If we let \vec{k} approach zero in (54.1) and (54.5) we see, by comparison with the fluctuation formulae (25.6) and (25.7), that the expressions become proportional to the static compressibility and susceptibility, respectively! In other words the small angle elastic scattering ($\theta \rightarrow 0$) gives an alternative measure of the K_T and $\chi(T)$.

Now as the critical point of a fluid or ferromagnetic system is approached K_T and $\chi(T)$, respectively, diverge to infinity. It follows, conversely, that the low angle scattering intensity must become very large near the critical point of a fluid or ferromagnet. This sharp increase in $I(\vec{k})$ as $T \rightarrow T_C$ is the well-known critical scattering phenomenon, sometimes referred to in gases as critical opalescence. The increase in scattering may be understood more physically in terms of enhanced large scale density or spin alignment fluctuations. One may imagine the spontaneous formation of relatively large, although still microscopic, "clusters" or "domains" which will occur with increasing frequency near T_C since macroscopic phase separation (or alignment) is about to set in. The coherence and large size of such clusters leads to the strength and low angle of the scattering.

The original theory to explain the temperature and wavenumber dependence of critical scattering is due to Ornstein and Zernike (Proc. Acad. Sci. Amsterdam 17, 793(1914)). This theory is in many ways comparable to the classical or mean field approximations and, as might thus be anticipated, it proves not to be entirely accurate in its detailed predictions in the critical region. An account of the theory, its many rederivations, of its validity and of improvements upon it would, however, take us beyond the scope of these lectures. Instead we refer the interested reader to a recent review (J. Math. Phys. 5, 944(1964)).

Finally, let us mention that neutron scattering invariably has an important inelastic component which may, in turn, be related to the time dependent behaviour of the correlation functions. This time

variation is also relevant to the calculation of the transport coefficients such as the viscosity and the self-diffusion and thermal conductivity coefficients. The study of such inelastic and irreversible phenomena in the critical region promises to be a fascinating task both for the experimentalist and the theoretician.

Appendix

Existence and Properties of the Limiting Free Energy

In this appendix we will present a rigorous proof of the existence of the limiting free energy of a classical system and establish its important properties. For simplicity we will assume the potentials satisfy a "strong tempering" condition and will consider only a special sequence of cubic domains. Proofs under weaker conditions on the potentials for more general shapes of domain and for quantum-mechanical systems obeying Fermi, Bose and Boltzmann statistics are given in the recent literature.[†] The connection with the grand canonical partition function is also discussed in these references.

For convenience, let us first restate the relevant definitions. We suppose N identical classical point particles with position vectors \vec{r}_i are restricted to a three-dimensional domain Ω of volume $V = V(\Omega)$. We allow the domain to have an infinitely repulsive wall of thickness h which prevents the particles approaching the boundary of Ω more closely than h . The density and specific volume are then

$$\rho = N/V, \quad v = 1/\rho = V/N, \quad (\text{A. 1})$$

and the canonical partition function is

$$Z(\beta, N, \Omega) = \frac{\Lambda^{-3N}}{N!} \int_{\Omega} d^3r_1 \dots \int_{\Omega} d^3r_N \exp[-\beta U_N(\vec{r}_1 \dots \vec{r}_N)], \quad (\text{A. 2})$$

where U_N is the total potential energy. The free energy per particle is, of course, defined by

$$-\beta F(\beta, N, \Omega) = -\beta F_N/N = (1/N) \ln Z(\beta, N, \Omega) \quad (\text{A. 3})$$

but it is more convenient to consider the free energy density

$$g(\beta, \rho, \Omega) = [1/V(\Omega)] \ln Z(\beta, N, \Omega), \quad (\text{A. 4})$$

$$= -\beta v^{-1} F(\beta, N, \Omega). \quad (\text{A. 5})$$

[†]D. Ruelle, *Helv. Phys. Acta.* **36**, 183, 789(1963); M. E. Fisher, *Arch. Ratl. Mech. Anal.* **17**, 377 (1964).

For a given domain Ω , this defines $g(\rho, \Omega)$ only for densities which are integral multiples of $\Delta\rho = 1/V(\Omega)$. It is natural and convenient to define $g(\rho, \Omega)$ for arbitrary densities by linear interpolation. Thus if

$$\rho = (N + \eta)/V(\Omega), \quad (0 \leq \eta \leq 1) \quad (\text{A. 6})$$

we set

$$g(\rho, \Omega) = g(N/V, \Omega) + \eta[g((N+1)/V, \Omega) - g(N/V, \Omega)]. \quad (\text{A. 7})$$

This is equivalent to defining $F(\Omega)$ for all specific volumes by linear interpolation in v .

We anticipate that for an infinite sequence of domains Ω_k with $V_k \rightarrow \infty$ the limit

$$\lim_{k \rightarrow \infty} g(\beta, \rho, \Omega_k) = g(\beta, \rho) = -\beta v^{-1} F(\beta, v) \quad (\text{A. 8})$$

will exist and depend only on β and ρ (or v).

Potentials

To establish the existence of the thermodynamic limit for the free energy, two conditions must be imposed on the potentials—roughly speaking, one on the attractive part and one on the repulsive part. The first condition is

(A) Stability

$$U_N(\vec{r}_1 \dots \vec{r}_N) \geq -Nw_A$$

for all \vec{r}_i and all N (w_A fixed), (A. 9)

which simply states that the potential energy per particle is bounded below, however large the system. (This property of the potentials is familiar in nuclear physics as the "saturation" of nuclear forces.)

For a system of particles with hard cores of diameter \underline{a} which interact through pure pair forces with potential $\varphi(r)$, it is quite easy to see that stability will be insured by

$$\varphi(r) \geq -D/r^{3+\epsilon}, \quad (r > a) \quad (\text{A. 10})$$

where D and ϵ are positive constants. As stated in Section 11, however, hard cores are not necessary for stability: it is sufficient that $\varphi(r)$ is bounded below, satisfies (A.10) and the condition

$$\varphi(r) \geq C/r^{3+\epsilon'} \quad \text{as } r \rightarrow 0, \quad (\text{A. 11})$$

where C and ϵ' are positive.*

With the stability condition (A) we at once obtain from (A.2) the inequality

$$Z(\beta, N, \Omega) \leq \frac{\Lambda^{-3N}}{N!} e^{\beta N w_A} [V(\Omega)]^N. \quad (\text{A.12})$$

On using Stirling's formula in the form

$$\ln N! \geq N \ln N - N, \quad (\text{A.13})$$

we thus have the important upper bound

$$g(\beta, \rho, \Omega) \leq \rho [1 + \beta w_A - \ln(\rho \Lambda^3)], \quad (\text{A.14})$$

valid for any domain.

In order to state the second condition on the potentials, we define the mutual potential energy of two groups of N and N' particles by

$$\begin{aligned} \Phi_{N, N'}(\vec{r}_1 \dots \vec{r}_N; \vec{r}'_1 \dots \vec{r}'_{N'}) &= U_{N+N'}(\vec{r}_1 \dots \vec{r}_N, \vec{r}'_1 \dots \vec{r}'_{N'}) \\ &\quad - U_N(\vec{r}_1 \dots \vec{r}_N) - U_{N'}(\vec{r}'_1 \dots \vec{r}'_{N'}). \end{aligned} \quad (\text{A.15})$$

Suppose now that the two groups of particles are confined in two regions which are separated by a distance at least R . Then the condition,

(B) Strong Tempering

$$\Phi_{N, N'}(\vec{r}_1 \dots \vec{r}_N; \vec{r}'_1 \dots \vec{r}'_{N'}) \geq 0 \quad (\text{A.16})$$

for all N, N' whenever $R = \min_{ij} |\vec{r}_i - \vec{r}'_j| \geq R_0$ (fixed),

merely asserts that the forces between groups of particles are not 'repulsive' at large distances (i.e., the mutual potential is nonpositive). This is the case, for example, with Van der Waals forces.

For pure pair forces the condition (B) will be satisfied if, for some R_0 ,

*See D. Ruelle, Boulder Lectures 1963, Section 2.5 (University of Colorado Summer School in Theoretical Physics) and Ann. Phys. (N.Y.) 25, 109(1963); M. E. Fisher, Arch. Ratl. Mech. Anal. (1964).

$$\varphi(r) \leq 0, \quad \text{for} \quad r \geq R_0. \quad (\text{A. 17})$$

The less restrictive "weak tempering" condition

$$\Phi_{N,N'} \leq NN'w_B/R^{3+\epsilon} \quad (R \geq R_0, \epsilon > 0), \quad (\text{A. 18})$$

is sufficient for the existence of the free energy but the proof is then more involved.

Basic Inequality

We may use the tempering condition (B) to obtain an inequality between the partition function for a domain Ω containing $N = N' + N''$ particles, and the partition functions for two subdomains Ω' and Ω'' contained in Ω but separated by a distance $R \geq R_0$ and containing N' and N'' particles, respectively (see Figure A. 1). Since the integrand in (A. 2) is positive we may reduce the domain of integration of each \vec{r}_i from Ω to $\Omega' + \Omega''$ and then split up the domains of integration in all possible ways. This yields the inequality

$$Z(N, \Omega) \geq \frac{\Lambda^{-3}}{N!} \sum_{N'+N''=N} \frac{N!}{N'!N''!} \int_{\Omega'} d^3r_1 \dots \int_{\Omega'} d^3r_{N'} \int_{\Omega''} d^3r_{N'+1} \dots \int_{\Omega''} d^3r_{N'+N''} \exp[-\beta U_{N'} - \beta U_{N''} - \beta \Phi_{N',N''}] \quad (\text{A. 19})$$

where the arguments of $U_{N'}$, $U_{N''}$ and $\Phi_{N',N''}$ are assigned in the obvious way. Each integral in the sum over (N', N'') is positive so the inequality remains true if we merely retain a typical term! The

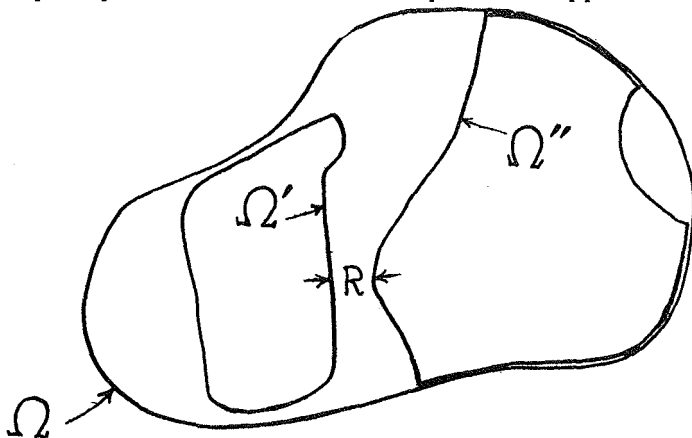


Figure A. 1. A domain Ω containing two separated subdomains.

interaction energy $\Phi_{N'N''}$ arises only between groups of particles separated by at least R_0 so that by condition (B) the factor $\exp[-\beta\Phi_{N'N''}]$ is never less than unity. The inequality can thus only be strengthened by dropping the mutual potential energy. The multiple integral then factorizes to yield the basic inequality

$$Z(N' + N'', \Omega) \geq Z(N', \Omega')Z(N'', \Omega''). \quad (\text{A.20})$$

On taking logarithms we find

$$Vg(\rho, \Omega) \geq V'g(\rho', \Omega') + V''g(\rho'', \Omega''), \quad (\text{A.21})$$

where

$$V\rho = V'\rho' + V''\rho'', \quad (\text{A.22})$$

and where

$$\rho = (N' + N'')/V, \quad \rho' = N'/V' \quad \text{and} \quad \rho'' = N''/V''.$$

By combining (A.20) with the three corresponding inequalities obtained by the replacements $(N', N'') \rightarrow (N'+1, N'')$, $(N', N''+1)$ and $(N'+1, N''+1)$ and using the definition (A.7), the relations (A.21) and (A.22) may be proved for arbitrary values of the densities.

If the domain Ω is divided into a number of subdomains $\Omega_1, \Omega_2, \dots$ so that the particles in any Ω_ℓ are always kept at least a distance R_0 from those in any other Ω_m , we may iterate (A.21) and (A.22) to get

$$g(\rho, \Omega) \geq \sum_{\ell=1}^n \omega_\ell g(\rho_\ell, \Omega_\ell) \quad (\text{A.23})$$

where

$$\rho = \sum_{\ell=1}^n \omega_\ell \rho_\ell, \quad \omega_\ell = V_\ell/V. \quad (\text{A.24})$$

Notice that the separation condition will be achieved for nonoverlapping (but possibly touching) domains if each Ω_ℓ has walls of thickness $h \geq \frac{1}{2}R_0$.

Limit for Sequence of Cubes

To take the thermodynamic limit suppose that the domains Ω_k are a sequence of cubes Γ_k with walls of fixed thickness $h \geq \frac{1}{2}R_0$ and such that the edge of Γ_{k+1} is double that of Γ_k . (In the limit $k \rightarrow \infty$ the volume excluded by the walls is negligible.) A cube Γ_{k+1} can thus be subdivided into eight nonoverlapping cubes Γ_k obeying the

separation condition. Let us, therefore, apply the basic inequality (A.23). Clearly,

$$\omega = V_k/V_{k+1} = 1/8. \quad (\text{A.25})$$

Setting $\rho_1 = \dots = \rho_4 = \rho'$ and $\rho_5 = \dots = \rho_8 = \rho''$ so that, by (A.24), $\rho = \frac{1}{2}\rho' + \frac{1}{2}\rho''$, yields

$$g(\frac{1}{2}\rho' + \frac{1}{2}\rho'', \Gamma_{k+1}) \geq \frac{1}{2}g(\rho', \Gamma_k) + \frac{1}{2}g(\rho'', \Gamma_k), \quad (\text{A.26})$$

for all ρ' and ρ'' .

To prove the existence of the limit, choose $\rho' = \rho'' = \rho$ to get

$$g(\rho, \Gamma_{k+1}) \geq g(\rho, \Gamma_k) \quad (\text{A.27})$$

Thus for each value of ρ the sequence $g(\rho, \Gamma_k)$ is increasing (monotonically nondecreasing). However, by (A.14), $g(\rho, \Gamma_k)$ is bounded above. Consequently, as $k \rightarrow \infty$ the sequence must tend to a limit!

This establishes the existence of the limiting free energy (A.8)—at least for the sequence of cubes Γ_k . To prove that the limit is the same for more general shapes of domain (with or without walls) the basic inequality may be used to compare the free energy of a general domain Ω_j with the free energies of the standard cubes by filling Ω_j with smaller cubes Γ_k and by filling a larger cube Γ_k with Ω_j and smaller cubes.†

Properties of the Free Energy

To determine the properties of the limiting function $g(\rho)$ take the limit $k \rightarrow \infty$ in (A.26). This yields the inequality

$$g(\frac{1}{2}\rho' + \frac{1}{2}\rho'') \geq \frac{1}{2}g(\rho') + \frac{1}{2}g(\rho''), \quad (\text{A.28})$$

which, in graphical terms, states that the curve of the function $g(\rho)$ versus ρ lies above the midpoint of any chord (see Figure A.2); such a function is said to be convex (upwards).

At first sight it might seem that nothing of much significance would follow from the convexity relation (A.28). However, the properties of a bounded‡ convex function are highly circumscribed. In particular such a function is (a) continuous, (b) differentiable

†See M. E. Fisher, Arch. Ratl. Mech. Anal. 17, 377 (1964).

‡The limit function $g(\rho)$ is bounded above by (A.14) and bounded below by virtue of (A.27).

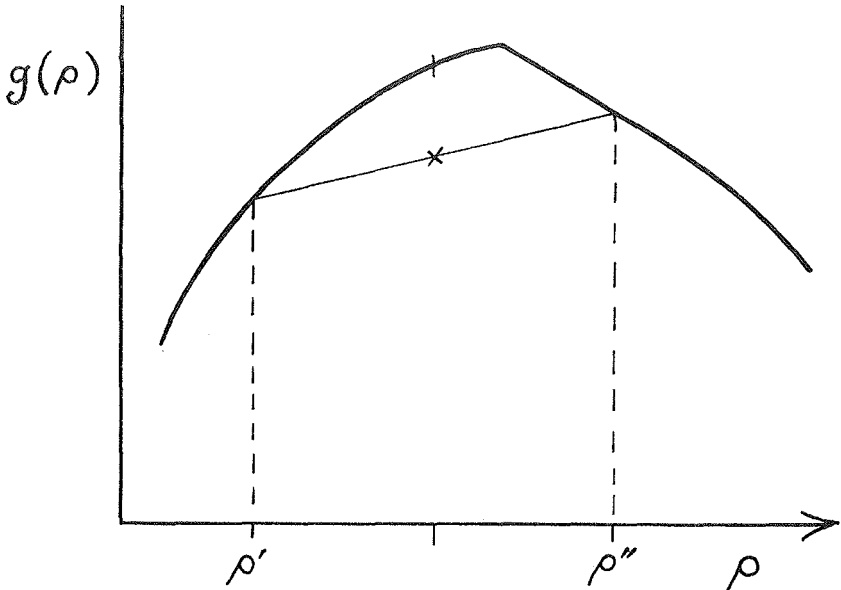


Figure A.2. Illustrating the convexity of the free energy density $g(\rho)$.

almost everywhere (that is, except at a countable number of points where the right and left derivatives exist but do not agree), and (c) its derivative is a monotonic function. These results are quite easily understood by graphical arguments based on drawing chords, but rigorous analytical proofs are available in the well known book by Hardy, Littlewood and Pólya ("Inequalities" Chap. 3, Cambridge (1934)).

We may thus conclude from (A.28) that

- (i) $g(\rho)$ is continuous in ρ , and hence from (A.8) the limiting free-energy per particle $F(v)$, is continuous in v ;
- (ii) by the continuity, the generalized convexity relation

$$g\left(\sum_{\ell} \theta_{\ell} \rho_{\ell}\right) \geq \sum_{\ell} \theta_{\ell} g(\rho_{\ell}) \quad (\text{A.29})$$

holds where

$$\sum_{\ell} \theta_{\ell} = 1, \quad (\theta_{\ell} \geq 0);$$

(iii) from this and (A.8) it follows that $F(v)$ is a convex (downwards) function of v ;

(iv) $g(\rho)$ and $F(v)$ are differentiable almost everywhere (the right and left derivatives exist everywhere) so that the pressure

$$p(\beta, v) = - \frac{\partial F}{\partial v} \quad (\text{A. 30})$$

is defined uniquely everywhere except, possibly, at a countable number of jump discontinuities;

(v) the derivatives of $g(\rho)$ and $F(v)$ are monotonic functions of ρ and v so that, in particular the pressure $p(v)$ is a monotonic nonincreasing function of the specific volume v .

It is easy to see that $F(v)$ is a nonincreasing function of v so that $p(v)$ is never negative. Notice, however, that we have not proved the continuity of $p(v)$. Although this is probably true under rather general conditions, it has only been proved for classical systems interacting with a pair potential $\varphi(r)$ which is bounded above.[†] Since $p(v)$ is monotonic it follows that its derivative, and hence the compressibility, exists almost everywhere[‡] and is nonnegative. (This expresses the "mechanical stability" of the thermodynamic limit.)

From the form of the canonical partition function as a Laplace integral in β and Schwarz's inequality, it follows that $g(\beta, \rho, \Omega)$, and hence $g(\beta, \rho)$, is convex in β . Thus the free energy $F(\beta, v)$ is also continuous and differentiable (almost everywhere) in the temperature variable β .

[†]See D. Ruelle, *Helv. Phys. Acta* **36**, 183(1963).

[‡]By Lebesgue's theorem; see, for example, F. Riesz and B. Sz. -Nagy, *Functional Analysis*, Ungar Publishing Co., New York (1955).